



Curtin University

THE INSTITUTE FOR
GEOSCIENCE RESEARCH (TIGeR)

TIGeR ANNUAL REPORT 2018

EXPLORING EARTH'S DYNAMIC EVOLUTION

Make tomorrow better.

scieng.curtin.edu.au

TIGeR: The Institute for Geoscience Research



About TIGeR - exploring Earth's dynamic evolution

The Institute for Geoscience Research (TIGeR) brings together active researchers across the spectrum of geosciences within Curtin University with the common goal of understanding the mechanisms and the timescales of the processes that control Earth's dynamic evolution.

TIGeR researchers study processes over a wide range of length scales, from the nanoscale to the macroscale – from reactions operating at grain boundaries in rocks to global tectonics and the origin of the Solar system.

Since the establishment of TIGeR, our researchers have been at the forefront of high-quality, world-leading research in the earth sciences. We produce geochronologic, geotectonic, geodetic and geochemical records, using the latest technology and field and laboratory data, to enhance our knowledge of the Earth's origin within the solar system, its evolution and its current configuration.

Our research forms the basis of understanding the element cycles operating on Earth and their application to the formation of natural resources such as mineral, oil, gas and coal deposits.

Widespread collaboration

TIGeR is a multidisciplinary group that brings together leading scientists in geology, inorganic and organic geochemistry, geodesy and geophysics with the common goal of advancing new and innovative geoscience research.

Our researchers are drawn from all the geoscience-related departments and centres across Curtin University, including the Department of Applied Geology, the John de Laeter Centre for Isotope Research, the Western Australian Centre for Geodesy, the Western Australian Organic and Isotope Geochemistry Group, the Department of Exploration Geophysics and the Department of Mining Engineering.

We work together with research teams across Australia and internationally and have an excellent track record of obtaining competitive national and international grants, publishing in leading international journals and producing highly-qualified postgraduates.

Contents

About TIGeR - Exploring Earth's Dynamic Evolution	
Director's comments	ii
2018 TIGeR Conference	iv
Research reports	
Mineral systems, fluids and ore deposits	1
Advanced Resource Characterisation Facility	31
Organic and isotope geochemistry	39
Tectonics and geodynamics	57
Planetary science	91
Spatial sciences	103
Computational geoscience	117
TIGeR publication list 2018	133
TIGeR membership 2018	161

Mission statement

To obtain a fundamental understanding of the mechanisms behind complex processes in the Earth.

To establish and maintain a reputation as an international leader in this field.

To enhance our interdisciplinary research by establishing new collaborations and joint ventures.

To actively seek greater involvement with industrial applications of our research.

To find efficient ways of transmitting our basic research to industry, the education sector and the public.

Director's comments



The Institute for Geoscience Research (TIGeR) promotes excellence across the wide spectrum of Earth science related activities at Curtin University. The 2018 Annual Report is the fourth of a regular series that summarizes the peer-reviewed research publications for each year and serves as both a source of information as well as an archive. The Reports are available on the TIGeR website (tiger.curtin.edu.au).

The articles in this Report are a selection from over 300 peer-reviewed publications by TIGeR members in 2018, mostly chosen by the authors themselves as representative of their research topics. The very high level of productivity is also typical of previous years and is why Curtin University continues to be a leader in the "solid earth" disciplines of geology and geochemistry. The 2019 Excellence in Research for Australia (ERA) results have acknowledged our international reputation with scores of 5 ("well above world standard") in both the categories of 'geology' and 'geochemistry'.

Notable successes for TIGeR members during 2018 include an ARC Laureate Fellowship to Julian Gale, an ARC Future Fellowship to Raffaella Demichelis, and ARC DECRA Fellowships to Denis Fougerouse and Amy Parker. Ian Fitzsimons was a recipient of the Stillwell Award of the Geological Society of Australia and Andrew Putnis received the 2018 Robert Wilhelm Bunsen Medal of the European Geoscience Union.

Katarina Miljkovic was awarded the highly prestigious 2018 ANZ L'Oreal-UNESCO for Women in Science Fellowship.

National and international collaboration is a characteristic of Geosciences research and TIGeR members continue to be active in multidisciplinary research projects as evidenced from the publications and projects reported here. TIGeR members are conspicuous at international conferences such as EGU, AGU and Goldschmidt and it is particularly pleasing to see young researchers and PhD students from Curtin presenting their work at such conferences through the financial help available from the TIGeR Small Grants Scheme.

The Annual TIGeR Conference is a highlight of the year and has already established itself as an international forum for in-depth discussion of specific research issues in Geosciences. In 2018 the Conference theme was "Coupling between Metamorphism and Deformation" and attracted a very impressive list of international and national speakers. As a result of this, new collaborations have been initiated that give Curtin University, through TIGeR, an international visibility and an ever-increasing world-wide reputation of excellence in geosciences research. The Conference programme and abstracts are available for download from the TIGeR website.

So 2018 was another excellent year!

Andrew Putnis
Director, The Institute for
Geoscience Research (TIGeR)

2018 TIGeR Conference

The fourth TIGeR Conference was held in September with > 120 international and national participants from Universities and industry.

The details of the 2018 TIGeR Conference programme as well as downloadable abstracts can be found at: tiger.curtin.edu.au/conferences/



2018 TIGeR Conference



Research reports

MINERAL
SYSTEMS,
FLUIDS
AND ORE
DEPOSITS

Mineral systems, fluids and ore deposits

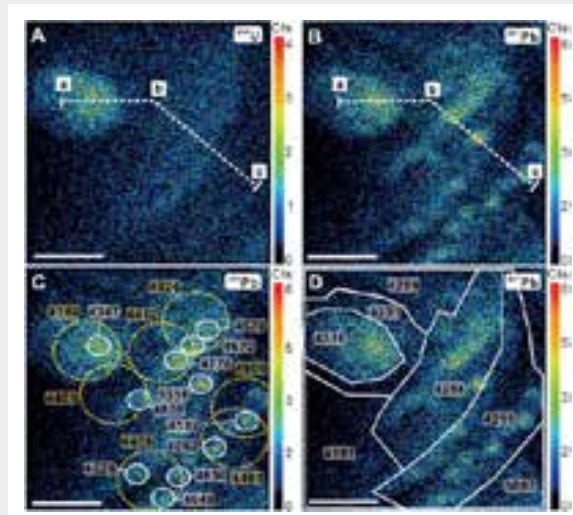
A 4463 Ma apparent zircon age from the Jack Hills (Western Australia) resulting from ancient Pb mobilization

Hadean (≥ 4.0 Ga) zircon grains provide the only direct record of the first half-billion years of Earth's history. Determining accurate and precise crystallization ages of these ancient zircons is a prerequisite for any interpretation of crustal evolution, surface environment, and geodynamics on the early Earth, but this may be compromised by mobilization of radiogenic Pb due to subsequent thermal overprinting.

Ge *et al.* (2018) report a detrital zircon from the Jack Hills (Western Australia) with 4486–4425 Ma concordant ion microprobe ages that yield a concordia age of 4463 ± 17 Ma (2σ), the oldest zircon age recorded

from Earth. However, scanning ion imaging reveals that this >4.4 Ga apparent age resulted from incorporation of micrometer-scale patches of unsupported radiogenic Pb with extremely high $^{207}\text{Pb}/^{206}\text{Pb}$ ratios and >4.5 Ga $^{207}\text{Pb}/^{206}\text{Pb}$ ages. Isotopic modeling demonstrates that these patches likely resulted from redistribution of radiogenic Pb in a ca. 4.3 Ga zircon during a ca. 3.8 Ga or older event. This highlights that even a concordia age can be spurious and should be carefully evaluated before being interpreted as the crystallization age of ancient zircon.

Ge, R., Wilde, S.A., Nemchin, A.A., Whitehouse, M.J., Bellucci, J.J., Erickson, T.M., Frew, A., Thern, E.R. (2018). A 4463 Ma apparent zircon age from the Jack Hills (Western Australia) resulting from ancient Pb mobilization. *Geology*, 46, 303–306.



Selected scanning ion images showing distribution of U and Pb isotopes and calculated $^{207}\text{Pb}/^{206}\text{Pb}$ ages for a detrital zircon grain. Color scale indicates counts (Cts) per pixel of image, and each image is 256×256 pixels. Scale bars are $20 \mu\text{m}$. A: ^{238}U image. B: ^{207}Pb image. C, D: Calculated $^{207}\text{Pb}/^{206}\text{Pb}$ ages (in Ma) for different regions of interest. Solid white and dashed yellow ellipses in C indicate $\sim 5 \mu\text{m}$ and $\sim 20 \mu\text{m}$ spots, respectively, that locate on, or partly overlap, hotspots and patches. Solid polygons in D indicate large areas that broadly follow individual domains seen in by cathodoluminescence.

What's the missing ingredient in the Earth's crustal composition?

The Earth's continental crust is a unique chemical environment due to the presence of liquid water and its highly evolved chemical composition. It also represents the most accessible part of our planet, yet its formation mechanism remains enigmatic. Models of continental crust formation involve partial melting of mantle peridotite and have developed from amalgamation of island arc-type magmatic rocks of andesite composition, magmatic recycling of chemically weathered material, to geodynamically more complex mechanisms involving melting of mantle metasomatites, reactions with overlying peridotite and differentiation of subducted material via buoyancy-driven delamination-relamination processes.

However, the chemical composition of the continental crust cannot be adequately explained by current models for its formation, because it is too rich in Ni and Cr

compared to that which can be generated by any of the proposed mechanisms. Estimates of the crust composition are derived from average sediment, while crustal growth is ascribed to amalgamation of differentiated magmatic rocks at continental margins.

Beinlich *et al.* (2018) show that chemical weathering of Ni- and Cr-rich, undifferentiated ultramafic rock equivalent to ~1.3 wt% of today's continental crust compensates for low Ni and Cr in formation models of the continental crust. Ultramafic rock weathering produces a residual that is enriched in Ni and also silica. In the light of potentially large volumes of ultramafic rock and high atmospheric CO₂ concentrations during the Archean, chemical weathering must therefore have played a major role in forming compositionally evolved components of the early Earth's crust.

Beinlich A., Austrheim H., Mavromatis V., Grguric B., Putnis C.V., Putnis A. (2018). Peridotite weathering is the missing ingredient of Earth's continental crust composition. *Nature communications*, 9, 634.



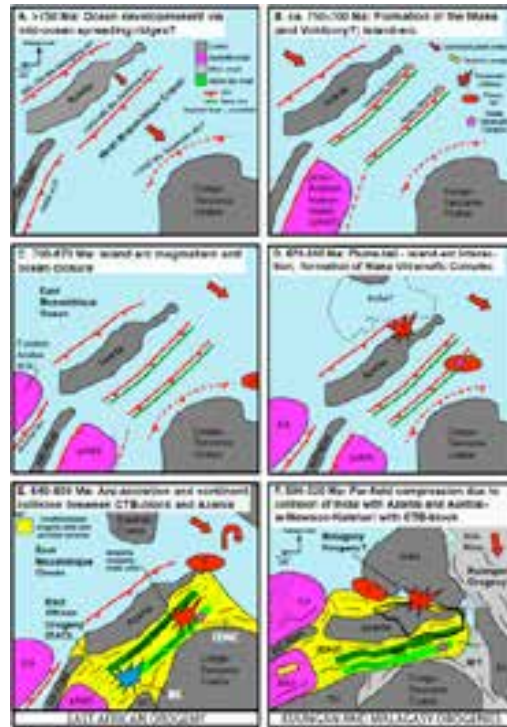
Quartz-carbonate rock (listvenite) formed by the reaction between peridotite and CO₂-bearing fluid, Linnajavri ophiolite, northern Norway.





A relic of the Mozambique ocean in south-east Tanzania

Mole *et al.* (2018) report a detailed assessment of the geology of the poorly exposed Nachingwea region of southeast Tanzania, based largely on geochemical and isotopic data on diamond drill core from the Ntaka Ultramafic Complex Ni-Cu exploration prospect. Linking the Cabo Delgado Nappe Complex of northern Mozambique and the Eastern Granulites of northern Tanzania, this region has a central location within the Neoproterozoic–Cambrian East African Orogen. The orogen represents a long-lived, cordilleran-style margin at the edge of the former Mozambique Ocean that closed during the amalgamation of Gondwana and subsequently Pangaea. The results of new zircon and monazite U–Pb dating combined with the geochemical evidence suggest that the newly named ‘Ntaka Terrane’ and neighbouring parts of the orogen represent an exotic Neoproterozoic island arc sequence that was accreted to either East Africa or the Azania microcontinent prior to their collision *ca.* 640–620 Ma. The interpreted history is similar in many respects to that of the Vohibory Terrane of southern Madagascar. The accompanying diagram from the paper shows a series of tectonic reconstructions of the geodynamic evolution of East Africa. Former TIGeR post-doctoral fellow David Mole is now based at Laurentian University in Sudbury, Canada.



Mole D.R., Barnes S.J., Taylor R.J.M., Kinny P.D., Fritz H. (2018) A relic of the Mozambique Ocean in south-east Tanzania. *Precambrian Research*, 305, 386-426.

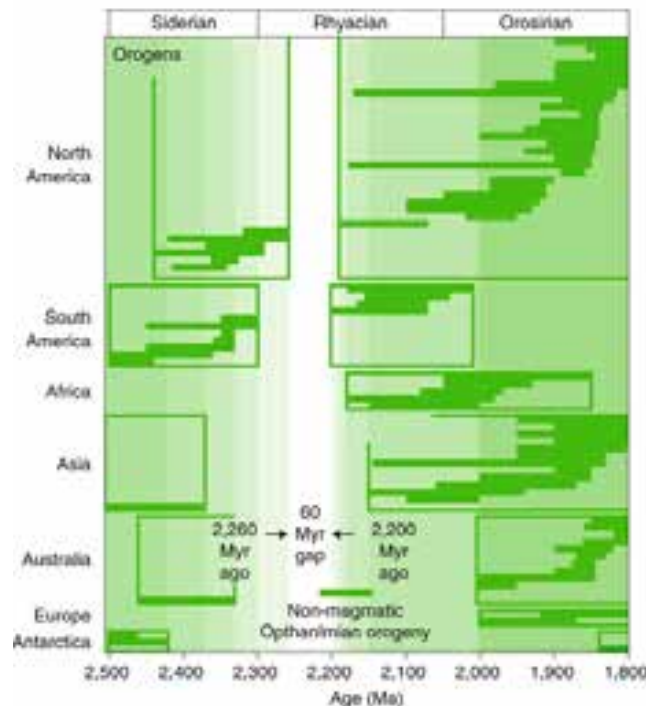
What may have triggered supercontinent cycles?

Research recently published by Spencer *et al.* in *Nature Geoscience* is likely to re-ignite debate over the earth's development, with scientists divided over what geologic processes occurred during the Palaeoproterozoic geologic Era. The research findings point to a near complete shutdown of continental magmatism during this period and has profoundly shaped the geologic record as we know it today. The early Paleoproterozoic was a significant time in Earth history. It was at this time when the atmosphere got its first whiff of oxygen and also the first global glaciation event. But this was also a period where other geologic processes effectively shut down. It's almost as if the Earth experienced a mid-life crisis.

The research involved compiling massive amounts of existing geological data as well as examination of rocks collected in

Western Australia's Stirling Ranges, China, Northern Canada and Southern Africa. Earth's mantle used to be much hotter than it is today and over time volcanoes allowed the mantle to cool and geologic processes are thought to have slowed down. We believe this continual slowdown led to dramatic geological changes such as those seen in the early Paleoproterozoic. This 'dormant' period lasted around 100 million years and signaled what we believe was a shift from 'ancient-style' tectonics to 'modern-style' tectonics more akin to those operating in the present day. Following this dormant period Earth's geology started to 'wake-up' again around 2.2 to 2.0 billion years ago with a 'flare-up' of volcanic activity and a shift in the composition of the continental crust.

Spencer, C.J., Murphy, J.B., Kirkland, C.L., Liu, Y., and Mitchell, R.N., 2018, A Palaeoproterozoic tectono-magmatic lull as a potential trigger for the supercontinent cycle: *Nature Geoscience*, v. 11, p. 97-101.



Temporal distribution of orogens through time groups by continent (after O'Neill *et al.*, 2007).

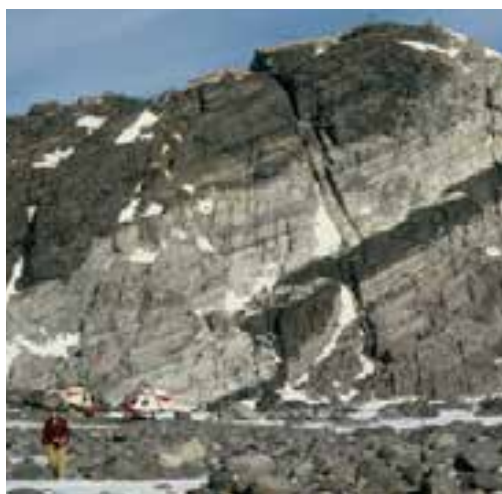
Long ultra-high temperature metamorphism in the Napier Complex, East Antarctica

The Napier Complex in East Antarctica preserves a record of ultrahigh-temperature (UHT) metamorphism during the late Archean to early Palaeoproterozoic. While there is little argument that the UHT metamorphic event began at c. 2580 Ma, the duration over which the rocks resided at UHT has been the subject of intense debate, with estimates for the end of metamorphism ranging from 2545 Ma to 2440 Ma—a discrepancy of some 105 Myr. To resolve the timescale of UHT metamorphism a zircon and garnet petrochronological (U-Pb, REE and Ti) dataset from a suite of rocks from the Tula Mountains region of the Napier Complex was analysed. Individual concordant populations define zircon U-Pb ages for (1) reset zircon cores of 2502 Ma to 2439 Ma; (2) zircon rims of 2491 Ma to 2454 Ma; and (3) neocrystallised sector-zoned zircons from 2492 Ma to 2443 Ma. Ti-in-zircon thermometry places a minimum estimate of 830 °C for zircon crystallization, with the majority of concordant populations yielding temperatures > 900 °C. Zircon-garnet partitioning (D_{Yb} vs $D_{Yb/Gd}$) arrays reveal that the bulk of metamorphic zircon defines an equilibrium relationship with the garnet that forms part of the peak assemblage.

Combined with existing geochronological constraints, the new petrochronological data demonstrate that the Napier Complex remained at UHT from c. 2585 Ma until at least 2450 Ma, a residence time of 135 Myr. In the absence of evidence for contemporaneous emplacement of large volumes of igneous rocks, a number of factors likely combined to drive and maintain these extreme temperatures. Clark *et al.* (2018) propose that the P - T conditions experienced by the Napier Complex were achieved through a combination of orogenic plateau formation, preconditioning of the crust by a high-temperature magmatic

and UHT metamorphic event at ca 2850 Ma, inefficient removal of heat-producing elements during partial melting, and slow exhumation. This style of long duration, regional, extreme metamorphism is becoming more commonly identified in the rock record as larger and more robust datasets are collected (e.g. the Eastern Ghats of India and the Gondwanan East African Orogen) and is commonly associated with the amalgamation phases of supercontinents/cratons.

Clark, C., Taylor, R. J. M., Kylander-Clark, A. R. C., & Hacker, B. (2018). Prolonged (>100 Ma) ultrahigh temperature metamorphism in the Napier Complex, East Antarctica: A petrochronological investigation of Earth's hottest crust. *Journal of Metamorphic Geology*, 36(9), 1117-1139.



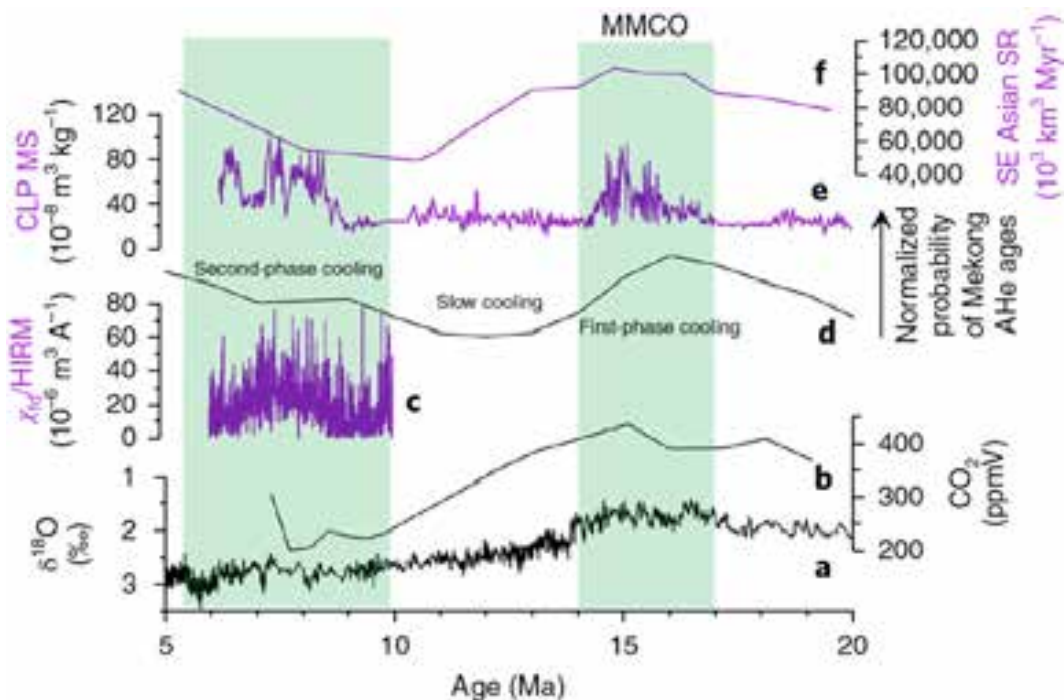
Mount Riiser-Larsen, Tula mountains, Napier Complex.

Thermochronology data from Mekong river bedrock samples reveals a phase of rapid downward incision (>700 m) associated with increased precipitation.

The uplift of orogenic plateaus has been assumed to be coincident with the fluvial incision of the gorges that commonly cut plateau margins. The Mekong River, which drains the eastern Qiangtang Terrane and southeastern Tibetan Plateau, is one of the ten largest rivers in the world by water and sediment discharge. When the Mekong River was established remains highly debated — with estimates that range from more than 55 to less than 5 million years ago — despite being a key constraint on the elevation history of the Tibetan Plateau. In our study published in *Nature Geoscience* (Nie *et al.* 2018) we report low-temperature thermochronology data from river bedrock samples that reveal a phase of rapid downward incision (>700 m) of the

Mekong River during the middle Miocene about 17 million years ago, long after the uplift of the central and southeastern Tibetan Plateau. However, this coincides with a period of enhanced East Asian summer monsoon precipitation over the region compared with the early Miocene. Using stream profile modelling, we demonstrate that such an increase in precipitation could have produced the observed incision in the Mekong River. In the absence of an obvious tectonic contribution, we suggest that the rapid incision of the Tibetan Plateau and the establishment of the Mekong River in the middle Miocene may be attributed to increased erosion during a period of high monsoon precipitation.

Nie J., Ruetenik G., Gallagher K., Hoke G., Garzzone C.N., Wang W., Stockli D., Hu X., Wang Z., Wang Y., Stevens T., Danišik M., Liu S. (2018). Rapid incision of the Mekong River in the middle Miocene linked to monsoonal precipitation. *Nature Geoscience*, 11(12), 944.



A comparison of Asian summer monsoon, atmospheric CO₂, Mekong River apatite (U-Th)/He age distribution and benthic oxygen isotope records between 20 and 5 Ma. Our apatite (U-Th)/He data revealed a phase of rapid incision of the Mekong River ~17 Ma, which coincides with a period of enhanced East Asian summer monsoon precipitation and is much younger than the uplift of the central and south eastern Tibetan Plateau.



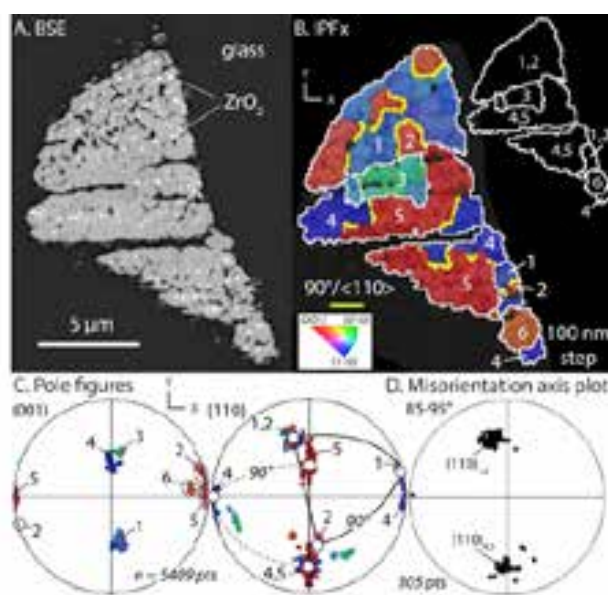


The Birth of FRIGN Zircon in 2018

TIGeR researchers at Curtin University are world-renowned for pushing the boundaries of microanalysis for accessory minerals, most notably zircon, that get shock-deformed during meteorite impact. Shocked zircon, and the rare high-pressure ZrSiO_4 polymorph reidite, provide critical information that helps to reconstruct impact conditions (pressure and temperature), and combined with U-Pb geochronology, can be used to date meteorite impact events. One of the more unusual varieties of shocked zircon are so-called granular grains, which consist of micrometer-sized neoblasts. Granular grains have long been known from impact glass and melt rocks, but the formation conditions have remained a mystery. In 2018 a series of publications by TIGeR members used electron backscatter diffraction (EBSD) to elucidate the formation mechanisms and conditions of granular zircon in impact melt. These grains first experience high-pressure

conditions, in excess of 30 GPa, at which they partially transform to reidite. However, reidite is unstable in high-temperature impact melt, and reverts back to neoblastic zircon. The transformations leave systematic orientation 'breadcrumbs' that can be detected by EBSD. Granular zircon grains were reported in Australasian tektites from Thailand (Cavosie *et al.*, 2018a), and also in melt from impact structures in Democratic Republic of the Congo (Luizi) and Nicaragua (Pantasma). Such grains that can be demonstrated to preserve crystallographic orientation evidence of high-pressure conditions are now known as 'Former Reidite In Granular Neoblastic' zircon, or FRIGN zircon (Cavosie *et al.*, 2018b).

Cavosie, A.J., Timms, N.E., Ferrière, L., and Rochette, P. (2018b). FRIGN Zircon, the Only Terrestrial High-pressure and High-temperature Mineral Diagnostic of Shock Deformation. *Geology*, 46, 891-894.



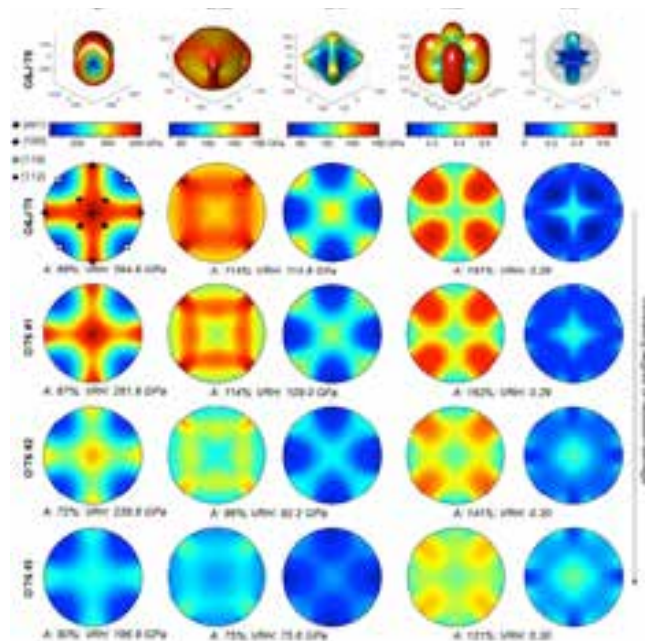
Images of a FRIGN zircon in impact glass from the Pantasma impact structure in Nicaragua. A: Backscattered electron image. B: Orientation map, showing systematic relations among zircon neoblasts. C: Pole figures, showing clusters related by $90^\circ/\langle 110 \rangle$, providing crystallographic evidence of former reidite. D: High-angle misorientation directions.

Influences of the elastic anisotropy of minerals on deformation and metamorphism

Rocks and minerals exhibit elastic behavior, which is important because it controls the transmission of acoustic waves through rocks, and precedes yield conditions for brittle and plastic deformation. All minerals have directional variations in elastic properties (elastic anisotropy) that relates to their crystallographic structure, yet are commonly assumed to be elastically isotropic in structural geology, rock mechanics, and metamorphic petrology. Recent research by Nick Timms, in collaboration with David Healy (University of Aberdeen), Mark Pearce (CSIRO), and others, focuses developing an open source toolbox of MATLAB scripts for visualization of elastic anisotropy in minerals in 2D and 3D (AnisoVis) and assessing the importance of this phenomenon in geosciences. In their landmark paper, Timms *et al.* (2018)

present visualizations of the complexity of Young’s modulus (E), shear modulus (G), and Poisson’s ratio (ν) of zircon, and their effects on zircon’s deformation mechanisms and polymorphic phase transformations in tectonic and impact settings. The research team are currently expanding their investigations to other rock-forming phases, clearly demonstrating that the directional variations of elastic properties of rocks and minerals have profound and significant consequences for their physical response to natural or imposed stresses.

Timms, N.E., Healy, D., Erickson, T.M., Nemchin, A.A., Pearce, M.A., Cavosie, A.J. (2018). The role of elastic anisotropy in the development of deformation microstructures in zircon. In: Moser, D., Corfu, F., Reddy, S., Darling, J., Tait, K. (Eds.), AGU Monograph: Microstructural Geochronology; Lattice to Atom-Scale Records of Planetary Evolution. AGU-Wiley, 183-202.



Top row: 3D visualizations of the directional variations (anisotropy) of Young’s and shear moduli and Poisson’s ratio of single crystal of zircon. The <c> axis is vertical in the diagrams, zircon’s tetragonal symmetry is evident in its elastic anisotropy. Below: Lower hemisphere stereographic projections of the elastic properties shown in the top row for zircon with different degrees of radiation damage. All elastic properties decrease with increasing radiation damage.





Argon dating of terrestrial pyroxene

Geochronological techniques such as U/Pb in zircon and baddeleyite and $^{40}\text{Ar}/^{39}\text{Ar}$ on a vast range of minerals, including sanidine, plagioclase, and biotite, provide means to date an array of different geologic processes. Many of these minerals, however, are not always present in a given rock, or can be altered by secondary processes (e.g. plagioclase in mafic rocks) limiting our ability to derive an isotopic age. Pyroxene is a primary rock forming mineral for both mafic and ultramafic rocks and is resistant to alteration process but attempts to date this phase with $^{40}\text{Ar}/^{39}\text{Ar}$ have been met with little success so far.

In this study, Ware and Jourdan (2018) analyzed pyroxene crystals from two different Large Igneous Provinces using a Multi-collector noble gas mass spectrometer (ARGUS VI) since those machines have been shown to significantly improve analytical precision compared to the previous single-collector instruments. We obtain geologically meaningful and relatively precise $^{40}\text{Ar}/^{39}\text{Ar}$ plateau ages ranging from 184.6 ± 3.9 to 182.4 ± 0.8 Ma (2σ uncertainties of $\pm 1.8\%$ to 0.4%) and 506.3 ± 3.4 Ma for Tasmanian and Kalkarindji dolerites, respectively. Those data are indistinguishable from new and/or published U-Pb and $^{40}\text{Ar}/^{39}\text{Ar}$ plagioclase ages showing that $^{40}\text{Ar}/^{39}\text{Ar}$ dating of pyroxene is a suitable geochronological tool.

Scrutinizing the analytical results of the pyroxene analyses as well as comparing them to the analytical result from plagioclase of the same samples indicates pure pyroxene was dated. Numerical models of argon diffusion in plagioclase and pyroxene support these observations. However, we found that the viability of $^{40}\text{Ar}/^{39}\text{Ar}$ dating approach of pyroxene can be affected by irradiation-induced recoil redistribution between thin pyroxene exsolution lamellae and the main pyroxene crystal, hence

requiring careful petrographic observations before analysis. Finally, diffusion modeling show that $^{40}\text{Ar}/^{39}\text{Ar}$ of pyroxene can be used as a powerful tool to date the formation age of mafic rocks affected by greenschist metamorphism and will likely play an important role in high temperature thermochronology.

Ware B., Jourdan F. (2018) $^{40}\text{Ar}/^{39}\text{Ar}$ dating of terrestrial pyroxene. *Geochim. Cosmochim. Acta* 230, 112-136.



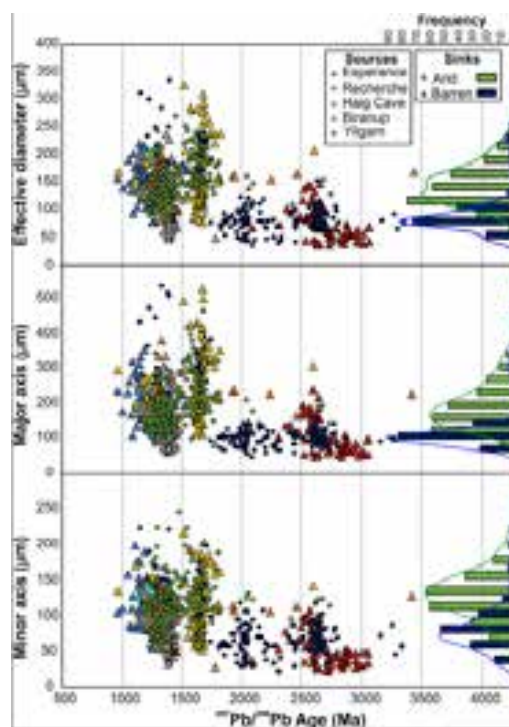
Photomicrographs of a dolerite from Ferrar Large igneous province, sampled in Tasmania: note the partial alteration of plagioclase contrasting with the freshness of pyroxene. Stringent picking of only fresh crystals of plagioclase yielded a plateau age of 181.69 ± 0.36 Ma – picking of pyroxene crystals yielded an indistinguishable age of 182.36 ± 0.75 Ma.

Using diagnostic characteristics of detrital zircon populations to inform sediment routing and basin evolution of parts of southern and northwestern Australia.

Barham *et al.* (2018) and Makulini *et al.* (2018) were focused on utilising diagnostic characteristics of detrital zircon populations to inform sediment routing, basin evolution and broader geological histories of parts of southern and northwestern Australia. Regardless of sediment age (basins studied ranged from the Mesoproterozoic to the Cretaceous), same-grain detrital zircon U-Pb geochronology integrated with Hf isotope or trace-element geochemistry were applied to enable more nuanced understanding of both surface and deeper crustal processes in their respective rift-influenced settings. Makulini *et al.* (2018) documented a novel approach to provenance analysis using zircon shape descriptors to track grain origins. Statistical tests demonstrate the power of the cheaper and faster technique in basins of the Albany-Fraser Orogen and suggest revision of the current model for sediment routing in the heavy mineral sand province of the southern margin may be necessary.

Barham, M., Reynolds, S., Kirkland, C.L., O'Leary, M.J., Evans, N.J., Allen, H., Haines, P.W., Hocking, R.M., McDonald, B.J. (2018). Sediment routing and basin evolution in Proterozoic to Mesozoic east Gondwana: a case study from southern Australia. *Gondwana Research*, 58, 122-140.

Makulini, P., Kirkland, C.L., Barham, M. (2018). Zircon grain shape holds provenance information: A case study from southwestern Australia. *Geological Journal*, 1-15.



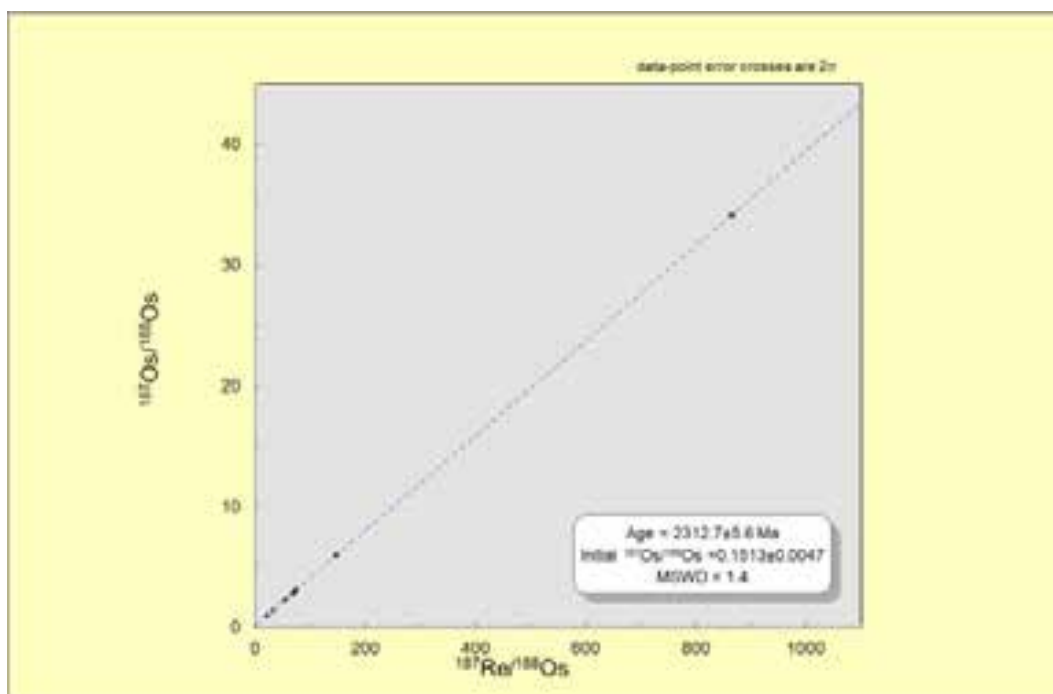
Age ($^{207}\text{Pb}/^{206}\text{Pb}$) versus specified grain shape parameter (effective diameter, major axis, and minor axis) plots for magmatic and detrital zircons of the Yilgarn Craton, Albany-Fraser Orogen, Madura Province, and Madura Shelf. Inset on right hand margin shows histograms of the shape parameter with a kernel density estimate. Source regions are indicated by triangles whereas sink regions are indicated by circles. Mu indicates median zircon grain shape for approximately 1,200 Ma Musgrave Province magmatic rocks. Mo indicates median zircon grain shape for the Moodini Supersuite of the Madura Province.

Globally asynchronous sulphur isotope signals require re-definition of the Great Oxidation Event

The Great Oxidation Event (GOE) has been defined as the time interval when sufficient atmospheric oxygen accumulated to prevent the generation and preservation of mass-independent fractionation of sulphur isotopes (MIF-S) in sedimentary rocks. Existing correlations suggest that the GOE was rapid and globally synchronous. Here we apply sulphur isotope analysis of diagenetic sulphides combined with U-Pb and Re-Os geochronology to document the sulphur cycle evolution in Western Australia spanning the GOE. Our data indicate that, from ~2.45 Gyr to beyond 2.31 Gyr, MIF-S

was preserved in sulphides punctuated by several episodes of MIF-S disappearance. These results establish the MIF-S record as asynchronous between South Africa, North America and Australia, argue for regional-scale modulation of MIF-S memory effects due to oxidative weathering after the onset of the GOE, and suggest that the current paradigm of placing the GOE at 2.33-2.32 Ga based on the last occurrence of MIF-S in South Africa should be re-evaluated.

Philippot P., Ávila J.N., Killingsworth B.A., Tessalina S., Baton F., Caquineau T., Muller E., Pecoits E., Cartigny P., Lalonde S.V., Ireland T.R., Thomazo C., Kranendonk M.J., Busigny V. (2018). Globally asynchronous sulphur isotope signals require re-definition of the Great Oxidation Event. *Nature Communications*, 9 (1).



Re-Os isochron plots for two pyrite separates and 5 bulk diamictite samples from the Meteorite Bore member (Turee Creek Formation) analysed at John de Laeter Centre using Carius tube in $\text{CrO}_3 - \text{H}_2\text{SO}_4$ digestion medium. Error bars are $\pm 2\sigma$. Regression based on Isoplot.

Response of zircon to melting and metamorphism in deep arc crust

Bhattacharya *et al.* (2018) report on zircon grains formed under magmatic/granulite facies conditions in the Cretaceous Mount Daniel Complex (MDC) in northern Fiordland, New Zealand and the criteria used to assign them to either magmatic or metamorphic origin.

Petrological assignment involved microstructure and additional parameters such as age, morphology, Th/U ratios, REE patterns and Ti-in-zircon temperature estimates. Using this integrative approach, assignment of analysed grains to metamorphic or igneous groupings improved to 98%.

A striking feature of the MDC is that only ~2% of all igneous zircon grains reflect emplacement, so that the zircon cargo was almost entirely inherited, even in dioritic magmas.

A comparison with lower- and upper-crustal, high Sr/Y metaluminous granites

elsewhere in Fiordland shows that zircon inheritance is common in the deep crust, near the source region, but generally much less so in coeval, shallow magma chambers (plutons). This is consistent with previous modelling on rapid zircon dissolution rates and high Zr saturation concentrations in metaluminous magmas. Accordingly, unless unusual circumstances exist, such as MDC preservation in the deep crust, low temperatures of magma generation, or rapid emplacement and crystallization at higher structural levels, information on zircon inheritance in upper crustal, Cordilleran plutons is lost during zircon dissolution, along with information on the age, nature and variety of the source material. The observation that dioritic magmas can form at these low temperatures (<750 °C) also suggests that the petrogenesis of mafic rocks in the arc root might need to be re-assessed.

Bhattacharya, S., Kemp, A.I.S., Collins, W.J. (2018). Response of zircon to melting and metamorphism in deep arc crust, Fiordland (New Zealand): implications for zircon inheritance in cordilleran granites. *Contributions to Mineralogy and Petrology*, 173:28



Base of a continental arc, Mt Daniel, Fiordland, New Zealand. This diatexitic migmatite formed part of a crystal-rich slurry of melt, residual minerals and restite in a magma-filled shear zone formed at ~40 km depth.

Arctic toilet with a view.





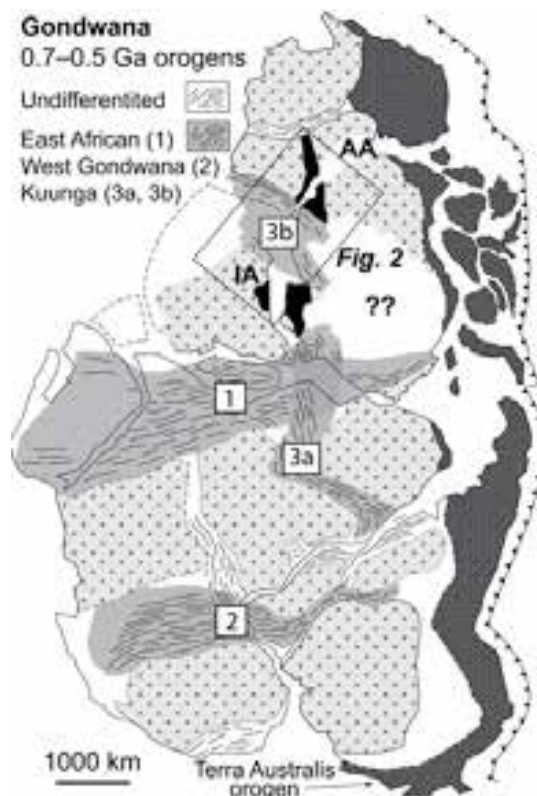
A cryptic Gondwana-forming orogen located in Antarctica

The most poorly exposed and least understood Gondwana-forming orogen lies largely hidden beneath ice in East Antarctica. Called the Kuunga orogen, its interpolation between scattered outcrops is speculative with differing and often contradictory trends proposed, and no consensus on the location of any sutures. While some discount a suture altogether, paleomagnetic data from Indo-Antarctica and Australo-Antarctica do require 3000–5000 km relative displacement during Ediacaran-Cambrian Gondwana amalgamation, suggesting that the Kuunga orogen sutured provinces of broadly Indian versus Australian affinity.

that fingerprint two coastal subglacial basement provinces between 60 and 130°E, one of Indian affinity with dominant ca. 980–900 Ma ages (Indo-Antarctica) and one of Australian affinity with dominant ca. 1190–1140 and ca. 1560 Ma ages (Australo-Antarctica). They combine this offshore compilation with existing and new onshore U-Pb geochronology and previous geophysical interpretations to delimit the Indo-Australo-Antarctic boundary at a prominent geophysical lineament which intersects the coast east of Mirny at ~94°E.

Daczko N.R., Halpin J.A., Fitzsimons I.C.W., Whittaker J.M. (2018). A cryptic Gondwana-forming orogen located in Antarctica. *Scientific Reports*, 8(1), 8371.

Daczko *et al.* (2018) use compiled data from detrital zircons offshore of East Antarctica



Cratons (>0.9 Ga; light grey-fill) and Pan-African orogens (0.7–0.5 Ga) of Gondwana modified from Fitzsimons (2016). Conjugate margin correlations of Indo-Antarctica (IA) and Australo-Antarctica (AA) are shown (black-fill).

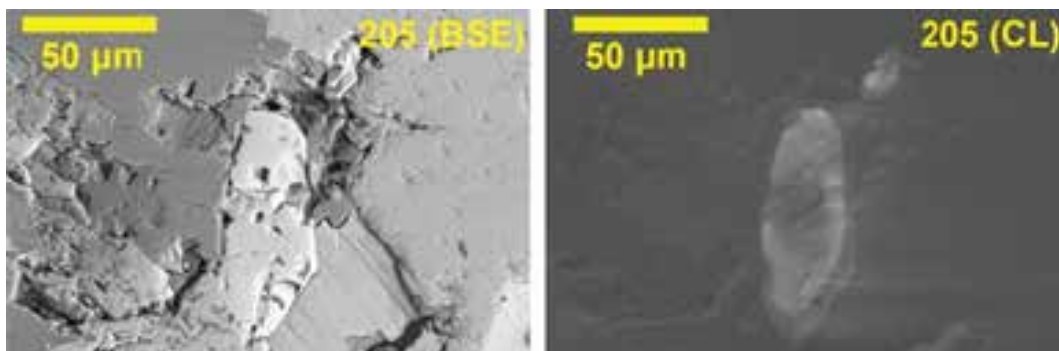
Apatite: a U-Pb thermochronometer or geochronometer?

Apatite is an accessory mineral that is frequently found in both igneous and clastic sedimentary rocks. It is conventionally considered to be characterized by a closure temperature range between 375 and 600 °C and hence has been employed to address mid-temperature thermochronology questions relevant to the reconstruction of thermal events in the middle to lower crust. However, questions remain as to whether apatite faithfully records thermally-activated volume diffusion profiles, or rather is influenced by recrystallization and new growth processes. Kirkland *et al.* (2018) present a case study of two apatite samples from the Akia Terrane in Greenland that help chart some of the post magmatic history of this region.

Apatite in a tonalitic gneiss has distinct U-enriched rims and its U-Pb apparent ages correlate with Mn chemistry, with a high Mn group yielding an age of c. 2813 Ma. The U-Pb and trace element chemistry and morphology support an interpretation in which these apatite crystals are

originally igneous and record cooling after metamorphism, with subsequent generation of discrete new rims. Epidote observed in the sample implies a <600 °C fluid infiltration event associated with apatite rims. The second sample, from a granitic leucosome, contains apparently homogeneous apatite, however U-Pb analyses define two distinct discordia arrays with different common Pb components. The chemical and age profiles do not directly correspond, implying different diffusion rates between trace elements and U and Pb. Results from these two samples show that recrystallization, dissolution and regrowth processes likely formed the younger rim overgrowths, and at temperatures below those often considered to be closure temperatures for Pb diffusion in apatite. The results from these samples imply many apatite grains may not record simple thermally activated Pb diffusion profiles and cautions against inversion of apatite U-Pb data to thermal histories without detailed knowledge of the grain growth/alteration processes.

Kirkland C., Yakymchuk C., Szilas K., Evans N.J., Hollis J. and McDonald B.J. (2018). Apatite: a U-Pb thermochronometer or geochronometer. *Lithos*, 318-319, 143-157.



Left; backscatter electron images of apatite from the Akia Terrane. Right; cathodoluminescence images of the same apatite. Note presence of clear overgrowths and embayed margin on sample 205 apatite. BSE: Backscatter-electron image, CL: Cathodoluminescence image.

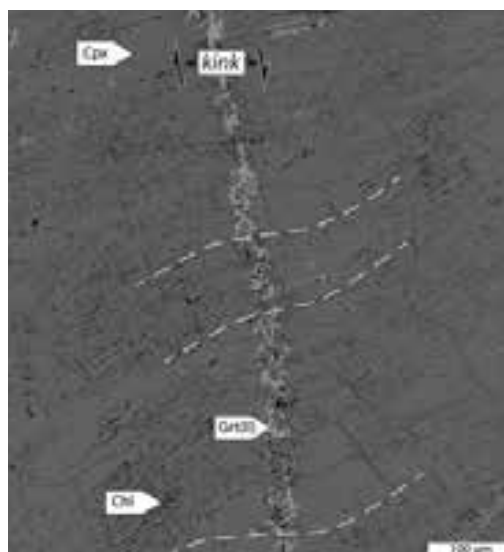
Do variations in pressure exist within a single crystal of pyroxene during hydration, deformation and retrograde metamorphism?

Centimetre-sized grains of Al-rich clinopyroxene within the granulitic anorthosites of the Bergen Arcs, W-Norway undergo deformation by faults and micro-shear zones (kinks) along which fluid has been introduced. The clinopyroxene reacts to the deformation and hydration in two different ways: reaction to garnet plus a less aluminous pyroxene along kinks and the replacement of the Al-rich clinopyroxene by chlorite along cleavage planes. These reactions only take place in the hydrated part of a hand specimen that is separated from dry, unreacted granulite by a sharp interface that defines the limit of hydration. Centrella *et al.* (2018) use electron probe microanalysis (EPMA) and X-Ray mapping together with electron backscatter diffraction (EBSD) mapping to investigate the spatial and possible temporal relationships between these two parageneses. Gresens' analysis has been used to determine the mass balance and the local volume changes associated with the two reactions.

The reaction to garnet + low-Al clinopyroxene induces a loss in volume of the solid phases whereas the chlorite formation gains volume. Strain variations result in local variation in undulose extinction in the parent clinopyroxene. EBSD results suggest that the density increasing reaction to garnet + low-Al clinopyroxene takes place where the strain is highest whereas the density-decreasing reaction to chlorite forms away from shear zones where EBSD shows no significant strain.

Arguing that the two reactions are contemporaneous at the same fluid infiltration event, Centrella *et al.* suggest on the basis of phase equilibria modelling that the thermodynamic pressure of the assemblage within the shear zones is >6 kbar higher than the pressure conditions for the whole rock for the same range of temperature (~650 °C). This result suggests that the stress redistribution within a rock may play a role in determining the reactions that take place during retrograde metamorphism.

Centrella S., Putnis A., Lanari P. and Austrheim H. Textural and chemical evolution of pyroxene during hydration and deformation: a consequence of retrograde metamorphism. *Lithos* 296-299, 245-264 (2018).



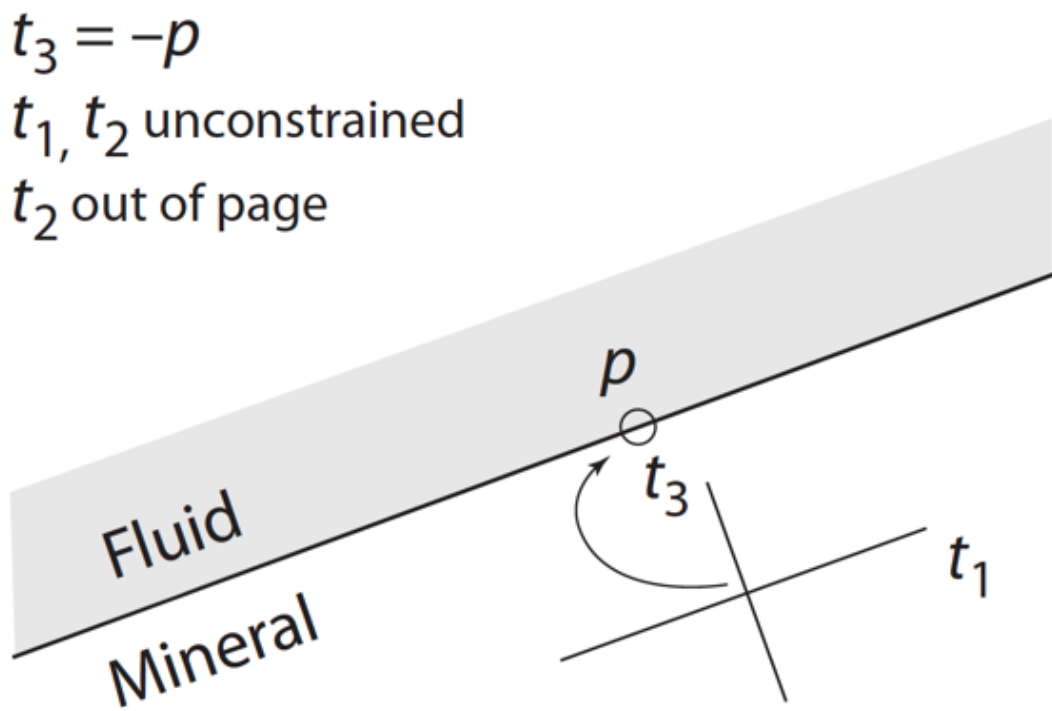
SEM BSE image of the kink containing the garnet bearing reaction with the chlorite-forming reaction within dilatational domains.

On equilibrium in non-hydrostatic metamorphic systems.

It has been proposed that rocks undergoing metamorphism are subject to non-hydrostatic stress, and that the differential stress is recorded by minerals, so that mineral zoning patterns, for example, can be used to recover the magnitude of differential stress. Evans *et al.* (2018) explore the consequences of non-hydrostatic stress for fundamental thermodynamic expressions that describe equilibrium in such a situation. Non-hydrostatic stress can occur at

equilibrium so long as there are conditions, such as the lattice constraint, that prevent processes that lead to hydrostatic stress. However, the magnitude of the effects of this non-hydrostatic stress are small, and would be hard to detect in metamorphic rocks, even when the differential stress is of the order of several kilobars.

Powell, R., Evans, K.A., Green, E.C.R., White, R.W., (2018). On equilibrium in non-hydrostatic metamorphic systems. *Journal of Metamorphic Geology* 36, 419-438.



Summarising the stress relationships at a solid–fluid grain boundary, using the cross to represent the principal axes of the stress tensor at the indicated point on the boundary, the length of the lines representing the relative magnitude of the principal stresses. The principal stress t_3 , designated to be normal to the grain boundary,





Pb-isotope composition of detrital feldspar as an indicator of sediment recycling

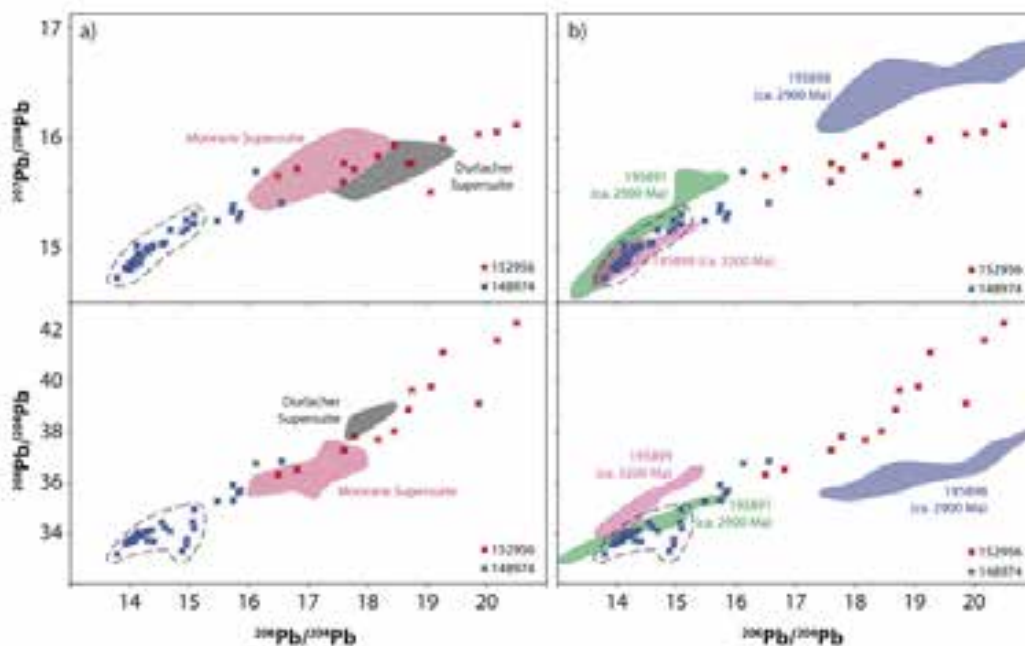
Detrital zircon U–Pb geochronology has become the gold standard in evaluating source to sink relationships in sedimentary basins. However, the physical and chemical robustness of zircon, which make it such a useful mineral for provenance studies, is also a hindrance as zircon can be recycled through numerous sedimentary basins, thus obscuring the first cycle source to sink relationship.

An elegant approach to addressing this potential issue is to compare the Pb isotope composition of detrital K-feldspar, a mineral which is unlikely to survive more than one erosion-transport-deposition cycle, with that of magmatic K-feldspar from potential basement source terranes. The Curtin node of the Centre for Exploration Targeting has partnered with the John de Laeter Centre to

develop Pb isotopes in feldspars as a powerful source characterization tool.

A case study of this new approach has been presented in Johnson *et al.*, (2018) where in situ Pb isotope data on detrital K-feldspar from two Proterozoic arkosic sandstones from Western Australia, and magmatic K-feldspar grains from potential igneous source rocks, as inferred by the age and Hf isotope composition of detrital zircon grains is evaluated. The data indicate that the detrital zircon and K-feldspar grains could not have been liberated from the same source rocks, and that the zircon has most likely been recycled through older sedimentary basins.

Johnson S. P., Kirkland C. L., Evans N. J., McDonald B. J., and Cutten H. N. (2018) The complexity of sediment recycling as revealed by common Pb isotopes in K-feldspar: *Geoscience Frontiers*, v. 9, no. 5, p. 1515-1527.



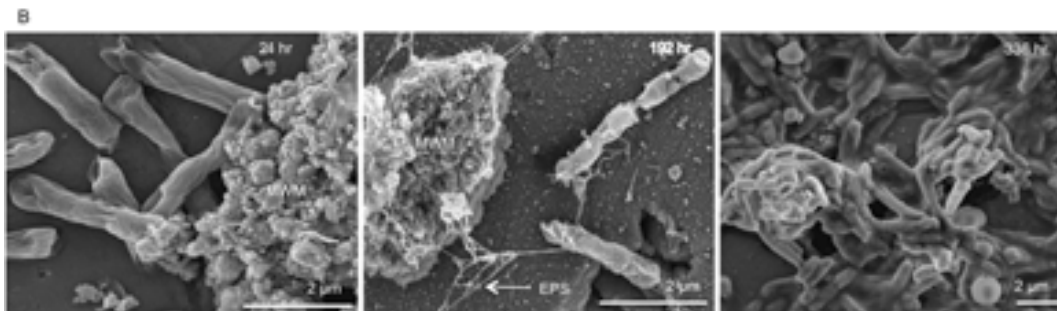
Pb isotope compositions of detrital K-feldspar in the studied samples versus the magmatic grains in the potential magmatic source rocks.

Microorganisms that leach Rare Earth Elements from Monazite

Bioleaching of monazite with phosphate solubilising bacteria (PSB) is limited by the decreasing pH challenging the viability of the PSB. Continuous bioleaching of monazite by combining heterotrophic and autotrophic acidophilic microorganisms was investigated. The co-culture of autotrophic, acidophilic *Acidithiobacillus ferrooxidans* and heterotrophic *Enterobacter aerogenes* was more effective in bioleaching rare

earth elements (REEs) from monazite than either species alone. This was likely due to a synergic interaction through the biogenic generation of both organic acids and sulfuric acid. The consortium solubilized REEs (Ce, La, Nd, Pr, and Y) up to a final concentration of 40 mg L⁻¹.

Fathollahzadeh *et al.* (2018). Better together: Potential of co-culture microorganisms to enhance bioleaching of rare earth elements from monazite. *Bioresource Technology Reports* 3 (2018) 109–118.



Scanning electron micrographs showing population changes of *Enterobacter aerogenes* over 336 h when incubated in the presence of Mount weld monazite (MWM) (EPS - extracellular polymeric substance). Corbett *et al.* (2018). *Research in Microbiology* 169; 558-568.



Greenbushes Lithium mine, Western Australia.

Research reports

ADVANCED
RESOURCE
CHARACTERI-
SATION
FACILITY

Advanced Resource Characterisation Facility



Geoscience Atom Probe.

The Advanced Resource Characterisation Facility (ARCF) is a multi-institutional facility comprising state-of-the-art analytical equipment located at Curtin, UWA and CSIRO. The facilities at Curtin include the Cameca LEAP 4000X HR atom probe microscope (Geoscience Atom Probe) and a Tescan LYRA Focused Ion Beam Scanning Electron Microscope (FIB-SEM), both housed within the John de Laeter Centre (JdLC). These laboratories have been particularly focused on the development of nanoscale analysis of geological materials, since their establishment in 2015, resulting in significant contributions to the literature on nanoscale geochemistry. In 2018, an Australian Research Council grant (LE190100053, \$1.267m) was awarded to expand the ToF-SIMS capability of the JdLC with funding received to purchase a dedicated instrument with significant improvements in sensitivity and mass resolution. This will further increase the ability to perform ground-breaking studies of geomaterials at the nanoscale.

The Geoscience Atom Probe (GAP) performed analyses on a wide range of geological samples in 2018, from extra-terrestrial plagioclase and baddeleyite to samples of pyrite ore, and nanoscale grains of goethite. Research outputs included several published works and many conference presentations.

The first demonstration of atom probe analysis for Re-Os systematics was published, using Re and Os standards and comparisons with TIMS results. The GAP laboratory also participated in an interlaboratory study of atom probe analyses of zircon using the GJ-1 reference material, which published a comparison of results from nine atom probe facilities around the world. Several studies were focussed on the mobility of trace elements in accessory mineral phases – in particular Pb and other elements in monazite and titanite. Publications from the facility also included a brief overview of progress in the field of geoscience applications of the atom probe, with speculation on future developments.

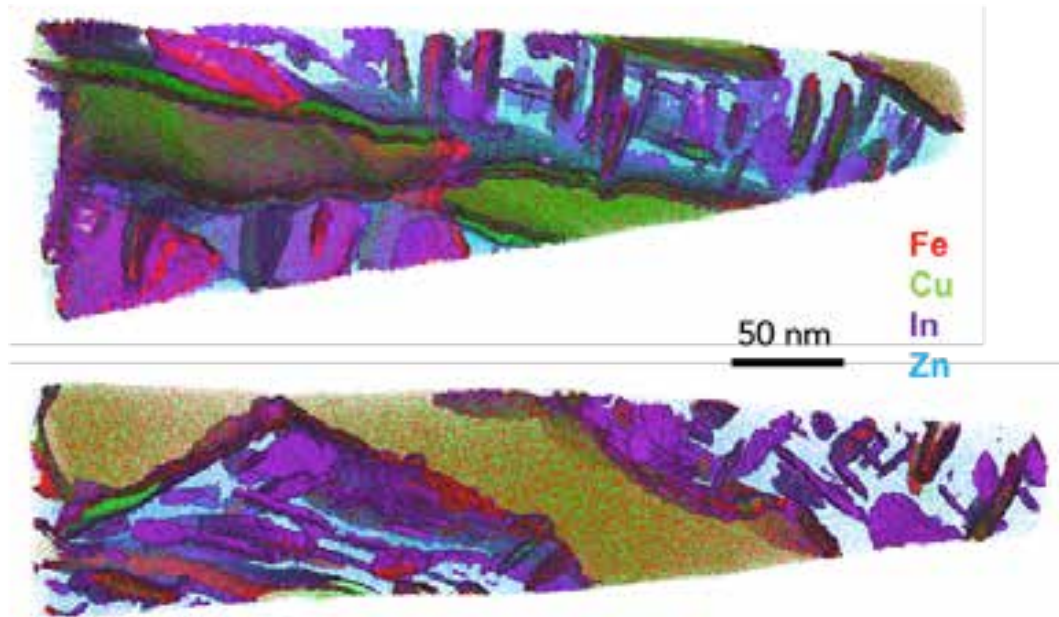


Figure 1. Atom probe analysis of indium-bearing sphalerites show complex distribution patterns of major and minor elements on a micrometer to sub-micrometer scale. Shown here are three-dimensional reconstructed atom maps, with surfaces corresponding to 7 at.% Fe (red) and 5 at.% (purple).

Atom probe analysis has been applied to several samples of an indium-bearing sulphide ore, in an example of resource-related applications from the past year. Many features in these samples cannot be resolved with the spatial resolution of conventional analytical methods, which do not indicate whether Cu, In and Fe are in solid solution in the sphalerite or form discrete phases.

Atom probe tomography combined with transmission Kikuchi diffraction was used to resolve the compositional heterogeneity and the nanostructure of these complex In-Cu-Fe-sphalerites. The obtained data indicate a complex structure with micro- to nanometre sized, plate-shaped inclusions of chalcopyrite in the sphalerite. In addition, a nanometre scale In-Cu-sulfide phase forms plate-like segregations in the sphalerite. All types of segregations have similar crystal structure and record the same crystal orientation, indicating that they likely formed by exsolution.

The results demonstrate that complex sulfides containing cations of more than one element as minor or major constituents may represent discrete, exsolved phases, rather than solid solutions. This heterogeneous nature will affect the nanoscale properties of the sphalerite, which may have implications for the economic extraction of precious elements such as indium. Furthermore, these nanoscale properties will open up new perspectives on formation processes of In-Cu-Fe-sphalerites, which may be relevant for other chemically complex minerals.



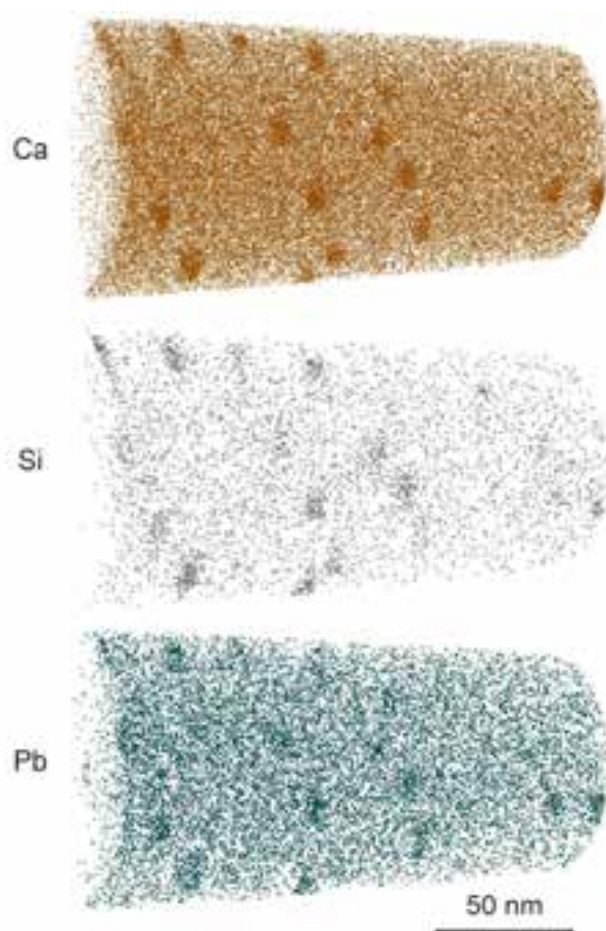


Nanoscale distribution of Pb in monazite revealed by atom probe microscopy

This study by Fougereuse *et al.* (2018) reports the first atom probe contribution of atom probe analysis of the rare Earth phosphate mineral monazite (REEPO₄). Monazite is widely used in the geosciences to date geological events and U-Th-Pb geochronology is underpinned by the assumption that monazite incorporates negligible amounts of Pb during initial growth, and that radiogenic Pb remains immobile after formation. The nanoscale investigation of monazite however revealed the presence of apatite nanoclusters enriched

in Pb. The composition of the clusters indicated that they formed soon after the crystallisation of the mineral by exsolution. The size and distribution of the clusters also indicate that they had no effects on ages acquired with other more conventional dating techniques (EPMA, SIMS and LA-ICPMS) as these methods would average enough clusters in their analytical volumes.

Fougereuse D., Reddy S.M., Saxey D.W., Erickson T.M., Kirkland C.L., Rickard W.D.A., Seydoux-Guillaume A.M., Clark C., Buick I.S. (2018). Nanoscale distribution of Pb in monazite revealed by atom probe microscopy. *Chemical Geology*, 479, 251–258.



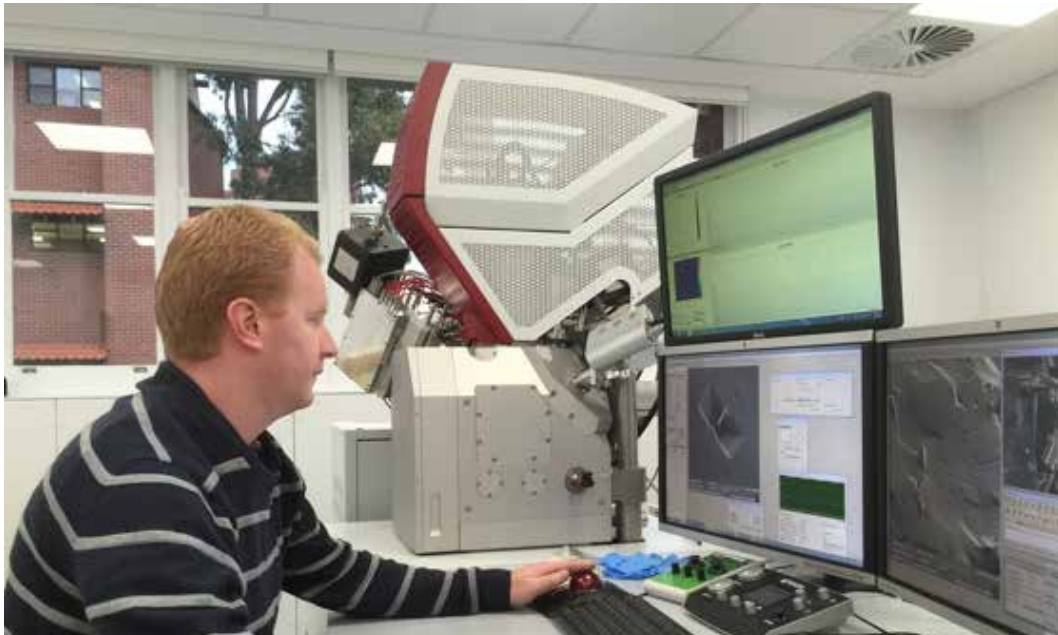
Reconstructed three-dimensional atom probe image of Ca, Si and Pb (²⁰⁶Pb+²⁰⁸Pb) distribution. Each sphere represents one atom. The maps show the presence of Ca-Si-Pb clusters.

Tescan Lyra FIB-SEM with ToF-SIMS

The Tescan Lyra FIB-SEM facility supports research involving the Geoscience Atom Probe and the Transmission Electron Microscope as well as being used for high spatial resolution Time of Flight Secondary Ion Mass Spectrometry (ToF-SIMS). The Lyra is central to a number of analysis workflows and thus was involved in broad range of projects in 2018. Data from the instrument was used in 12 journal articles and a number of conference presentations/papers that

were published in 2018. Research highlights include high spatial resolution mapping of the lithium distribution in spodumene and micaceous ores; and the discovery of graphitisation and other structural changes in thermally mature shales (figure 2).

Delle Piane C., Raven M.D., Bourdet J., Clennell M.B., Rickard W.D.A., Saunders M., Sherwood N., Li Z., Dewhurst D.N. (2018). Organic matter network in post-mature Marcellus Shale: Effects on petrophysical properties. *AAPG Bulletin*, 102, 2305-2332.



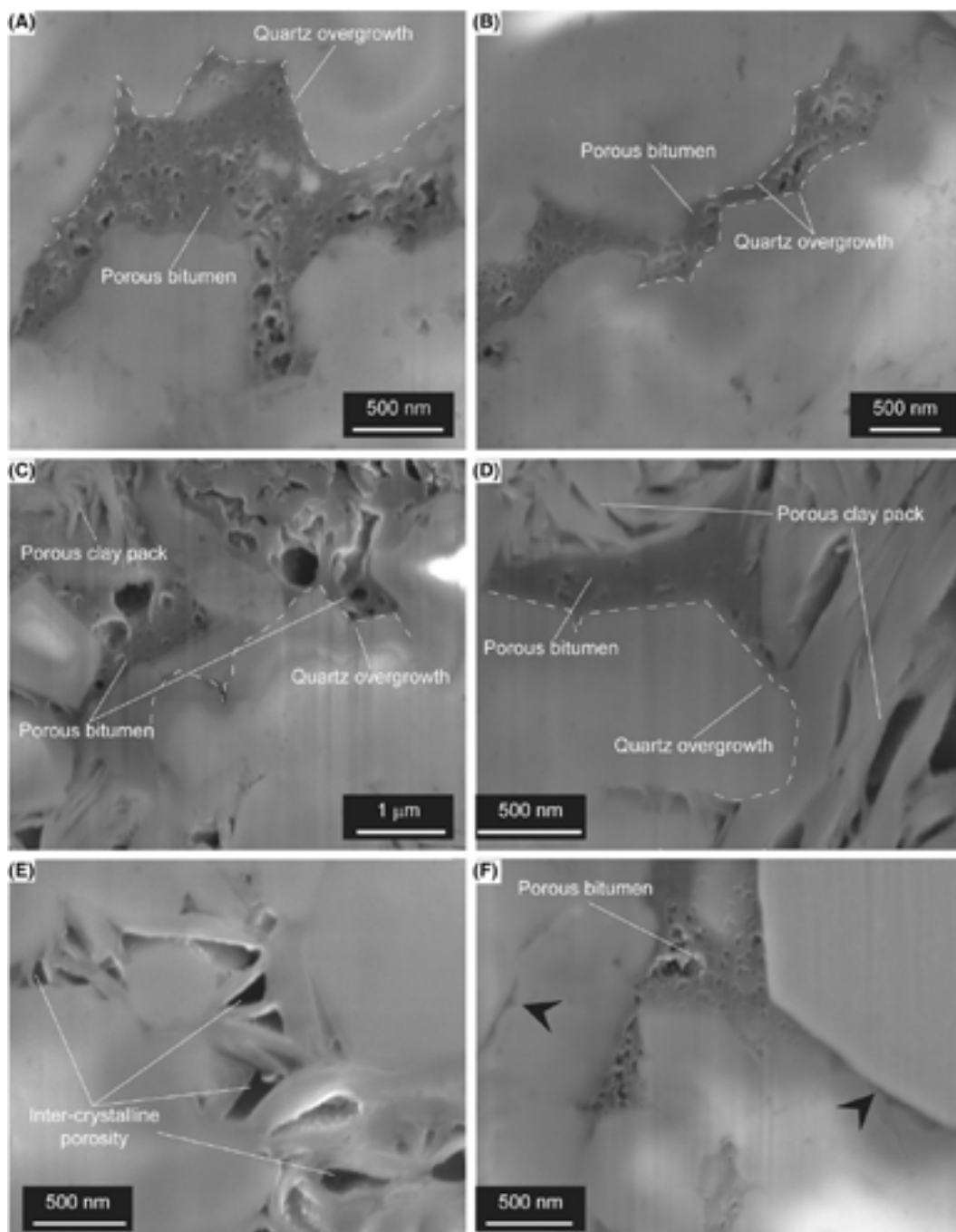


Figure 2. FIB-SEM images showing occurrence of porosity in a Marcellus Shale (USS). (A, B) Organic porosity juxtaposed to quartz overgrowths. (C, D) Examples of coexistence of organic-hosted and clay-hosted pores; note the juxtaposition between organic matter and quartz overgrowth. (E) Inter-crystalline porosity between clays and nanograins of quartz. (F) Interstitial porous pyrobitumen and organic lining coating mineral grain boundaries (indicated by the black arrows).

Research reports

ORGANIC AND ISOTOPE GEOCHEMISTRY

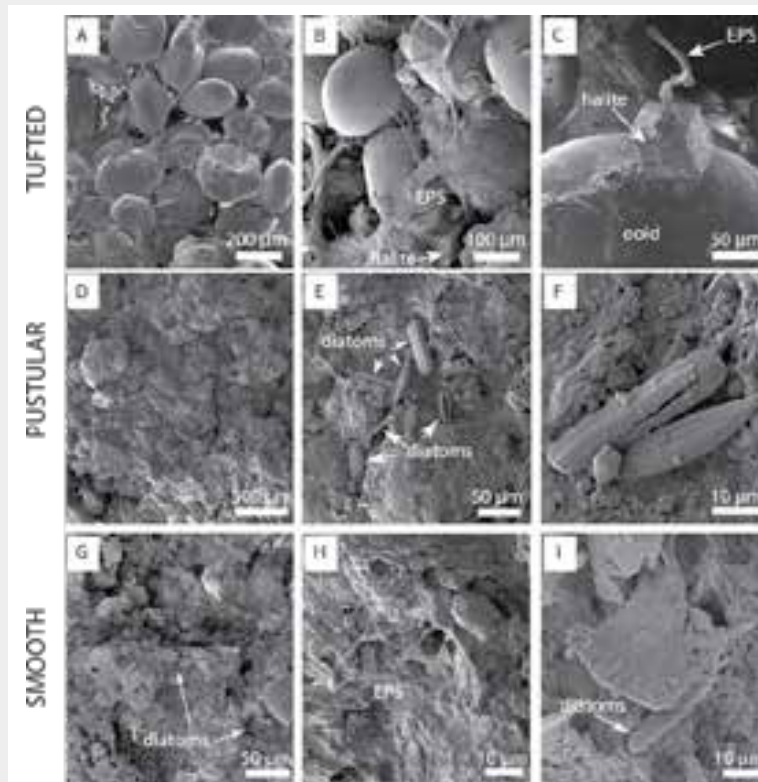
Organic and Isotope Geochemistry

Using lipid biomarkers, stable carbon isotopes and micofabrics to characterise Shark Bay biomats

The microbial mats of Shark Bay are commonly thought to be living analogues of Precambrian mats. Three types of microbial mats from Hamelin Pool (Shark Bay, Western Australia) were subject to multi-proxy characterisation including biolipids, stable isotopes and imaging techniques. The three mat types (tufted, pustular and smooth) exist in the shallowest section of a tidal flat gradient, and all are composed of complex microbial communities. The complimentary analytical techniques used in this study allowed for detailed characterisation of mat communities, including cyanobacteria, sulfate reducers, diatoms and ciliates.

Eukaryotic input was detected in all three mat types, including aquatic macrophytes suggesting a contribution from the seagrass meadows that separate Hamelin Pool from the ocean. This study shows the benefits of a multi-proxy analytical approach in characterising such complex microbial ecosystems, which could also be applied to studies investigating the earliest life on Earth.

Plet, C., Pagès A., Holman A.I., Madden R.H.C., Grice K. (2018). From supratidal to subtidal, an integrated characterisation of Carbla Beach shallow microbial mats (Hamelin Pool, Shark Bay, WA): Lipid biomarkers, stable carbon isotopes and microfibrils. *Chemical Geology*, 493, 338-352.



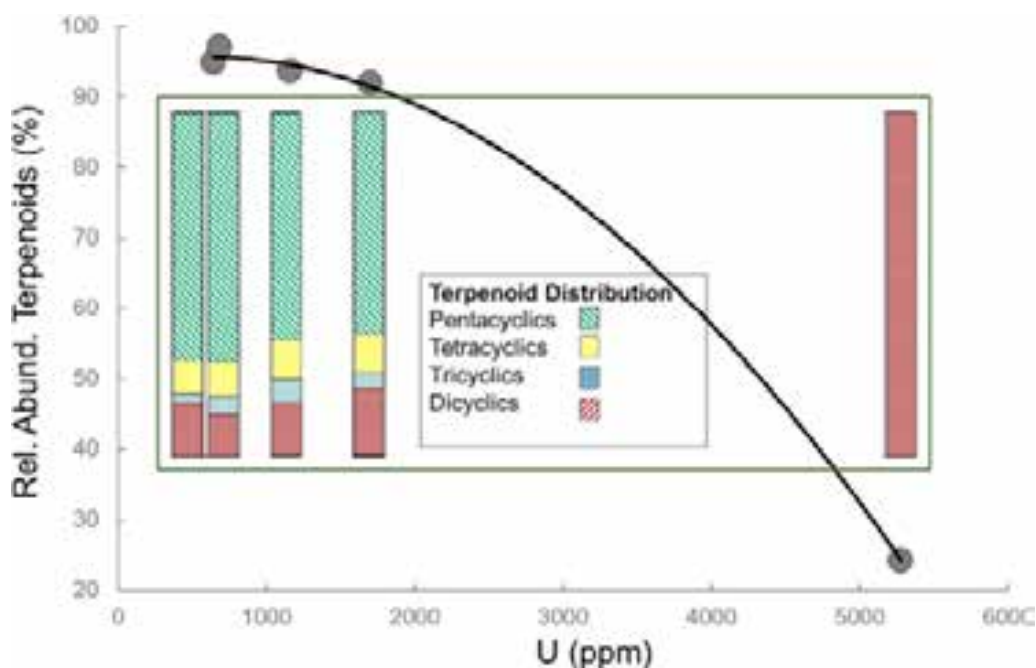
Scanning electron microscopy images from the three studied mat types, showing ooids and halite crystals in the tufted mat, abundant diatoms in the pustular mat, and predominantly EPS (exo-polymeric substances) in the smooth mat.

Aromatic hydrocarbons in sedimentary organic matter from the Mulga Rock (Australia) uranium deposit

Sedimentary organic matter has long been known to be associated with major U deposits, but the effects of ionizing radiation on organic matter have historically been underexplored. Samples from the Mulga Rock U deposit (Western Australia) were taken along a gradient of 173–5280 ppm U. The aromatic fraction of extractable organic matter showed an increase in aromatisation with increasing U

concentration, with plant-derived terpenoids being transformed into smaller aromatic molecules by dehydrogenation and bond cleavage reactions. A small ^{13}C -enrichment in the aromatised products was observed, attributed to preferential cleavage of ^{12}C -H bonds.

Greenwood P.F., Shan C., Holman A.I., Grice K. (2018). The composition and radiolysis impact on aromatic hydrocarbons in sedimentary organic matter from the Mulga Rock (Australia) uranium deposit. *Organic Geochemistry*, 123, 103-112.



A decrease in relative abundance of plant-derived terpenoids with increasing U. Also observed is a change in structure from mostly pentacyclic compounds at low U amounts, to 100% dicyclic compounds at the highest U concentration.

$\delta^{13}\text{C}$ of aromatic compounds in sediments, oils and atmospheric emissions: A review.

The $\delta^{13}\text{C}$ measurement of oils and sedimentary organic matter has become routine over the past ~ 40 years. These measurements have historically been done primarily on the saturated fraction of organic matter, but an increasing number of studies have demonstrated the utility of $\delta^{13}\text{C}$ measurements of aromatic compounds. This review by Holman and Grice (2018) summarises the range of applications of aromatic $\delta^{13}\text{C}$, from the early uses of bulk $\delta^{13}\text{C}$ for oil classification, to more recent compound-specific measurements for source differentiation and palaeo-environmental reconstruction. The ongoing development of position-specific isotope measurements which have the potential to provide valuable information on the formation of aromatic compounds during diagenesis are also discussed.

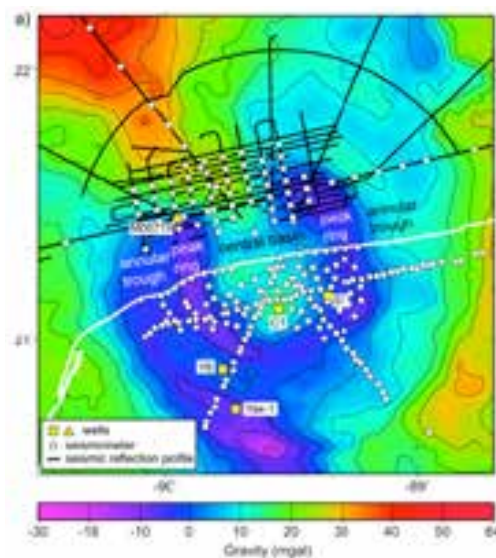
Holman A.I., Grice K. (2018). $\delta^{13}\text{C}$ of aromatic compounds in sediments, oils and atmospheric emissions: A review. *Organic Geochemistry*, 123, 27-37.

Extraordinary rocks from the peak ring of the Chicxulub impact crater

The peak ring of the Chicxulub impact crater was drilled in April of 2016 through the joint International Ocean Discovery Program (IODP) and International Continental Scientific Drilling Program (ICDP) Expedition 364. P-wave velocity, density, and porosity measurements from Hole M0077A revealed unusual physical properties of the peak-ring rocks. A sharp decrease in velocity and density, and an increase in porosity was measured across the boundary between post-impact sedimentary rock and suevite (impact melt-bearing breccia). The low velocity, low density, and high porosity of suevite and impact melt rock imply rapid emplacement, hydrothermal alteration

products, and the presence of pore space, vugs, and vesicles. Unaltered granite has higher velocity and density and lower porosity than what was measured in the uplifted granitic peak ring materials indicative of considerable rock damage. Our results were integrated with previous seismic datasets to map the suevite near the borehole. Suevite thickness is 100–165 m on the top of the peak ring but 200 m in the central basin, suggesting that suevite flowed downslope from the collapsing central uplift during and after peak-ring formation, accumulating preferentially within the central basin.

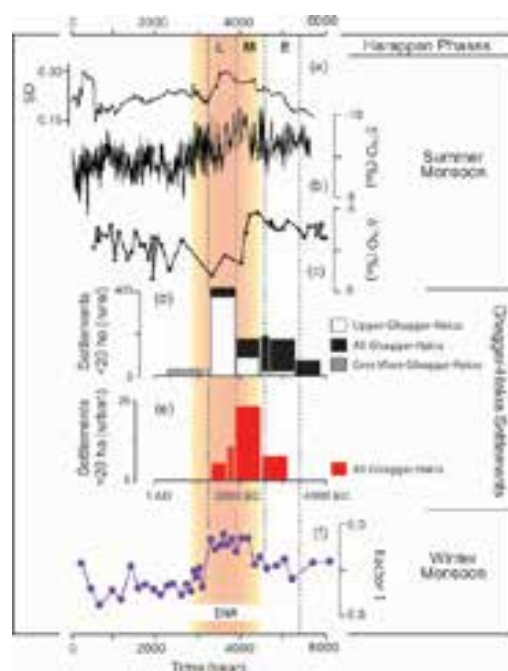
Christeson, G. L., S. P. S. Gulick, J. V. Morgan, C. Gebhardt, D. A. Kring, E. Le Ber, J. Lofi, C. Nixon, M. Poelchau, A. S. P. Rae, M. Rebolledo-Vieyra, U. Riller, D. R. Schmitt, A. Wittmann, T. J. Bralower, E. Chenot, P. Claeys, C. S. Cockell, M. J. L. Coolen, L. Ferrière, S. Green, K. Goto, H. Jones, C. M. Lowery, C. Mellett, R. Ocampo-Torres, L. Perez-Cruz, A. E. Pickersgill, C. Rasmussen, H. Sato, J. Smit, S. M. Tikoo, N. Tomioka, J. Urrutia-Fucugauchi, M. T. Whalen, L. Xiao and K. E. Yamaguchi (2018). Extraordinary rocks from the peak ring of the Chicxulub impact crater: P-wave velocity, density, and porosity measurements from IODP/ICDP Expedition 364. *Earth and Planetary Science Letters* 495: 1-11.



Bouguer gravity anomaly map (gravity data courtesy of A. Hildebrand and M. Pilkington) over the Chicxulub impact crater. The coastline is displayed with the white line.

Neoglacial climate anomalies and the Harappan metamorphosis

Climate has impacted growth and decline of past human societies, but our knowledge of temporal and spatial climatic patterns is generally restricted to address causal connections. At a global scale, the inter-hemispheric thermal balance provides a framework for understanding regional Holocene climate variability. As the thermal balance adjusted to gradual changes in the seasonality of insolation, the Inter-Tropical Convergence Zone migrated southward accompanied by a weakening of the Indian summer monsoon. Superimposed on this trend, anomalies such as the Little Ice Age point to asymmetric changes in the non-tropical latitudes of both hemispheres. In this study, Giosan *et al.* (2018) reconstructed the Indian winter monsoon in the Arabian Sea for the last 6000 years based on paleobiological records in sediments from the continental margin of Pakistan: sedimentary ancient DNA stratigraphy revealed a comprehensive overview of plankton responses to past water column environmental conditions and microscopic analysis revealed fossil planktonic foraminifers sensitive to winter conditions. The data show the presence of strong winter monsoons between ~4,500 and 3,000 years ago during a period characterized by a series of weak interhemispheric temperature contrast intervals. They infer this period as the Early Neoglacial Anomaly (ENA). The strong winter monsoons during ENA were accompanied by changes in wind and precipitation patterns that are particularly evident across the eastern Northern Hemisphere and Tropics. This coordinated climate reorganization may have helped trigger the metamorphosis of the urban Harappan civilization into a rural society through a push-pull migration from summer flood-deficient river valleys to the Himalayan piedmont plains with augmented winter rains.



Monsoon hydroclimate changes since the middle Holocene and changes in settlement distribution on the Ghaggar-Hakra interfluvium. (a) variability in summer monsoon calculated as 200-year window moving standard deviation of the detrended monsoon record of Katahayat *et al.* (2017) and (b) the speleothem $\delta^{18}\text{O}$ -based summer monsoon reconstruction of Katahayat *et al.* (2017); (c) lacustrine gastropod $\delta^{18}\text{O}$ -based summer monsoon reconstruction (Dixit *et al.*, 2014); (d and e) changes in the number of settlements on the Ghaggar-Hakra interfluvium as a function of size and location; and (f) winter monsoon paleo-DNA-based reconstruction for the NE Arabian Sea (this study – in purple). The period corresponding to the Early Neoglacial Anomalies (ENA) is shaded in red hues and durations for Early (E), Mature (M) and Late (L) Harappan phases are shown with dashed lines.

Giosan, L., W. D. Orsi, M.J.L. Coolen, C. Wuchter, A. G. Dunlea, K. Thirumalai, S. E. Munoz, P. D. Clift, J. P. Donnelly, V. Galy and D. Q. Fuller (2018). Neoglacial climate anomalies and the Harappan metamorphosis. *Climate of the Past* 14: 1669-1686.



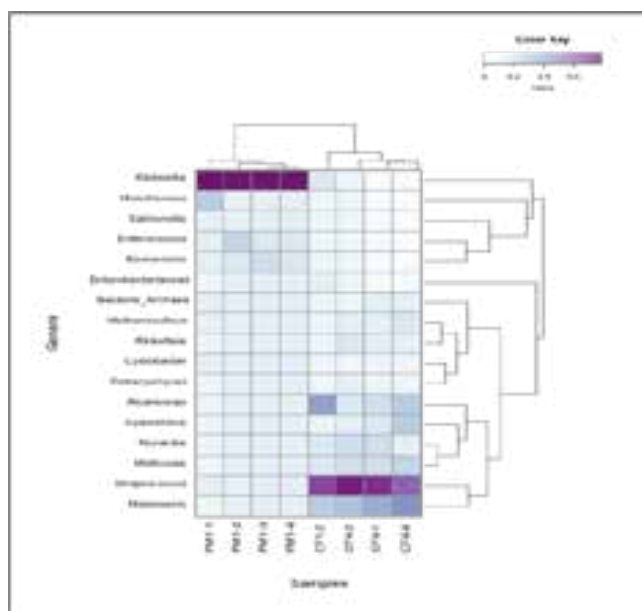


Gallstones: The putative role of bacteria

Bacteria are thought to play a role in the pathogenesis and formation of pigmented gallstones from humans. Prior studies mainly involved cultivation of gallstone-associated bacteria and/or the identification of the presence of bacteria through taxonomic 16S rRNA profiling. Only a small percentage of bacteria in environmental samples can be cultivated and 16S profiling only provides information about who is there without a direct link between processes involved in gallstone formation by the bacteria present. Here, we provide functional metagenomic evidence of a range of genes involved in bile stress response, biofilm formation, and anaerobic energy metabolism by Gram-negative *Klebsiella* in pigmented gallstones from a 76-year-old male patient. *Klebsiella* was also present in one cholesterol type stone in a 30-year-old female patient who had additional

cholesterol gallstones characterized by Gram-positive bacteria. Pigmented stones further revealed a predominance of genes involved in carbohydrate metabolism, whilst cholesterol stones indicated a profile dominated by protein metabolism possibly reflecting known chemical differences between Gram-negative and Gram-positive biofilm matrices. Complementary carbon and hydrogen isotopic analyses of cholesterol within the patients' stones revealed homogeneity, suggesting a common diet or cholesterol biosynthesis pathway that has little influence on microbial composition. This pilot study provided a framework to study microbial processes that play a potential role in gallstone formation across markedly different types of stones and patient backgrounds.

Kose, S. H., K. Grice, W. D. Orsi, M. Ballal and M. J. L. Coolen (2018). "Metagenomics of pigmented and cholesterol gallstones: the putative role of bacteria." *Scientific Reports* 8.



Heatmap with the major bacterial genera identified in the gallstones (n = 4) of patients PM1 (pigmented) and CF4 (cholesterol). The color key shows the relative abundance of the genera in the gallstones. The dendrograms illustrate the relationship between samples showing that the distribution of genera is relatively similar between replicate stones, but greatly differ between the two patients.

Coccolithovirus facilitation of carbon export in the North Atlantic

Marine phytoplankton account for ~50% of global primary productivity. Viruses are thought to recycle more than 25% of oceanic photosynthetically fixed organic carbon, which can stimulate nutrient regeneration, primary production and upper ocean respiration via lytic infection and the 'virus shunt'. Ultimately, this limits the trophic transfer of carbon and energy to both higher food webs and the deep ocean. Using the Moderate Resolution Imaging Spectroradiometer (MODIS) onboard the Aqua satellite, along with a suite of diagnostic lipid- and genetic biomarkers, as well as in situ optical sensors and sediment traps, this study showed that *Coccolithovirus* infections of mesoscale (~100 km) *Emiliania huxleyi* blooms in the North Atlantic are coupled with particle aggregation, high zooplankton grazing and greater downward vertical fluxes of both particulate organic and particulate inorganic carbon from the upper mixed layer. We captured blooms in different phases of infection (early, late and post) and revealed the highest export flux in 'early-infected blooms' with sinking particles being disproportionately enriched with infected cells and subsequently remineralized at depth in the mesopelagic. Our findings reveal viral infection as a previously unrecognized ecosystem process enhancing biological pump efficiency.

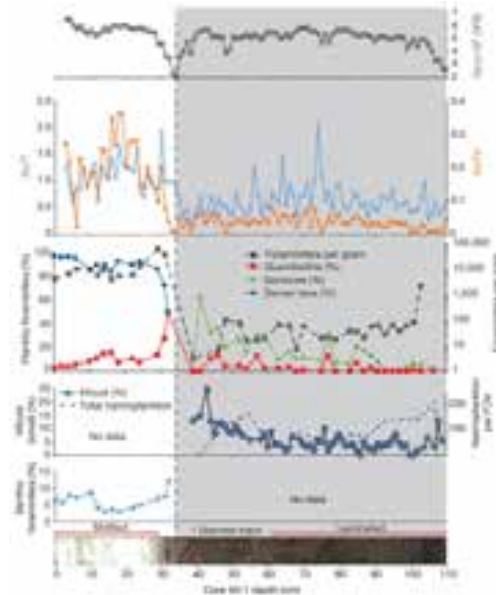
Laber, C. P., J. E. Hunter, F. Carvalho, J. R. Collins, E. J. Hunter, B. M. Schieler, E. Boss, K. More, M. Frada, K. Thamatrakoln, C. M. Brown, L. Haramaty, J. Ossolinski, H. Fredricks, J. I. Nissimov, R. Vandzura, U. Sheyn, Y. Lehahn, R. J. Chant, A. M. Martins, M. J. L. Coolen, A. Vardi, G. R. DiTullio, B. A. S. Van Mooy and K. D. Bidle (2018). Coccolithovirus facilitation of carbon export in the North Atlantic. *Nature Microbiology* 3: 537-547.

Rapid recovery of life at ground zero of the end-Cretaceous mass extinction

The impact of an asteroid on the Yucatán carbonate platform in the southern Gulf of Mexico 66 million years ago, forming the Chicxulub impact crater, caused the Cretaceous/Palaeogene mass extinction (K/Pg) which whipped out 76% of species on Earth including all non-avian dinosaurs. Previous studies from K/Pg deposits suggest that the global marine ecosystem, measured as primary productivity, was geographically heterogeneous, and took 300 kyr to return to levels prevailing during the Late Cretaceous. If there is a relationship between the distance from the impact and the recovery of marine productivity, we would expect recovery rates to be slowest in the crater itself. This would imply an impact-related environmental control, such as toxic metal poisoning, on the rate of recovery and could help to predict future patterns of recovery in anthropogenically perturbed ecosystems. This paper provides a record of foraminifera, calcareous nannoplankton, trace fossils and elemental abundance data from within the Chicxulub crater, dated to approximately the first 200 kyr of the Palaeocene. Our results imply that life reappeared in the basin just years after the impact and a high-productivity ecosystem was established within 30 kyr, which indicates that proximity to the impact did not delay recovery and that there was no impact-related environmental control on recovery.

Ecological processes probably controlled the recovery of productivity after the K/Pg mass extinction and are therefore likely to be important for the response of the ocean ecosystem to other rapid extinction events.

Lowery, C. M., T. J. Bralower, J. D. Owens, F. J. Rodriguez-Tovar, H. Jones, J. Smit, M. T. Whalen, P. Claeys, K. Farley, S. P. S. Gulick, J. V. Morgan, S. Green, E. Chenot, G. L. Christeson, C. S. Cockell, M. J. L. Coolen, L. Ferriere, C. Gebhardt, K. Goto, D. A. Kring, J. Lofi, R. Ocampo-Torres, L. Perez-Cruz, A. E. Pickersgill, M. H. Poelchau, A. S. P. Rae, C. Rasmussen, M. Rebolledo-Vieyra, U. Riller, H. Sato, S. M. Tikoo, N. Tomioka, J. Urrutia-Fucugauchi, J. Vellekoop, A. Wittmann, L. Xiao, K. E. Yamaguchi and W. Zylberman (2018). Rapid recovery of life at ground zero of the end-Cretaceous mass extinction. *Nature* 558:288-291.



The shaded area is the transitional unit and the dashed line represents the contact with the overlying pelagic limestone. Top to bottom: X-ray fluorescence-derived calcium abundance in counts per second (CPS); Ba/Ti and Ba/Fe ratios; percentage abundances of key planktic foraminiferal groups, including percentage of *Guembelitria*, percentage of survivors (that is, Cretaceous species known to survive the impact) and percentage of Danian taxa (that is, species that evolved after the impact) as a percentage of total foraminifera; foraminifera per gram of sediment, plotted on a logarithmic scale; percentage of *Micula* smaller than 2 μm (against total nannoplankton) and nannoplankton abundance (total occurrences per field of view (FOV)); percentage of benthic foraminifera (against total foraminifera); and core image of 364-M0077A-40R-1 0–110 cm (616.58–617.33 m below seafloor), with discrete trace fossils highlighted by arrows

A 43 kyr record of protist communities and their response to oxygen minimum zone variability in the Northeastern Arabian Sea

An extensive oxygen minimum zone (OMZ) occurs in the northeastern (NE) Arabian Sea where sedimentary records show evidence of alternating strong vs. weak OMZs that correlate with North Atlantic climate variability during the last glacial-interglacial cycle. OMZs are thought to be expanding world-wide in coastal areas due to anthropogenic activities leading to enhanced stratification (eutrophication and global warming). Information on long-term OMZ-ecosystem interactions is mainly limited to fossilized species, notably foraminifera. In this study, we provide a first comprehensive ancient sediment DNA (*sed aDNA*) record of (non)fossilizing unicellular eukaryotes (protists) and their response to OMZ variability in the NE Arabian Sea over the last 43 ka. Protist communities changed significantly during strong vs. weak OMZ conditions coincident with interstadials and stadials respectively. Dinoflagellates were identified as significant indicator taxa for strong OMZs during glacial as well as interglacial interstadials, whereas diatoms were significant indicators for strong OMZs only during glacial interstadials. The green alga *Chlorella* was found to be the main photosynthetic protist in nutrient-depleted surface waters during glacial stadials. Notably, strong OMZ conditions shaped past protist communities by creating isolated habitats for those capable of sustaining oxygen depletion either by adapting a parasitic life cycle (e.g. apicomplexans) or by establishing mutualistic connections with others (e.g. radiolarians and mixotrophic dinoflagellates) or by forming cysts (e.g. colpodeans). Notably, a long-term increase in eutrophication and a decrease in the diatom/dinoflagellate ratio was observed during the late Holocene favouring the pelagic component of the marine food web. A similar

scenario could be expected in the context of predicted worldwide expansion of coastal OMZs associated with global climate change.

More, K. D., W. D. Orsi, V. Galy, L. Giosan, L. J. He, K. Grice and M. J. L. Coolen (2018). A 43 kyr record of protist communities and their response to oxygen minimum zone variability in the Northeastern Arabian Sea. *Earth and Planetary Science Letters* 496: 248-256.



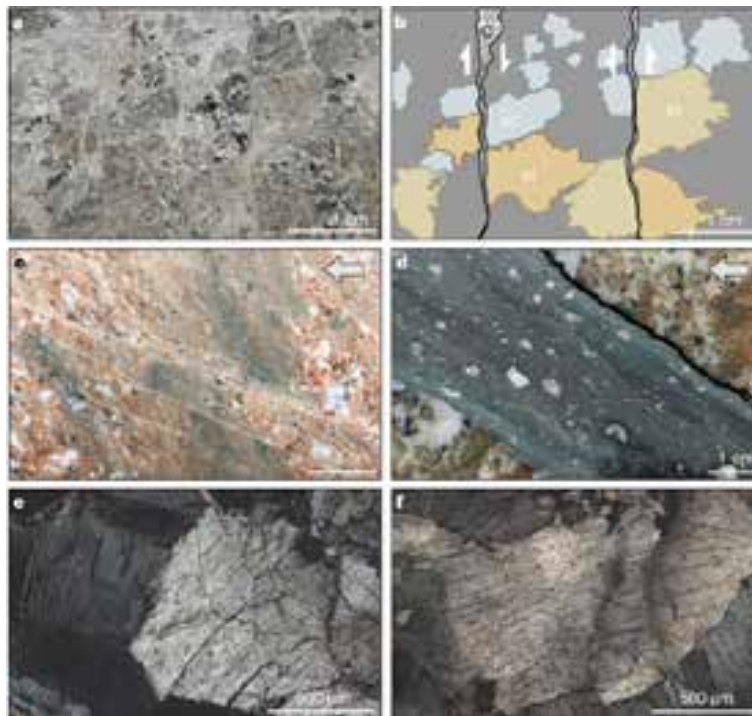


Rock fluidization during peak-ring formation of large impact structures

Meteorite impact structures that are several hundreds of kilometers in diameter contain topographic rings rising above flat crater floors that formed from uplifted rocks within minutes of impact. In order to flow rapidly over large distances, target rocks need to weaken drastically, but subsequently have to regain sufficient strength to build and sustain topographic rings. The mechanisms of rock deformation accomplishing such extreme change in mechanical behavior during cratering are largely unknown and heavily debated. Recent drilling of the ~200 km diameter Chicxulub crater, México, unveiled an unprecedented record of brittle and viscous deformation mechanisms within peak ring rocks. This study shows how this deformation evolved during cratering, and demonstrates that initial catastrophic rock weakening is followed by a gradual increase

in rock strength that culminated in peak-ring formation. The observations point to quasi-continuous rock flow and, thus, acoustic fluidization as the dominant physical process controlling initial cratering followed by increasingly localized faulting.

Riller, U., M. H. Poelchau, A. S. P. Rae, F. M. Schulte, G. S. Collins, H. J. Melosh, R. A. F. Grieve, J. V. Morgan, S. P. S. Gulick, J. Lofi, A. Diaw, N. McCall, D. A. Kring, J. V. Morgan, S. P. S. Gulick, S. L. Green, J. Lofi, E. Chenot, G. L. Christeson, P. Claeys, C. S. Cockell, M. J. L. Coolen, L. Ferriere, C. Gebhardt, K. Goto, H. Jones, D. A. Kring, L. Xiao, C. M. Lowery, R. Ocampo-Torres, L. Perez-Cruz, A. E. Pickersgill, M. H. Poelchau, A. S. P. Rae, C. Rasmussen, M. Rebolledo-Vieyra, U. Riller, H. Sato, J. Smit, S. M. Tikoo-Schantz, N. Tomioka, M. T. Whalen, A. Wittmann, K. E. Yamaguchi, J. U. Fucugauchi, T. J. Bralower and I.-I. D. E. S. Part (2018). Rock fluidization during peak-ring formation of large impact structures. *Nature* 562: 511-518.



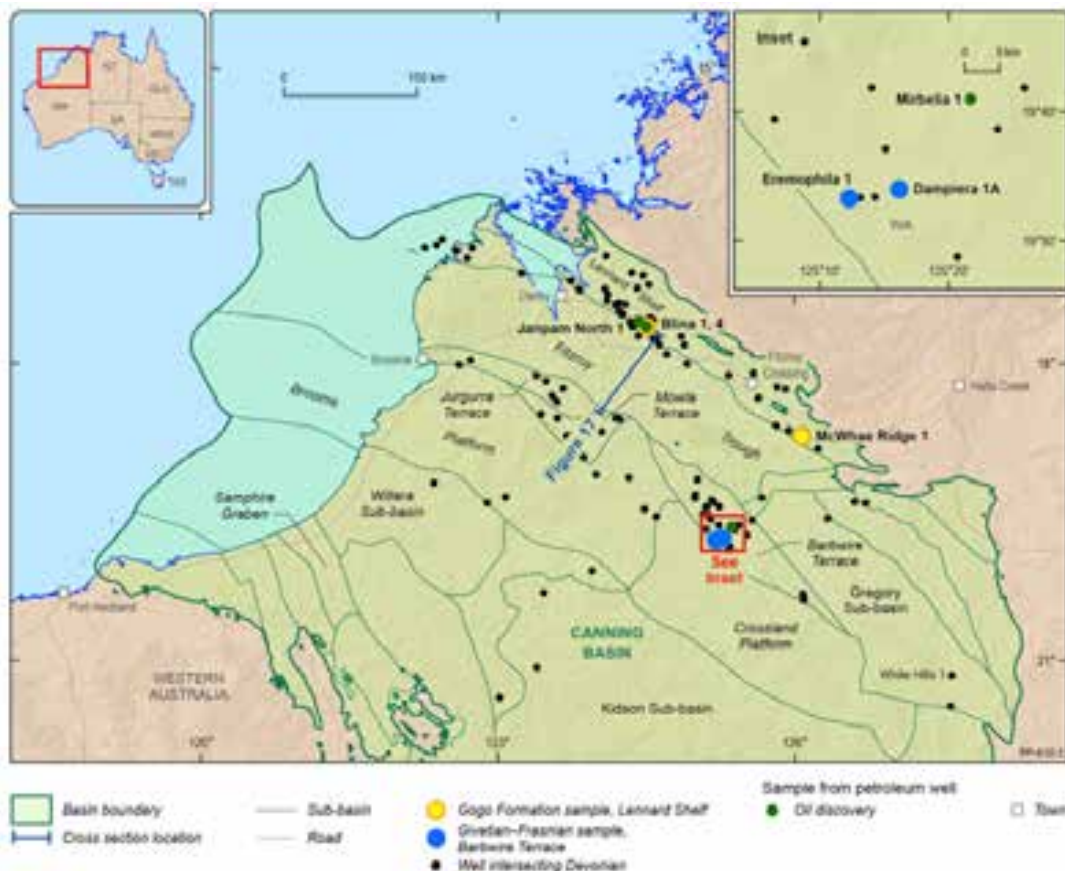
Deformation structures at the impact site. Cataclasites and planar deformation features.

Extent and persistence of photic zone euxinia in Middle-Late Devonian seas

During the Late Devonian, the Canning Basin (Western Australia) was characterised by an inland sea. Photic Zone Euxinia (PZE) prevailed during this time and this study reports geochemical evidence for PZE on the northern (Lennard Shelf), and southern (Barbwire Terrace) margins of the Fitzroy Trough. On the Lennard Shelf, shales record episodic pulses of PZE associated with high algal activity due to enhanced nutrient supply, whereas a restricted marine setting on the Barbwire Terrace is thought to be the main driver for the development of

persistent PZE and associated bacterial predominance. These insights are combined with oil geochemistry to pinpoint the source of the Mirbelia-1 oil. Results show some genetic affinity between the Mirbelia-1 oil and the Givetian–Frasnian rock extracts from the Barbwire Terrace, suggesting that local source rocks are developed in the region.

Spaak, G., D. S. Edwards, H. J. Allen, H. Grotheer, R. E. Summons, M. J. L. Coolen and K. Grice (2018). Extent and persistence of photic zone euxinia in Middle-Late Devonian seas - Insights from the Canning Basin and implications for petroleum source rock formation. *Marine and Petroleum Geology* 93: 33-56.



Location of wells that intersect Devonian strata in the Canning Basin. Wells from which oil and rock samples were analysed in this study are labelled.

How our ability to identify individual compounds can help us understand the mechanism of biodegradation of petroleum hydrocarbons

The biotransformation of petroleum hydrocarbons is of major importance for oil production systems and for environmental pollution. The mechanisms for this alteration is poorly understood due to the highly complex nature of the matrix. Using comprehensive two-dimensional gas chromatography-mass spectrometry (GC×GC-TOFMS) it was possible to identify individual aromatic acids and diacid metabolites, plus their intermediate succinic acids, produced under sulphate-reducing conditions over a two year period within mesocosms (Aitken *et al.*, 2018). The results demonstrated that the fumarate addition mechanism applies to the alteration of monoaromatic hydrocarbons within a range of alkylation and that functionalisation of up to three ring aromatic hydrocarbons occurred.

Many aromatic acids, including diaromatic naphthoic acids, were identified during the study reported by Aitken *et al.* (2018). It had previously been hypothesised that aromatic acids were responsible, at least in part, for the developmental abnormalities observed in fish exposed to oil sands process-affected water in which carboxylic acids are highly concentrated. In a study reported by Dogra *et al.* (2018) a range of aromatic acids were first screened for toxicity using a *Thamnocephalus platyrus* (beavertail fairyshrimp) assay, then a subset selected to test for lethality and developmental abnormalities using *Danio rerio* (zebrafish) embryos. Exposure to monoacids produced concentration-dependent deformities including yolk-sac and pericardial edema, fin abnormalities, tail flexure and truncation, and reduced growth. Interestingly, 2-naphthoic acid (Fig. 1), identified by Aitken *et al.* (2018)

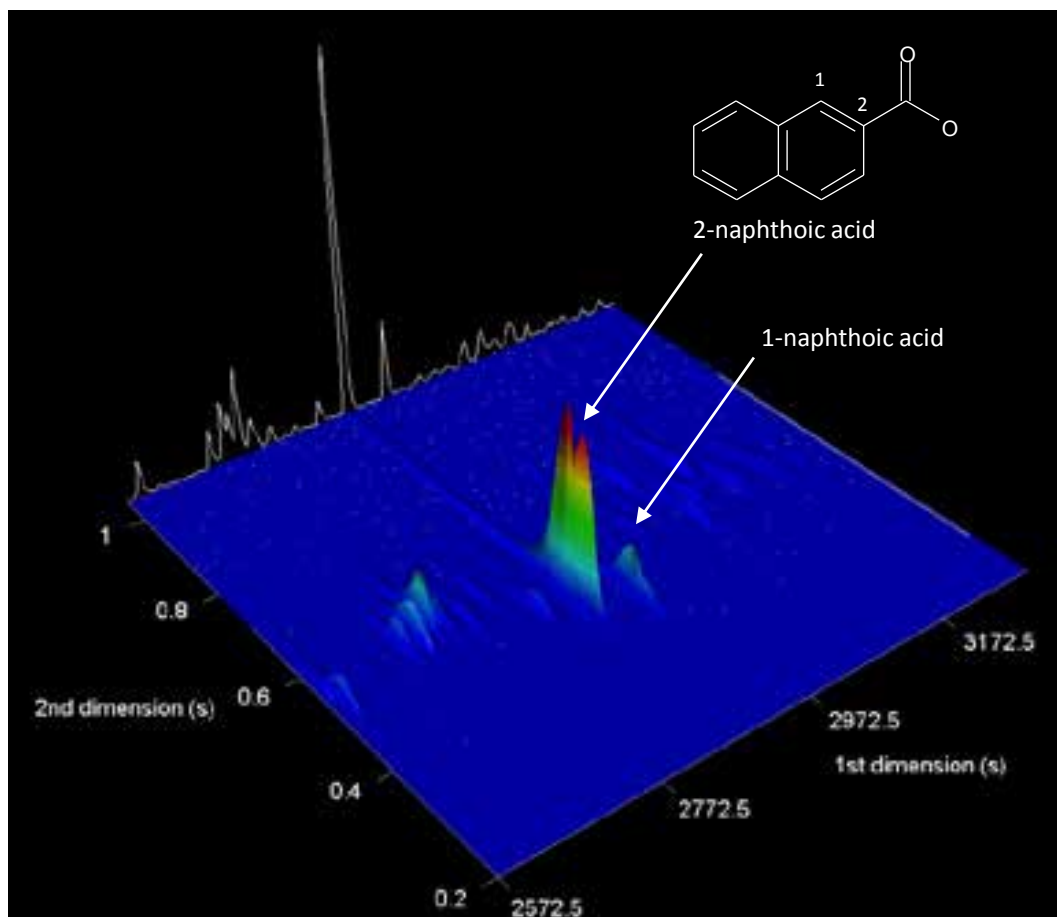
as the predominant isomer produced by anaerobic biodegradation, was found to cause very unusual head and ocular edemas in zebrafish embryos.

These two very different studies have demonstrated how our ability to identify individual compounds can help us understand the mechanism of biodegradation of petroleum hydrocarbons and how acid metabolites can affect the health of organisms that might be exposed to them. The key to analyses of such complex mixtures is GC×GC-TOFMS, which is a powerful tool now routinely used by WA-OIGC. For example, we were able identify a range of carboxylic acids, including naphthoic acids, present in the polar fraction of Montara oil. A large oil spill occurred in 2009 due to an accident at a wellhead platform drill rig of the Montara oil field in the Timor off the northern coast of Australia. Our ability to detect metabolites of oil is now under investigation by WA-OIGC funded by an ARC linkage grant.

Aitken, C.M., Head, I.M., Jones, D.M., Rowland, S.J., Scarlett, A.G., West, C.E., 2018. Comprehensive two-dimensional gas chromatography-mass spectrometry of complex mixtures of anaerobic bacterial metabolites of petroleum hydrocarbons. *Journal of Chromatography A*, 1536, 96-109.

Dogra, Y., Scarlett, A.G., Rowe, D., Galloway, T.S., Rowland, S.J., 2018. Predicted and measured acute toxicity and developmental abnormalities in zebrafish embryos produced by exposure to individual aromatic acids. *Chemosphere*, 205, 98-107.

Rowland, S.J., Sutton, P.A., Belt, S.T., Fitzsimmons-Thoss, V., Scarlett, A.G., 2018. Further spectral and chromatographic studies of ambergris. *Natural Product Research*, 1-7.



GCxGC-TOFMS extracted ion chromatogram (m/z 127, 155, 186) highlighting the presence of both 1- and 2-naphthoic acid isomers (as methyl esters) in the polar fraction of Montara crude oil.



Granites at Freycinet National Park, Tasmania.

Research reports

TECTONICS AND GEODYNAMICS

Tectonics and geodynamics

Tectonics and geodynamics involve the understanding of processes related to the motion of tectonic plates through time such as mountain building, basin formation and cyclic evolution of supercontinents, and the interaction of tectonic plates with the Earth's deep interior. Such knowledge is essential for understanding life evolution, environmental changes, and the exploration of mineral and energy resources.





The Earth Dynamics Research Group's annual science meeting with international visitors, March 2019.

Earth Dynamics Research Group — How the Earth Works

The Earth Dynamics Research Group (<http://geodynamics.curtin.edu.au>) focuses on discovering how the Earth engine works. We study the dynamic distribution and evolution of tectonic plates on Earth through time, geodynamic driving mechanisms and tectonic processes, and their relevance to Earth resources and environments. We have a particular focus on supercontinent cycles, global plume records, and 4D geodynamic modelling. Our research involves palaeomagnetism, all aspects of field-based studies, geochemical, petrological, and geochronological analyses, data-mining, numerical modelling, and regional to global syntheses.

The Research Group is mainly funded by an ARC Laureate Fellowship grant and Curtin University's co-support to Zheng-Xiang Li. Funding from the ARC Center of Excellence for Core to Crust Fluid Systems (CCFS; <http://ccfs.mq.edu.au>) finished in 2018, but CCFS will continue its existence for three more years.

Our field regions cover all major cratons of Australia, and many other parts of the world. In 2018 our research programs continue to produce groundbreaking results, including field-based program to investigate northeastern Australia's record of the assembly and breakup of the supercontinent Nuna, geochronological and palaeomagnetic investigations of Precambrian mafic igneous rocks, 4D geodynamic modeling, and global syntheses. Some of the results were published during the year, but most will be published in 2018.







Tea break, East Desert, Egypt.

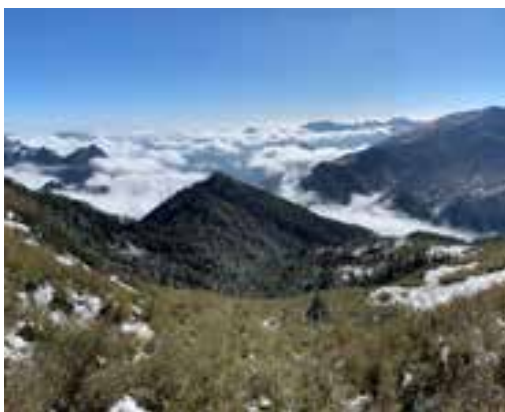


ZX Li with PhD student Hamed Mohammed Gamal El Dien at East Desert, Egypt.

Our research program goes hand-in-hand with the UNESCO/IUGS-funded IGCP 648 project: Supercontinent Cycles and Global Geodynamics (<http://geodynamics.curtin.edu.au/igcp-648/>). A highlight of IGCP 648 in 2018 include the successful and exciting session at the Australian Geoscience Council Convention (Adelaide, 14-18 October, 2018) on “Decoding Earth’s supercycles: from the core to the crust” (<https://geodynamics.curtin.edu.au/australian-geoscience-council-convention-14-18-oct-2018/>) and the successful IGCP 648 Field Symposium – From Rodinia to Pangea: Geodynamics, Life and Climate (Yichang and Shennongjia region, China, 1-9 November, 2018) (<http://geodynamics.curtin.edu.au/igcp-648-2018-field-symposium/>). The Project was highly rated by the IGCP Scientific Board, given an overall score of 5 out of 5.



Curtin's Earth Dynamic Research Group showing in force at the AGCC, Adelaide, 14-18 October, 2018.



Shennongjia field region close to the northern edge of the South China Craton.



IGCP 648 field symposium, Yichang, China.

Decoding Earth's Supercycles

It has been increasingly recognized over the past two decades that there have been repeated, and possibly cyclic, events of supercontinent assembly and breakup. The latest of such events was the supercontinent Pangaea (ca. 320–170 Ma), preceded by Rodinia (ca. 900–700 Ma), and by Nuna (ca. 1600–1400 Ma), implying a cyclicity of $\sim 600 \pm 100$ Myr. A similar cyclicity, with a 50–100 Myr time lag, is found in global mantle plume intensity, leading to the geodynamic model of a coupled supercontinent-superplume cycle in Earth history. However, variations in global zircon Hf isotopic signatures and seawater Sr isotope ratios are both characterized by a longer-term variation trend that is approximately double the wavelength of a typical supercontinent cycle. Such a billion-year variation trend (or supercycle) is also exhibited in global juvenile crust generation, by the distribution of ages of certain global-scale mineral deposits (such as lead and zinc deposits and orogenic gold deposits, but why?

Li *et al.*, (2018) suggested that the answer lies in the evolution of the World's ocean basins. According to the model, supercontinents appear to assemble through two alternating pathways. One is extroversion (e.g., the assembly of Pangaea) where the previous supercontinent (Rodinia) was turned inside-out to form the new supercontinent, and in the process the superocean surrounding Rodinia got consumed (see Figures 1c to 1f). The other is called introversion (e.g., the assembly of Rodinia), where the previous superocean surrounding Nuna survived the supercontinent cycle. In this latter case, the assembly of the new supercontinent occurred through the collapse of the internal oceans formed during the break-up of the previous supercontinent Nuna (Figures 1a to 1c).

More intriguingly, these two alternating methods of supercontinent assembly determine not only whether the superocean survives, but also whether the circum-Pacific ring of fire (e.g., the present-day Pacific ring of fire, which is scientifically referred to as the subduction girdle) survives. If this ring of fire survives along with the superocean, then the mantle structure maintains a similar pattern as during the previous supercontinent cycle (the so-called degree-2 mantle structure; Fig. 2a). If not (in the case of extroversion supercontinent assembly), then the Earth's mantle structure gets completely reorganised from a degree-2 pattern into a so-called degree-1 pattern (Fig. 2b), with the new supercontinent formed over a giant mantle downwelling (shown in blue). The researchers speculate that such alternating pathways of supercontinent assembly (along with the survival or regeneration of the superocean and ring of fire) led to the presence of an Earth cycle which is twice as long as the ca. 600 Myr supercontinent cycle, influencing the formation of some of Earth's resources.

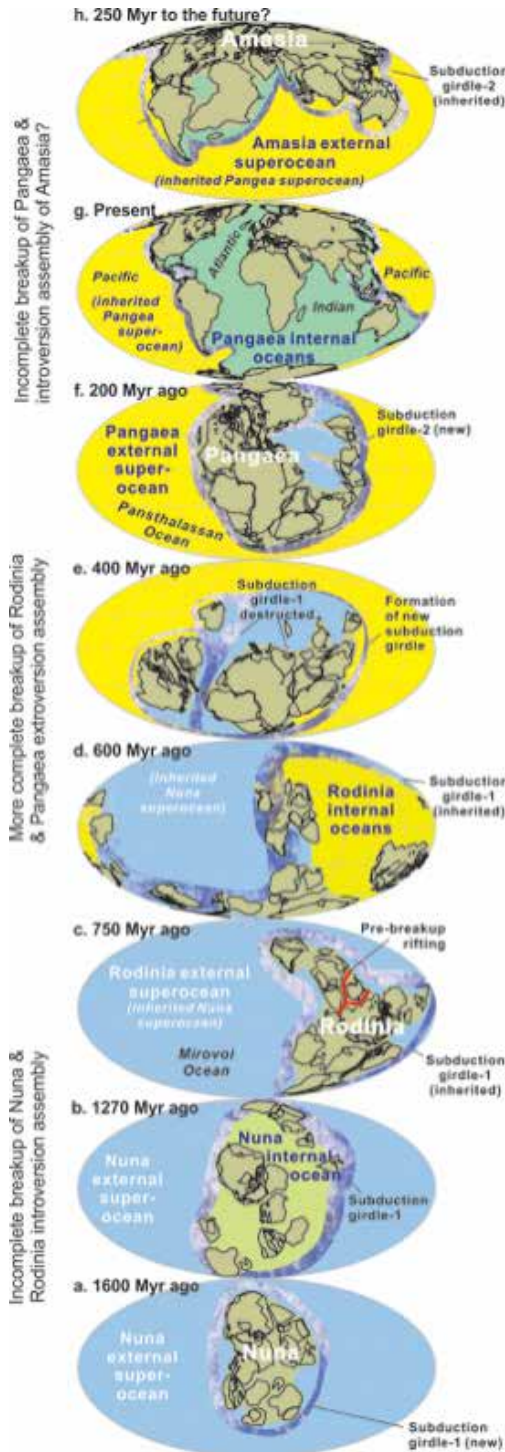


Figure 1. Survival of an external superocean over two supercontinent cycles as evidenced by global palaeogeography over the past 2000 Myr (a-h), and speculated corresponding mantle structures (i-n). Each major internal or external ocean system is colour-coded throughout the series of reconstructions. The assembly of Rodinia at 900 Ma (also future Amasia) is shown to be predominantly achieved through the closure of the internal ocean system formed as Nuna at 1400 Ma (or Pangaea at 170 Ma) fragmented (i.e., introversion), whereas the assembly of Pangaea was predominantly accomplished through the closure of the external ocean that once surrounded Rodinia (i.e., extroversion).





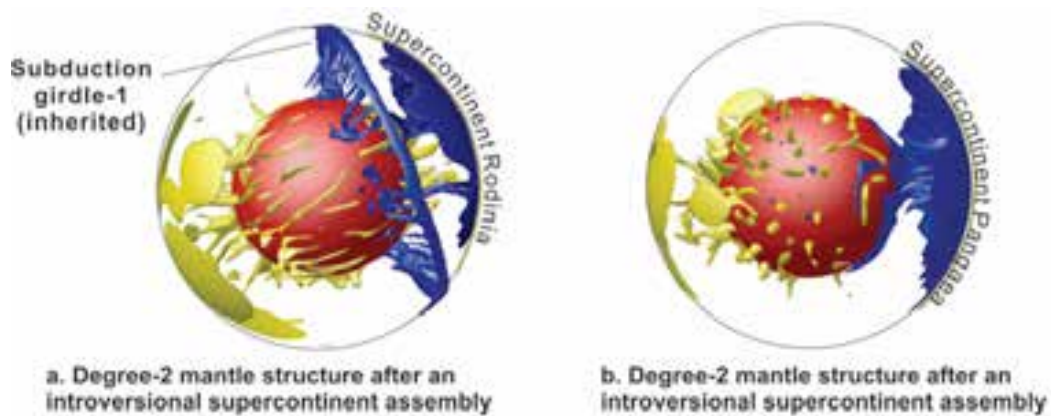


Figure 2. Different mantle structures related to the two different ways of supercontinent assembly. (a) A dominantly introverted supercontinent assembly inherits the pre-existing subduction girdle and degree-two mantle structure, along with the external superocean outside the subduction girdle. (b) A dominantly extroverted supercontinent assembly is accompanied by the destruction of the subduction girdle and the previous external superocean, where the new supercontinent forms above a superdownwelling. The mantle dynamics models were modified from Zhong *et al.* (2007), where Earth's core is shown in red, mantle upwellings in yellow, and mantle downwellings in blue.

Li, Z.X., Mitchell, R.N., Spencer, C.J., Ernst, R., Pisarevsky, S., Kirscher, U., Murphy, J.B.: Decoding Earth's rhythms: Modulation of supercontinent cycles by longer superocean episodes. *Precambrian Research* 323, 1-5, 2019.

Earth's mid-life crisis: New research backs 'lull' in the geologic record

Spencer *et al.* (2018) back recent research that claims that the Earth experienced a 'geological lull' in its development around 2.3 to 2.2 billion years ago. This work is likely to re-ignite the debate over the Earth's development, with scientists divided over what geologic processes occurred during the Palaeoproterozoic geologic era. The research findings point to a near complete shutdown of continental magmatism during this period and has profoundly shaped the geologic record as we know it today. The research shows a bona fide gap in the Palaeoproterozoic geologic record, with not only a slowing down of the number of volcanoes erupting during this time, but also a slow-down in sedimentation and a noticeable lull in tectonic plate movement.

The early Paleoproterozoic was a significant time in Earth history. Oxygenation of the atmosphere began and there was the first global glaciation event, but this was also a period where other geologic processes effectively shut down. It's almost as if the Earth experienced a mid-life crisis. The research involved compiling massive

amounts of existing geological data as well as examination of rocks collected in Western Australia's Stirling Ranges, China, Northern Canada and Southern Africa. As more rocks and data were collected, it became clearer that there is very little preserved record for this period.

This 'dormant' period lasted around 100 million years and is believed to signal a shift in the style of tectonism, from 'ancient-style' tectonics to those more akin to the present day. Earth's geology started to 'wake-up' again around 2.2 to 2.0 billion years ago with an increase in volcanic activity and a shift in the composition of the continental crust.

These findings could provide greater insight into our understanding of the world's natural resources and where they exist. Continued research into this time period is necessary to better determine how the earth's geological processes were impacted.

Spencer C.J., Murphy J.B., Kirkland C.L., Yebo Liu Y. and Mitchell R.N. (2018) A Palaeoproterozoic tectono-magmatic lull as a potential trigger for the supercontinent cycle. *Nature Geoscience* 11, 97-101 (2018).

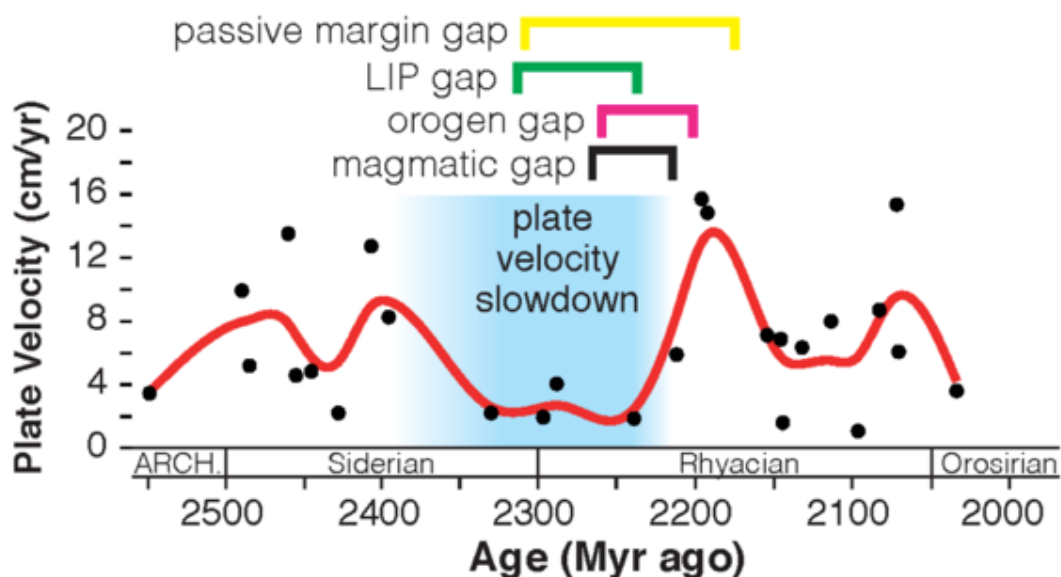
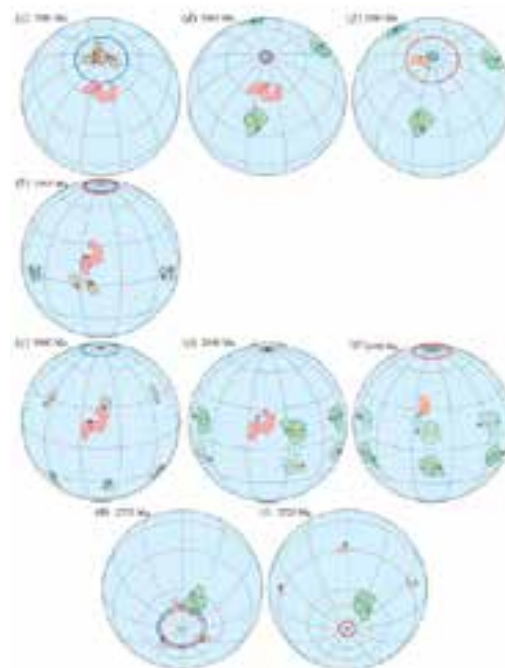


Plate velocity slowdown and geologic gaps/lulls. The black dots are velocities for individual plates (as measured by palaeomagnetic data from six individual cratons) with the red line representing a best-fit spline.

Geological archive of the onset of plate tectonics

Plate tectonics is a characteristic feature of our planet, but estimates of how long it has been the *modus operandi* of lithospheric formation and interactions range from the Hadean to the Neoproterozoic. Cawood *et al.* (2018) review sedimentary, igneous and metamorphic proxies along with palaeomagnetic data to infer both the development of rigid lithospheric plates and their independent relative motion, and conclude that significant changes in Earth behaviour occurred in the mid- to late Archaean, between 3.2 Ga and 2.5 Ga. These data include: sedimentary rock associations in passive continental margin settings, marking the onset of seafloor spreading; the oldest foreland basin deposits associated with lithospheric convergence; a change from thin, new continental crust of mafic composition to thicker crust of intermediate composition, increased crustal reworking and the emplacement of potassic and peraluminous granites, indicating stabilization of the lithosphere; replacement of dome and keel structures in granite-greenstone terranes, which relate to vertical tectonics, by linear thrust imbricated belts; the commencement of temporally paired systems of intermediate and high dT/dP gradients, with the former interpreted to represent subduction to collisional settings and the latter representing possible hinterland back-arc settings or ocean plateau environments. Palaeomagnetic data from the Kaapvaal and Pilbara cratons for the interval 2780–2710 Ma and from the Superior, Kaapvaal and Kola-Karelia cratons for 2700–2440 Ma suggest significant relative movements. We consider these changes in the behaviour and character of the lithosphere to be consistent with a gestational transition from a non-plate tectonic mode, arguably with localized subduction, to the onset of sustained plate tectonics.

Cawood P.A., Hawkesworth C.J., Pisarevsky S.A., Dhuime B., Capitanio F.A., Nebel O. (2018). Geological archive of the onset of plate tectonics. *Phil. Trans. R. Soc. A* 376: 20170405,



Palaeomagnetic reconstructions of Superior, Kola-Karelia and Kaapvaal cratons at 2680 Ma (a,d,f), 2505 Ma (b), 2440 Ma (c,e,g), of Kaapvaal and Pilbara cratons at 2775 and 2720 Ma (h,i). Arrows denote directions to the present data north. Alternative polarity option is shown with dashed outlines.

A piece of America found in northern Australia: Legacy of the 1.6-billion-year-old supercontinent Nuna — Legacy of the 1.6-billion-year-old supercontinent Nuna

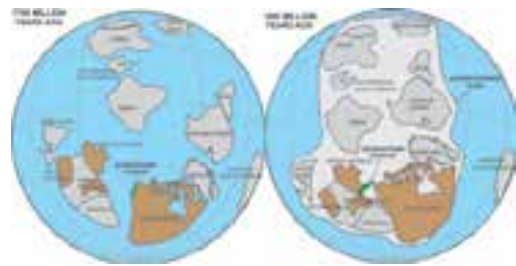
Throughout Earth's 4-billion-year history, as continents shift around the globe, periods occur where the continents amass to form supercontinents. Most recently this occurred about 300 million years ago to form the supercontinent Pangea, where the southern continents (Africa, South America and Australia and Antarctica) were connected to Eurasia and North America. It is now recognised that a supercontinent termed Nuna formed about 1.6 billion years ago. Although previous researchers have speculated that north-east Australia was near North America, Siberia, or North China in Nuna, solid evidence have been hard to find from the ancient rocks.

In Australia, approximately two thirds of the country consist of basement rocks older than 600 million years. In North Queensland, 1.7 billion-year-old rocks are found in Mt. Isa and 500 km away in the Georgetown region. New sedimentological field data in conjunction with new and existing geochronological data from both regions revealed an unexpected constituent of the Australian continent. As expected, in Mount Isa rocks, we found a strong resemblance to known Australian basement rocks. However, sedimentary rocks in Georgetown revealed surprising signatures that are unknown in Australia. Instead, they show a strong resemblance to sedimentary rocks along present-day Canada, sourced from American basement rocks.

The simplest explanation for our findings is that at 1.7 billion-year ago when the Georgetown rocks were deposited in a shallow sea, the Georgetown area was part of North America. It then rifted from North America, and only collided with the Mt Isa region of northern Australia at around 1.6 billion-year ago when almost all continents on Earth at the time assembled together to

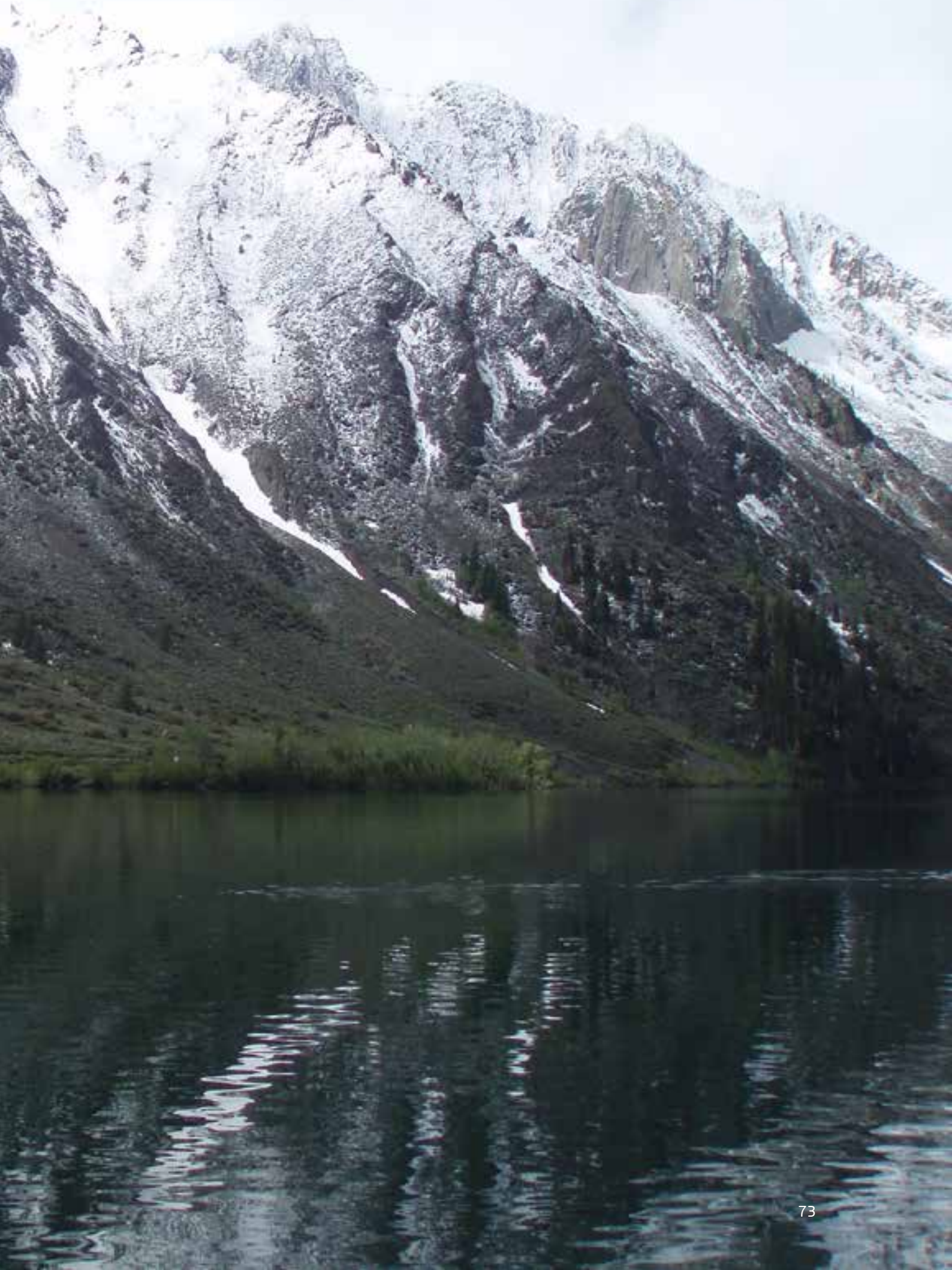
form a Pangea-like supercontinent called Nuna (Figures 1). When Nuna broke apart some 300 million years later, the Georgetown area had become a new piece of real estate permanently stuck to Australia.

Nordsvan A.R., Collins W.J., Li Z-X., Spencer C.J., Pourteau A., Withnall I.W, Betts P.G. and Volante S. (2018) Laurentian crust in northeast Australia: Implications for the assembly of the supercontinent Nuna. *Geology* 46(3), 251-254.



Cartoon illustrating that the Georgetown terrane of present-day northern Queensland was originally part of North America some 1700 million years ago. It then joined Australia at around 1600 million years ago during the formation of the supercontinent Nuna, and has remained part of Australia since.



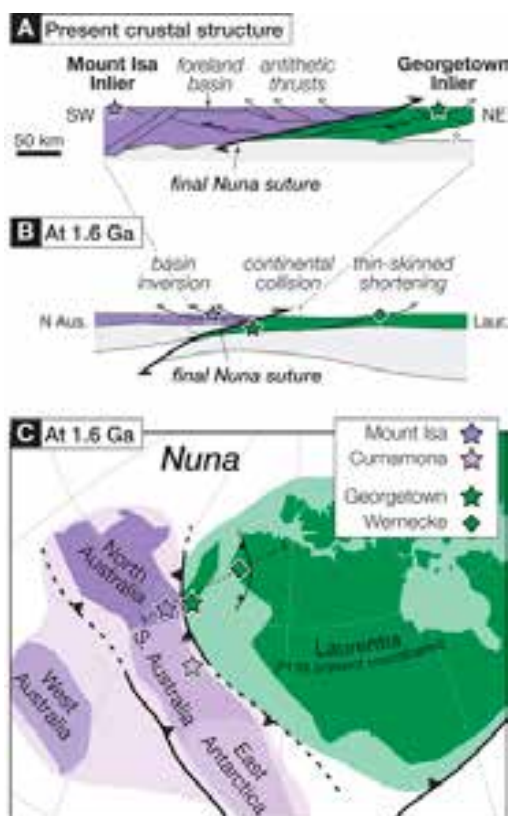


1.6 Ga crustal thickening along the final Nuna suture

Precisely defining the nature and timing the collision of proto-Australia and Laurentia (North America) during the final assembly of the supercontinent Nuna has remained elusive. It has previously been speculated that this final suture zone is concealed in northeastern Australia, but definitive evidence for crustal thickening across the suture zone has been critically lacking. In our latest publication we report new garnet petrological and geochronological results of samples from both sides of the inferred suture. The precise dates (from Lu-Hf of garnet) show synchronous prograde metamorphism between 1606- and 1598-million years ago, representing crustal thickening in the Georgetown Inlier and simultaneous basin inversion in the Mount Isa Inlier. Large-scale collision is further supported by interpretation of deep seismic reflection images of the northeastern Australia continental crust.

The precisely dated collision-related processes in northeastern Australia correlate with 1.61–1.59 Ga orogenesis recorded within South Australia and North America, suggesting a large-scale collision of Laurentia with Australia–East Antarctica, and pinpointing the final assembly of the supercontinent Nuna.

Pourteau, A., Smit, M.A. Li, Z.X., Collins, W.J., Nordsvan, A.R., Volante, S. and Li, J. (2018) 1.6 Ga crustal thickening along the final Nuna suture. *Geology* 46 (11), 959-962.



North eastern Australian Nuna suture. (A) Present-day crustal structure adapted from Korsch *et al.*'s (2012) geophysical imaging and modeling. (B) Schematic lithospheric cross section across the Nuna suture at ca. 1.6 Ga (C) Possible Nuna Australia–Antarctica Laurentia configuration at 1.6 Ga marking the final supercontinent assemblage. Presently emerged continents are shown with their possible original extensions (faded colors).

Supercontinent Nuna formed in two stages

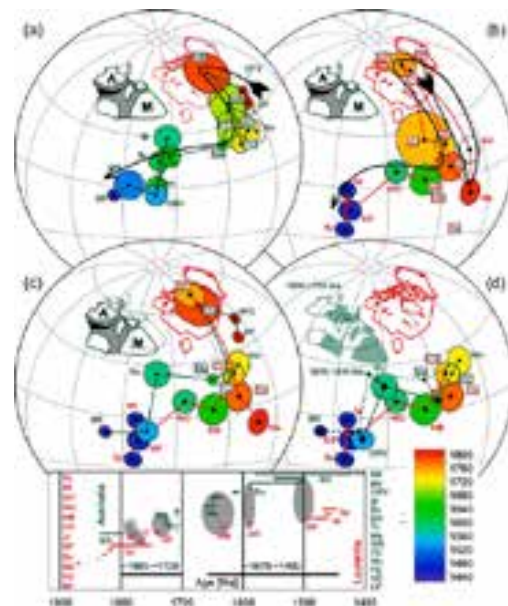
While there exists a general consensus regarding the configuration of the Earth's youngest supercontinent, Pangea, much uncertainty still surrounds that of arguably the oldest supercontinent, Nuna. Recent work suggests Nuna's final assembly was not completed until ca. 1600 Ma, and that the preceding interval of ca. 2000–1700 Ma might represent a time when the building blocks of Nuna, including proto-Laurentia, proto-Australia and proto-Baltica were assembled.

Current paleomagnetic constraints are still insufficient for establishing a detailed paleogeography for this assembly process. This is especially true for one of the key continent-continent connections in building Nuna, the speculated connection between western Laurentia and eastern proto-Australia. A 1976 preliminary study of the ca. 1.8 Ga Hart Dolerite in the eastern Kimberley craton, north-western Australia, showed some promising results, although a subsequent study in 2008 in western Kimberly proved to be less successful. We undertook a meticulous sampling of the Hart Dolerite from the eastern Kimberley craton, which yielded well defined paleomagnetic directions with dual polarities. A comparison of our resulting paleopole with other Australian poles for the period of 1800–1600 Ma indicates that proto-Australia, as a whole, underwent only very minor amounts of plate motion during that time. Our published results, along with existing data, also support the previously interpreted 40° intracontinental rotation between the North Australia and South Australia cratons during the Neoproterozoic.

A comparison of the Australian poles with that of Laurentia for the time between 1800 Ma and ~1400 Ma yielded more important findings: there are two distinct segments in the apparent polar wander paths (APWPs) of both continents for that time interval, suggesting similar movements of the two continents during these two time intervals.

Comparable APWPs between 1800 Ma and 1730 Ma imply that the two continents were already close to each other then and shared similar plate motions (Fig. 1a). This was followed by a ca. 1000 km relative plate motion between them before ca. 1650 Ma, leading to the final assembly of Nuna by ca. 1600 Ma. The two continents as a core part of Nuna again shared common APWPs after 1650 Ma that lasted at least until ~1400 Ma (Fig. 1b). We therefore suggest that there was a two-stage assembly between Australia and Laurentia as part of the assembly of the supercontinent Nuna.

Kirscher, U., Liu, Y., Li, Z.X., Mitchell, R., Pisarevsky, S., Denyszyn, S., Nordsvan, A.: Paleomagnetism of the Hart Dolerite (Kimberley, Western Australia) – A two-stage assembly of the supercontinent Nuna? *Precambrian Research*, In Press (2018).



(a) Apparent polar wander paths of Australia (poles shown as squares and diamonds) and Laurentia (poles shown as black dots), colour coded with ages between 1900 and 1400 Ma after rotating proto-Australia to Laurentia to match their 1800–1730 apparent polar wander paths, or APWPs. (b) Proto-Australia rotated further to Laurentia, moving from the pre-1730 Ma position (green cratonic outlines) to its Nuna position after 1650 Ma (green shaded cratons), to match their APWPs for the 1650–1400 Ma time interval, signalling the final assembly of the supercontinent Nuna soon after 1650 Ma.

First Precambrian palaeomagnetic data from the Mawson Craton (East Antarctica) confirms the vast ~40° intracratonic rotation of Australia

East Antarctica has been a key piece in Precambrian palaeogeographic reconstructions. As one of the most effective methods used to reconstruct supercontinents, palaeomagnetic studies have encountered great difficulties in East Antarctica due to inaccessibility, limited outcrops, and difficulties in conducting fieldwork in the Antarctic. There are only two Precambrian palaeomagnetic poles available from East Antarctica: the ca. 1130 Ma “BM” pole from the Borgmassivet intrusions in Dronning Maud Land and the ca. 1100 Ma “CL” pole from Coats Land (Fig. 1). However, it is likely that neither the Dronning Maud Land nor Coats Land terranes joined the Mawson Craton until the final assembly of Gondwana ca. 520 Ma. Therefore, the BM and CL poles cannot be used to constrain the location of the Mawson Craton in pre-530 Ma palaeogeographic reconstructions. Additionally, for much of the Precambrian time, the Mawson Craton is thought to have been a part of Australia, connected to the Gawler craton, which is also lacking reliable pre-800 Ma palaeomagnetic constraints. We conducted a pilot palaeomagnetic study on the ca. 1134 Ma Bungler Hills dykes of the Mawson Craton. Of the six dykes sampled, three revealed meaningful results providing the first well-dated Precambrian palaeopole at 40.5°S, 150.1°E (A95 = 20°) for the Mawson Craton.

Although it is generally agreed that Precambrian Australia (west of the Tasman line; Fig. 1) is composed of three Archaean to Palaeoproterozoic cratons (the West, North, and South Australian cratons – WAC, NAC and SAC respectively), when and how the present-day configuration took form is still a matter of debate. In an effort to reconcile some mismatching coeval poles of Australia,

Li & Evans (2011, *Geology*) proposed that WAC+SAC (with Mawson) rotated ~40° relative to the NAC ca. 650 – 550 Ma to form the Precambrian part of Australia as we know it today (Fig. 1). Our new pole and the coeval Lakeview Dolerite pole make up another group of coeval poles from the NAC and WAC + SAC + Mawson, respectively, with which the intraplate rotation may be further tested. With the rotation applied, the area of overlap of the 95% confidence circles of the BHD and LD poles increases (Fig. 2), which constitutes a positive test for the relative rotation model between WAC+SAC(+Mawson) and NAC. The vast intracratonic rotation hypothesis not only reconciles discrepant coeval palaeopoles, but also provides a mechanism for the enigmatic Paterson and Petermann orogenies that accounts for significant mineralisation such as the massive Telfer Au deposit.

Liu, Y., Li, Z.X., Pisarevsky, S.A., Kirscher, U., Mitchell, R.N., Stark, J.C., Clark, C., Hand, M. (2018) First Precambrian palaeomagnetic data from the Mawson Craton (East Antarctica) and tectonic implications. *Scientific Reports* 8, 16403.

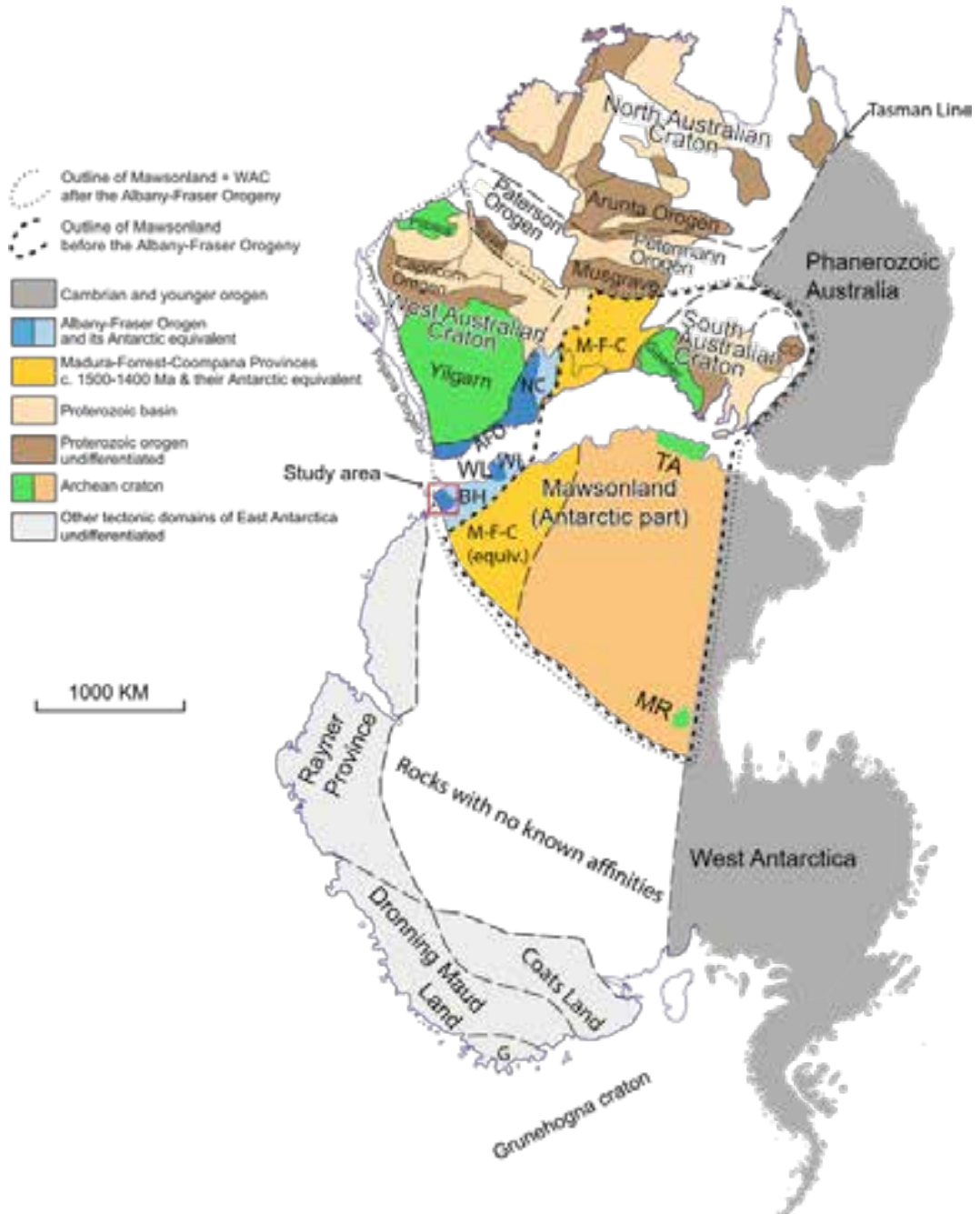


Fig. 1 Tectonic map of Australia and Antarctica in a Gondwana configuration. Antarctica is rotated to Australia coordinates using a Euler pole at 1.3°N, 37.7°E, rotation = 30.3°. Abbreviations: AFO, Albany-Fraser Orogen; BH, Bungar Hills; CC, Curnamona Craton; M-F-C, Madura-Forrest-Coompana Provinces; MR, Miller Range; NC, Nornalup Complex; TA, Terre Adélie craton; WI, Windmill Islands; WL, Wilkes Land.





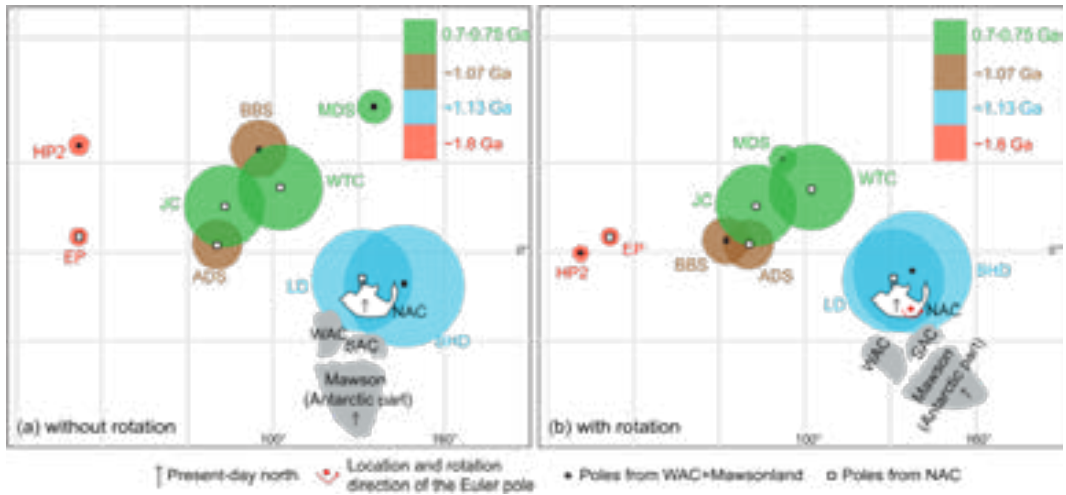


Fig. 2. Four groups of coeval poles from the WAC + Mawson and NAC plotted in Mercator projection. Mawson (Antarctic Part) rotated to SAC in its Gondwana configuration using a Euler pole at 1.3°N, 37.7°E, rotation = 30.3°. (a) Australia in its present-day configuration; (b) WAC + SAC + Mawson rotated to NAC about a Euler pole at 20°S, 135°E, rotation = 40°. Poles from the NAC: EP – Elgee-Pentecost Formations; LD – Lakeview dolerite; ADS – Alcurra dykes and sills; JC – Johnny’s Creek Member (Bitter Springs Formation); WTC – Walsh Tillite Cap Dolomite. Poles from WAC+SAC+Mawson: HP2 – Hamersley Overprint 2; BHD – Bungar Hills dykes; BBS – Bangemall Basin sills; MDS – Mundine Well dykes.

New insights into the Tibetan Plateau

The occurrence of the magnitude 7.9M Wenchuan earthquake on 12 May 2008, at the eastern foothill of the Tibetan Plateau, surprised many in the earthquake community. More intriguingly, the large number of aftershocks related to that earthquake almost exclusively occurred northeast of the main shock along the Longmenshan Fault Zone (LFZ), a phenomena that current models have trouble explaining.

In a recently published article we combine gravity modelling with a synthesis of an array of geological and geophysical observations to establish a regional hypothesis featuring (1) contrasting behaviors between the southern and central-northern LFZ, with the southern LFZ being a crustal-scale thrust zone, whereas the central-northern LFZ being a

lithospheric-scale fault zone with strong episodic dextral transpressional motions; (2) such contrasting behaviors are driven by differential motions of two crustal blocks from the western highland (the Tibetan Plateau), pushed by India's northward motion; (3) as a consequence, the LFZ features a twisted fault plane with the Wenchuan earthquake being located at the junction of the LFZ and the bounding fault between the two crustal blocks to the west; and (4) the LFZ has been behaving like this since around 40 Myr ago and it became an external boundary for a northeasterly-directed extrusion-style growth of the Tibetan Plateau.

Jiang, X., Li, Z.X., Li, C., Gong, W. (2019) A gravity study of the Longmenshan Fault Zone: New insights into the nature and evolution of the fault zone and extrusion-style growth of the Tibetan Plateau since 40 Ma. *Tectonics* 38, 176-189.

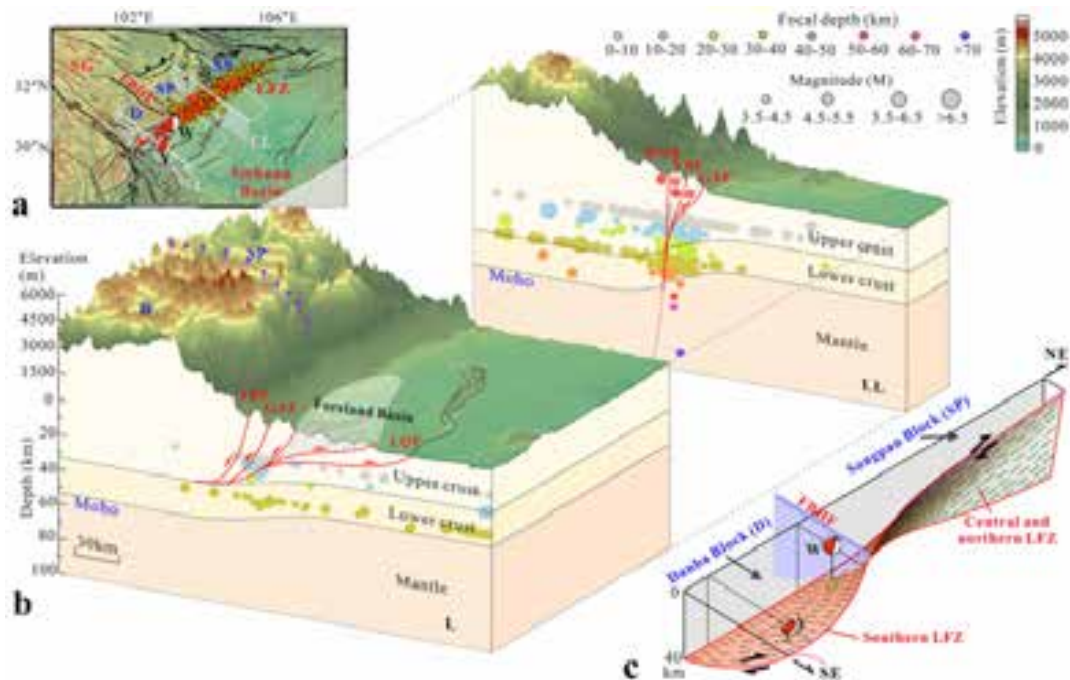


Figure 2. Contrasting structure, topography and behaviors between the southern and the central-northern LFZ. (a) Subdivision of crustal blocks in the eastern Tibetan Plateau (after Burchfiel *et al.* [2008]) and positions of the two lithospheric block diagrams as in (b). Focal solutions of the M7.9 Wenchuan earthquake (W) and aftershocks (orange dots), and that of the M6.7 Ya'an event (Y), are shown. D - Danba Block; SP - Songpan Block; XS - Xue Shan Block. (b) A 3D tectonic model for the eastern margin of Tibet along the LFZ. The 895 earthquake events of magnitude > 3.5 ruptured within ~100 km of transects L and LL (positions shown in (a)) between August 1933 and April 2015 are projected onto the two transects. The purple dot line marks the boundary between the Danba and Songpan crustal blocks - note the contrasting topography on the two sides of this boundary fault. (c) A schematic diagram illustrating a twisted fault plane along the LFZ driven by different block motion directions along the eastern margin of the Tibetan Plateau, with the hypocenter of the M7.9 Wenchuan earthquake (W) located near the twisting zone. The thrust plane in southern LFZ is within the crust, whereas in central and northern LFZ the increasingly more strike-slip fault cuts through the lithosphere.

Australia-China Joint Research Centre for Tectonics and Earth Resources (ACTER)

ACTER (<http://tectonics.curtin.edu.au>) is a joint research centre led by two top geoscience research organisations in Australia and China – the Institute for Geoscience Research at Curtin University, and the Institute of Geology and Geophysics of the Chinese Academy of Sciences, and participated by key collaborating institutions from the two countries. It aims to facilitate collaborative research and research training in geotectonics and mineral and hydrocarbon resources.

A highlight of ACTER in 2018 was the annual ACTER Field Symposium on the **Tectonic evolution of the North Qilian Mountains**, 25 Aug. – 3 Sept., 2018.

The fourth annual ACTER field symposium, thematically titled “Tectonic evolution of the North Qilian Mountains: from Paleozoic oceanic subduction to Cenozoic plateau expansion”, was held from 25th August to 3rd September, 2018 in the Gansu Province, a historical and cultural province lying between the Tibetan and Loess plateaus in north-western China. This year, the field trip and symposium was jointly led by Prof. Shuguang Song from Peking University and A/Prof. Lei Wu from Zhejiang University. Prof. Song has spent over 30 years in the Qilian Mountains, studying the Paleozoic tectonic events and associated magmatism and metamorphism of the Qilian orogenic belt, and is an expert in the field of the Qilian geology. While A/Prof. Lei Wu, as a rising star of young Chinese geologists, has spent years working on the Cenozoic basin history and tectonic evolution of NE Tibet region, publishing over ten high-impact scientific papers on this region.



The event was well attended, with 16 staff and graduate students from Curtin University, University of Illinois (Urbana-Champaign), Peking University, Zhejiang University, the Institute of Geology and Geophysics – Chinese Academy of Sciences, Guangzhou Institute of Geochemistry – Chinese Academy of Sciences, Sun Yat-sen University, Northwest University and Lanzhou University. In particular, Dr. Yan Zhao from Northwest University contributed a wealth of knowledge on the Precambrian and Paleozoic metamorphic and magmatic events in the Dunhuang area to enhance the success of the trip.

After landing in the Jiayuguan airport and being spoiled with iconic views of the ancient Jiayu Pass (originally constructed in the year 1372), the group travelled east to the Sunan County for the first taste of the Silurian turbiditic sediments that developed as part of the Ordovician back-arc basin. Here they also observed the angular unconformity between the Carboniferous limestone and the Silurian turbidites, which geologically locates the north Qilian region. The first three days were spent in the region near the Sunan County, to examine the early Paleozoic subduction systems of the north Qilian suture zone and their associated magmatism, metamorphism and sedimentation. On the fourth day the group started to travel westward to Jiayuguan and Dunhuang, examining the contact between, and the deformation of, the Cenozoic red sandstone sequence and the Silurian granitic plutons in the Jinfosi area. Along with this geological stop, the trip 'officially' moved from the Paleozoic oceanic subduction and subsequent block collision into the Cenozoic intracontinental tectonics, related to the expansion of the Tibetan Plateau, which also brought the group very exciting geology and landscapes in the following days. Neogene and Quaternary sedimentary sequences and structures impressed in many ways, including a visit to the first oil well of China at the old Yumen town built in 1939. Everyone

in the group was impressed by A/Prof. Lei Wu and his way of calculating the rising rate of various terraces on the last day, not to mention the excellent Paleozoic intrusions and granulite outcrops along with Dr. Yan Zhao's knowledgeable introduction of the Mogutai region and geology the day before.

Aside from the incredible geology, the group enjoyed many fantastic evenings filled with scientific discussions, genuine local cuisine and great relaxing company. The 2018 ACTER Field Symposium was another definitive success, giving members the great opportunity to see some spectacular rocks of the Qilian Mountains as well as iconic landscapes of the vast north-western China, with people crossing different institutions, career stages, gender, disciplines and cultural backgrounds. Such a series of annual symposiums is becoming a regular and impactful event across all ACTER institutions. It will continue to be a platform for research training and education of geoscientists of all career stages, and for promoting cross-institutional and cross-disciplinary networking and collaboration.

For a full report and photos from this event, see <http://tectonics.curtin.edu.au/2017-acter-field-symposium-23-29-october-2017/>





Western Australia Palaeomagnetic and Rock-Magnetic facility

The Western Australia Paleomagnetic and Rock-magnetic Facility is a national research infrastructure supported by the Australian Research Council and collaborating institutions including Curtin University, the University of Western Australia (UWA), the Australian National University, Macquarie University and University of Queensland. The facility was established at UWA in 1990 by CCFS CI Z.X. Li, and has been progressively upgraded over the years. The facility is now completely housed in purpose built laboratories on Curtin University's Bentley campus.

A significant component of the facility is the magnetically shielded room (constructed in mid-2015 by Dr Gary Scott's team) which provides a 20m² laboratory space with ambient magnetic fields less than 0.5% of the local geomagnetic field. Within this shielded room are: a 2G 755 superconducting rock magnetometer with a vertical Model 855 automated sample handler (the RAPID system), an AGICO JR-6A spinner magnetometer, and ASC TD-48SC and MAGNETIC MEASUREMENTS thermal demagnetisers. An earlier model 2G 755 cryogenic magnetometer, which underwent repair and upgrade during 2017-18, will be installed within the shielded room during the first half of 2019.

Other apparatus is housed in the renovated laboratory spaces surrounding the shielded room and include: a MAGNETIC MEASUREMENTS MMPM5 pulse magnetiser, an AGICO MFK-1FA Kappabridge, and the Petersen Instruments Variable Field Translation Balance (VFTB). In mid-2018 both the Kappabridge and VFTB were upgraded to bring them up to the current state-of-the-art. A temperature-susceptibility (K-T) module was added to the Kappabridge and a full electronics upgrade was performed on

the VFTB system, improving the sensitivity and response time, as well as providing additional functionality (First Order Reversal Curve measurement). An additional module has also been recently installed on the RAPID system to enable acquisition, and subsequent measurement, of Isothermal Remanent Magnetisation (IRM).

The recent purchases, upgrades and co-location of all instruments represent a major enhancement to the productivity and capabilities of the facility. Apparatus in the facility include:

- a 2G 755 superconducting rock magnetometer with a vertical Model 855 automated sample handler (the RAPID system) and other accessories (including; AF coils, susceptibility meter, ARM and IRM modules),
- an earlier model 2G 755 cryogenic magnetometer upgraded to a 4K DC SQUID system (plus a recent upgrade carried out by 2G enterprises, including the repair of the lightning-damaged cold head),
- an AGICO JR-6A spinner magnetometer,
- 1x MMTD80, 2x MMTD18 and a TD-48-SC thermal demagnetiser,
- a Petersen Instruments Variable Field Translation Balance (VFTB),
- an AGICO MFK-1FA Kappabridge with K-T capacity, and
- a MAGNETIC MEASUREMENTS MMPM5 pulse magnetiser.

The facility supports a wide range of research topics, including reconstruction of global paleogeography (the configuration and drifting history of continents) through Earth's history, reconstructing the evolving geomagnetic field (e.g. paleointensity) through time, analyses of regional and local structures and tectonic histories, dating sedimentary rocks and thermal/chemical (e.g. mineralisation) events, studying past climate changes, and orienting rock cores from drill-holes.

A national workshop on paleomagnetism, rock magnetism and their applications to tectonics, paleoclimate research, and Earth resource exploration will be conducted in February 2020. It will include a tour of the facilities along with training on the operation of all instruments for potential users of the laboratory.



Inside the shielded room.

The 2G RAPID superconducting magnetometer

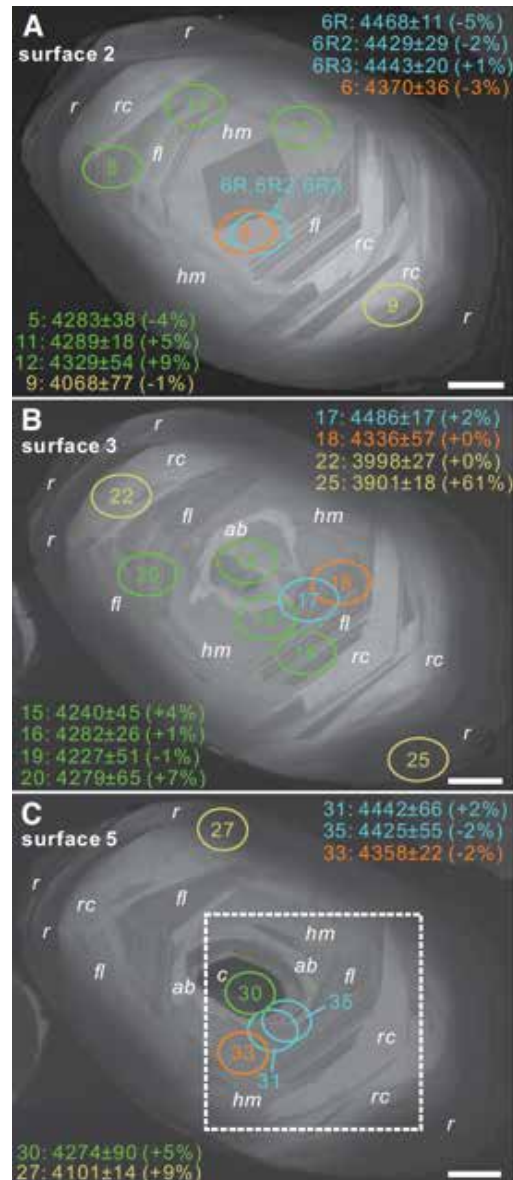


The VFTB system.

The Wilde Group

Research work published during 2018 was focussed on three broad aspects of global geology: (1) early Earth studies; (2) the Central Asian Orogen Belt; and (3) South China.

Early Earth studies included publication of three contributions in the Second Edition of Elsevier's *'Earth's Oldest Rocks'*, with chapters on the Narryer Terrane, Jack Hills and the Hadean to Eoarchean record of China. Specific studies included two papers on the geology of the ancient rocks of the Saglek Block in Labrador, one on the oldest identified rocks in the Tarim Craton of China and a major paper published in *Geology* on Jack Hills that identified how the mobilisation of radiogenic lead in zircon can lead to spuriously old, yet concordant, ages.



Selected cathodoluminescence images and sensitive high-resolution ion microprobe (SHRIMP) 207Pb/206Pb ages (in Ma, $\pm 1\sigma$, discordance in parentheses) of three sequential surfaces for detrital zircon grain 14041, Jack Hills, Western Australia.

Five papers were published on various aspects of the Central Asian Orogenic Belt, including one on the now inaccessible Alay area of Kyrgyzstan utilising rocks I had collected on a Soviet field trip in 1991 (never throw away your old samples!). Other papers included an overview of the distribution of continental fragments throughout the Paleo-Asian Ocean, the closure of which led to the formation of the Central Asian Orogenic Belt. The location of that closure is marked by the Solonker Suture Zone and joint work with staff and students from the China University of Geosciences in Wuhan on part of this zone was published in *Tectonics*. Work published on South China included studies on Neoproterozoic and Cretaceous granitoids, Neoproterozoic high-MgO basalts and isotopic studies of rocks hosting two significant Pb-Zn deposits.



Collecting ophiolite sample from Solonker, North China, with staff and students of the Chinese Academy of Geological Sciences (Prof Ying Tong on left).

Fieldwork undertaken in 2018 include sample collection of ophiolites on the Chinese side of the border with Inner Mongolia and a field excursion in September to the Beishan area as part of the inaugural meeting of IGCP 662 'Orogenic architecture and crustal growth from accretion to collision', both within the Central Asian Orogenic Belt. Work also commenced on the metamorphism and igneous activity in the Andes and Guyana Craton of Colombia. The former included sampling of the Western, Central and Eastern Cordillera and the latter involved

collaboration with the Geological Survey of Colombia in Bogota to investigate if rocks older than the early Paleoproterozoic are present in the craton.



View across the Western Cordillera near Jerico, Colombia.

Work on the Yenisei Ridge in Siberia continued in association with Prof Valery Vernikovskiy of the University of Novosibirsk, including a visit by Prof Vernikovskiy to Perth with new SHRIMP analyses undertaken on samples prepared in 2017.

Peking University cotutelle PhD student Kai Liu obtained his Chinese doctorate during the year and is now finalising the English-language version in order to obtain his doctorate through Curtin. His research work was focussed on the relationship between the Sikote-Alin orogenic belt of Far East Russia and the Central Asian Orogenic Belt to the west.



Carbonate precipitation along the Anatolian Fault, Turkey.

Research reports

PLANETARY SCIENCE

Planetary science



The Space Science and Technology Centre (SSTC) at Curtin University was officially launched on the 7th of December 2018. The SSTC represents the largest group of planetary scientists in the Southern Hemisphere, and acts as the central location of the SSERVI Australian Node.

Planetary science is a historical area of strength at Curtin: John de Laeter was a world-renowned cosmochemist and planetary scientist. That strength continues through to the present day. With 26 members, TIGeR is home to the largest planetary science group in Australia, with 14 members of staff publishing in the field as their principal area of interest and 8 PhD students full time on planetary projects.

Partnering with NASA

The Planetary Science group direct the Australia node for the NASA Solar System Exploration Research Virtual Institute (SSERVI), representing Australia's planetary research community to NASA. Curtin researchers in mission concept development have enhanced opportunities for collaboration directly with NASA teams.

The partnership will result in great scientific discoveries in planetary science as well as advancing lunar and planetary science research, and human exploration of the solar system.

Chasing Fireballs

The Desert Fireball Network (DFN) uncovers mysteries surrounding the origins of the Solar System by studying meteorites, fireballs and their pre-Earth orbits.

Digital skyward facing cameras capture pictures of meteors as they fall, while purpose-built computer programs calculate the speed, direction, and potential landing zone so the meteorite can be recovered and analysed.

Lockheed Martin FireOPAL

FireOPAL is a joint Curtin and Lockheed Martin project, building on 6 years engineering heritage from the Desert Fireball Network. The FireOPAL system is designed to be a cost effective optical SSA solution that tracks objects in LEO, MEO, and GEO. During 2018 the initial trial system grew to be a fully functional space situational awareness network – a sovereign SSA solution for Australia.

Global Fireball Observatory

The Global Fireball Observatory (GFO), based on the existing Desert Fireball Network (DFN) infrastructure, has continued to expand internationally. GFO cameras are now operational in Australia, the USA, England, Scotland, Canada, Mexico, Saudi Arabia, and Morocco. In total there are 18 collaborating institutions working on this project. The GFO will see hundreds of bright fireballs every month, providing a unique window into the evolution of small bodies in the inner solar system.

The completed GFO will allow researchers to make sense of the compositional diversity seen in meteorites and track samples back to their source regions in the main asteroid belt to eventually build a map of the geological structure of the asteroid belt and near-Earth space. With more than 150 installations planned, the GFO aims to observe 2% of the Earth's skies for fireball phenomenon by 2020.





Workshop in Geology and Geophysics of the Solar System, Petnica Science Center, Serbia, June 23 - July 1, 2018.

Petnica Workshop June/July 2018

This multidisciplinary workshop was held at the Petnica Science Center in Serbia from the 23rd of June to the 1st of July 2018. Katarina Milkjovic of Curtin University was the lead scientific organizer and one of 14 international speakers to present at the workshop.

Presentations covered a wide range of topics relating to the formation, structure and dynamics of Solar System bodies, and was aimed at graduate students and young researchers of various backgrounds and different levels of experience in the fields of planetary science and space exploration. There were 44 participants from 19 different countries, including Australia.

Planetary Perceptions of our Time

Planetary Perceptions of our Time features original artworks by illustration students based on current research from the Space Science and Technology group at Curtin University. Drawing inspiration from the retro-futuristic styling of NASA's Visions of the Future project, the students and researchers collaborated to produce illustrations that would effectively communicate the science to a wider audience, while remaining visually engaging and playful.

The exhibition was first displayed in July 2018 at Curtin University, and has since travelled nationally and internationally for display at various planetary events and conferences. The artworks are on display permanently in several locations around the Curtin University Bentley campus, and have also been published as greeting cards which are shared with the public at outreach events. The entire collection can be viewed here: <https://sstc.curtin.edu.au/engagement/community/planetary-perceptions-time/>



Asteroid Families by Curtin University students Alise Sciano and Marsquakes by Gabrielle Goetz, two posters from the Planetary Perceptions of Our Time exhibition.



Katarina Miljkovic was awarded the prestigious L'Oréal UNESCO For Women in Science Fellowship in 2018.



Katarina Miljkovic, Phil Bland, Fiona Roche and Peter Klinken at the 2018 WA Premier's Science Awards. Katarina and Phil were finalists in the Early Career Scientist of the Year and Scientist of the Year categories respectively.





Earth's Oldest Crust-Like Rocks Produced by Meteorite Impact?

Earth's oldest felsic rocks, the 4.02 billion-year-old Idiwhaa gneisses of the Acasta Gneiss Complex, northwest Canada, have compositions that are distinct from the felsic rocks that typify Earth's ancient continental nuclei, implying they formed through a different process. Using phase equilibria and trace element modelling, Johnson *et al.* (2018) show that the Idiwhaa gneisses were produced by partial melting of iron-rich amphibolite host rocks at very low pressures, equating to the uppermost ~3 km of mafic crust.

The heat required for such shallow melting is most easily explained through meteorite impacts. Hydrodynamic impact modelling shows that, not only is this scenario physically plausible, but the region of shallow melting appropriate to formation of the Idiwhaa gneisses would have been widespread. Given the predicted high flux of meteorites during the late Hadean, impact melting may have been the predominant mechanism that generated Hadean felsic rocks.

Johnson, T. E., Gardiner, N. J., Miljković, K., Spencer, C. J., Kirkland, C. L., Bland, P. A. & Smithies, R. H. (2018). An impact melt origin for Earth's oldest known evolved rocks. *Nature Geoscience*, 11, 795–799.



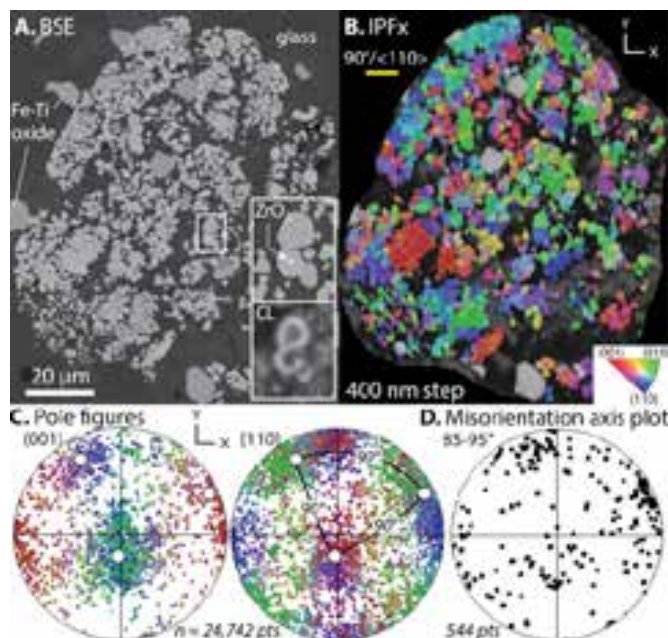
Hadean rocks of the Acasta Gneiss Complex (Image: Martin Schmieder/Lunar and Planetary Institute).

High P,T shock events recorded by granoblastic zircons transformed from reidite

Minerals that record high-pressure deformation from meteorite impact are relatively common on Earth; however, minerals that record both high-pressure and high-temperature effects of impact are rare, and they occur mostly in meteorites. Cavosie *et al.* (2018) report new occurrences of a type of granular zircon that is the only terrestrial mineral known that uniquely records both high-pressure and high-temperature conditions diagnostic of impact. Granular zircon grains in impact melt rock from the Luizi impact structure (Democratic Republic of the Congo) and in

glass from the recently described Pantasma structure (Nicaragua) consist of $\sim 1\text{-}\mu\text{m}$ -sized neoblasts in multiple domains that are systematically oriented such that all (001) poles are approximately orthogonal and coincide with a $\langle 110 \rangle$ direction from adjacent domains. The neoblast orientations are produced uniquely by transformation to the high-pressure polymorph reidite and its subsequent reversion to neoblastic zircon at high-temperature conditions, as evidenced by the occurrence of ZrO_2 .

Cavosie, A.J., Timms, N.E., Ferrière, L., and Rochette, P. (2018b). FRIGN Zircon, the Only Terrestrial High-pressure and High-temperature Mineral Diagnostic of Shock Deformation. *Geology*, 46, 891-894.



Former reidite in granular neoblastic (FRIGN) zircon in Luizi (Democratic Republic of the Congo) impact melt rock. A: Backscattered electron (BSE) image showing a granular zircon with ZrO_2 inclusions. CL cathodoluminescence image. B: Inverse pole figure map (IPF) showing neoblast orientations. Former reidite is indicated by $90^\circ/\langle 110 \rangle$ boundaries. C: Pole figures showing data from B that reveal three dominant orientations that are each highly dispersed. The 90° misonorientations are shown for $\{110\}$ pole clusters that each coincide with a (001) pole cluster. D: Plot showing high-angle (85° to 95°) misonorientation axes; clusters coincide with poles for $\{110\}$. Stereonets are equal-area, lower-hemisphere projections in sample x - y - z reference frame.

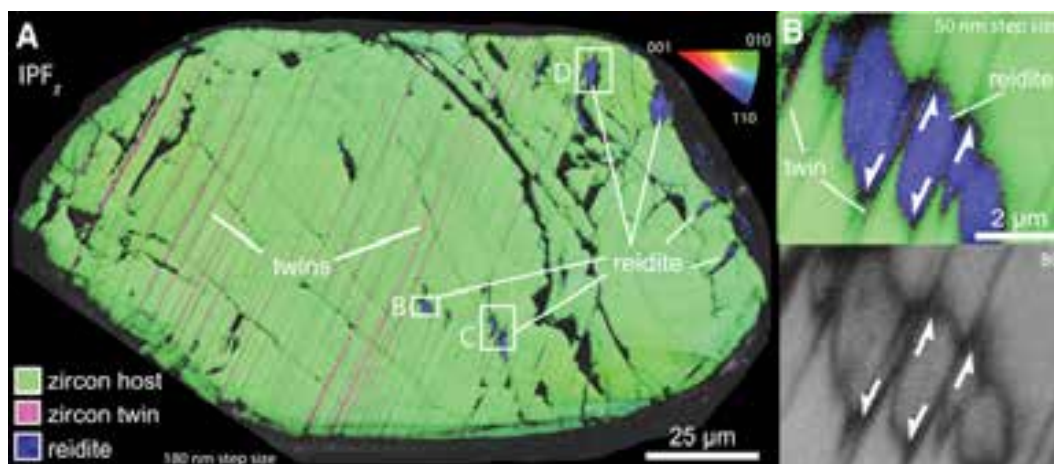
Microstructural dynamics of central uplifts: Reidite offset by zircon twins at the Woodleigh impact structure, Australia

Impact cratering is a dynamic process that is violent and fast. Quantifying processes that accommodate deformation at different scales during central uplift formation in complex impact structures is therefore a challenging task. The ability to correlate mineral deformation at the microscale with macroscale processes provides a critical link in helping to constrain extreme crustal behaviour during meteorite impact.

Cox *et al.* (2018) describe the first high-pressure- phase-calibrated chronology of shock progression in zircon from a central uplift. They report both shock twins and reidite, the high-pressure $ZrSiO_4$ polymorph, in zircon from shocked granitic gneiss drilled from the center of the >60-km-diameter Woodleigh impact structure in Western Australia. The key observation is that in zircon grains that contain reidite, which forms at >30 GPa during the crater

compression stage, the reidite domains are systematically offset by later-formed shock deformation twins (~20 GPa) along extensional planar microstructures. The {112} twins are interpreted to record crustal extension and uplift caused by the rarefaction wave during crater excavation. These results provide the first physical evidence that relates the formation sequence of both a high-pressure phase and a diagnostic shock microstructure in zircon to different cratering stages with unique stress regimes that are predicted by theoretical and numerical models. These microstructural observations thus provide new insight into central uplift formation, one of the least-understood processes during complex impact crater formation, which can produce many kilometers of vertically uplifted bedrock in seconds.

Cox, M.A., Cavosie, A.J., Bland, P.A., Miljković, K. and Wingate, M.T.D. 2018. "Microstructural dynamics of central uplifts: Reidite offset by zircon twins at the Woodleigh impact structure, Australia." *Geology* 46 (November): 983–86.



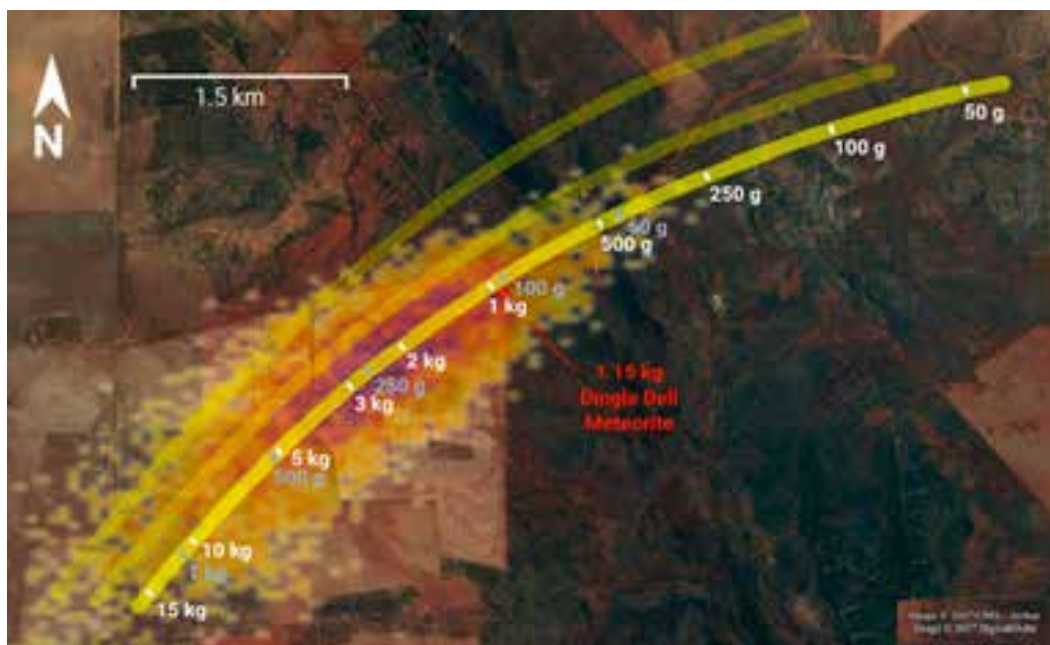
Electron back-scatter diffraction maps for zircon 112. A–D: Orientation map with an inverse pole figure (IPFz) color scheme showing prominent {112} twin lamellae, which cross-cut reidite, producing apparent sinistral offset. Reidite is shown in blue. Arrows indicate apparent sense of offset.

The Dingle Dell meteorite: A Halloween treat from the Main Belt

Devillepoix *et al.* (2018) describe the fall of the Dingle Dell (L/LL 5) meteorite near Morawa in Western Australia on October 31, 2016. The fireball was observed by six observatories of the Desert Fireball Network (DFN), a continental-scale facility optimized to recover meteorites and calculate their pre-entry orbits. The 30 cm meteoroid entered at 15.44 km s^{-1} followed a moderately steep trajectory of 510 to the horizon from 81 km down to 19 km altitude, where the luminous flight ended at a speed of 3.2 km s^{-1} . Deceleration data indicated one large fragment had made it to the ground. The four person search team recovered a 1.15 kg meteorite within 130 m of the predicted fall line, after 8 h of searching, 6 days after the fall.

Dingle Dell is the fourth meteorite recovered by the DFN in Australia, but the first before any rain had contaminated the sample. By numerical integration over 1 Ma, we show that Dingle Dell was most likely ejected from the Main Belt by the 3:1 mean motion resonance with Jupiter. This makes the connection of Dingle Dell to the Flora family (currently thought to be the origin of LL chondrites) unlikely.

Devillepoix, H.A.R., Sansom, E.K. Bland, P.A., Towner, M.C., Cupák, M., Howie, R.M., Jansen-Sturgeon, T. *et al.* 2018. "The Dingle Dell meteorite: A Halloween treat from the Main Belt." *Meteoritics and Planetary Science* 53 (October).

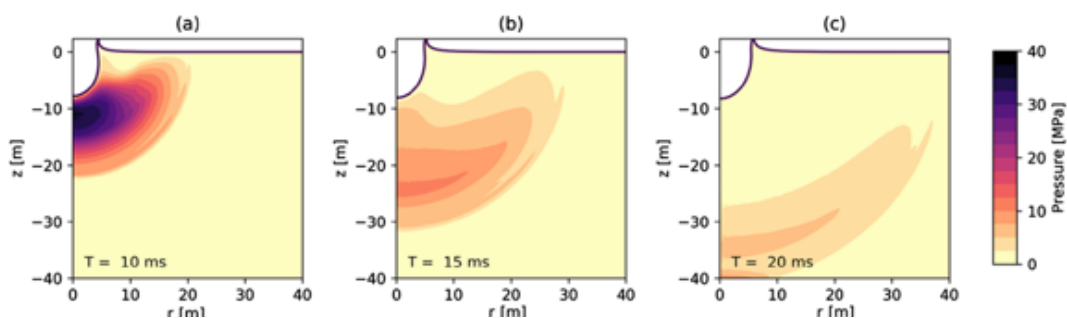


Fall area around Dingle Dell farm and Koolanooka Hills. Fall lines in yellow represent different wind model solutions: W1 (bottom), W2 (middle), and W3 (top). Mass predictions for the preferred wind model are shown for spherical (light blue markings; $A=1.21$) and cylindrical (white markings $A=1.5$) assumptions.

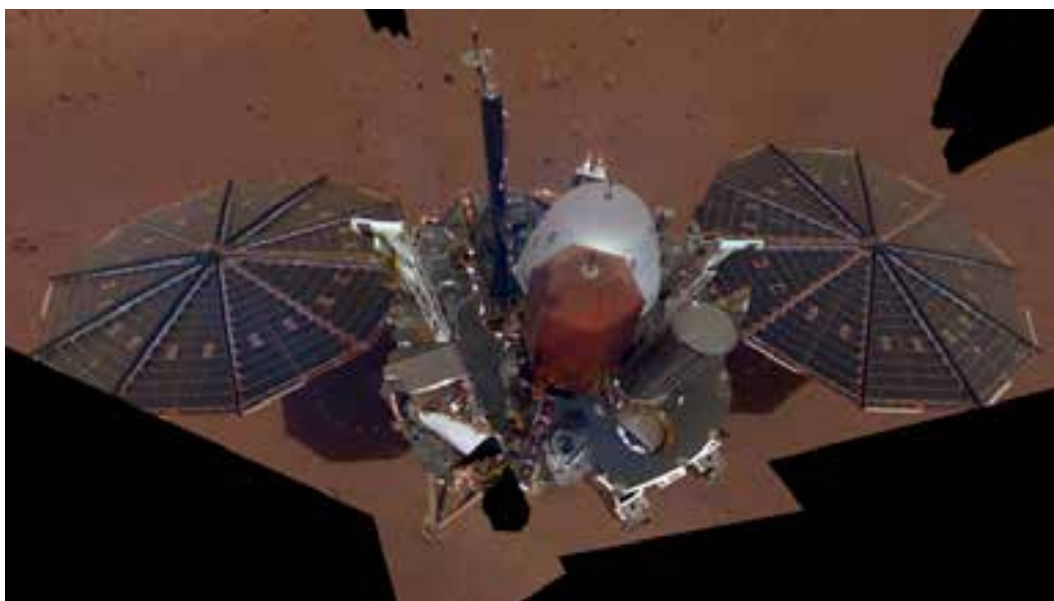
Impact-seismic investigations of the InSight mission

Impact investigations will be an important aspect of the InSight mission. One of the scientific goals of the mission is a measurement of the current impact rate at Mars. Impacts will additionally inform the major goal of investigating the interior structure of Mars.

Daubar, I.J., P. Lognonné, N. Teanby, K. Miljković, J. Stevanović, J. Vaubaillon, B. Kenda, T. Kawamura, J. Clinton, A. Lucas, M. Drilleau, C. Yana, G. Collins, D. Banfield, M. Golombek, S. Kedar, N. Schmerr, R. Garcia, S. Rodriguez, T. Gudkova, S. May, M. Banks, J. Maki, E. Sansom, F. Karakostas, M. Panning, N. Fuji, J. Wookey, M. von Driel, M. Lemmon, V. Ansan, M. Boese, S. Stähler, H. Kanamori, J. Richardson, S. Smrekar, B. Benerdt (2018) Impact-seismic investigations of the InSight mission, *Space Sci. Rev.*, 214: 132.



An example of an iSALE-2D hydrodynamic simulation showing a 1-m radius basalt impactor striking Mars regolith at 7 km/s; snapshot 10 ms (a); 15 ms (b) and 20 ms (c) after the impact. Note the expansion of the hemispherical shock wave; this is the primary source of seismic signal.



The Interior Exploration using Seismic Investigations, Geodesy and Heat Transport (InSight) mission robotic lander.

Research reports

SPATIAL SCIENCES

Geodesy and Spatial Sciences

Geodesy

Geodesy involves the study of the Earth's shape and gravity field. It forms the scientific basis for precise positioning over large areas, navigation, mapping and charting, and studies of the physics and dynamics of the Earth. It therefore contributes to the Earth-present theme in TIGeR.

Earth and planetary gravity field modelling

The Geodesy Group's continuing work on gravity field modelling in 2018 has focussed on new gravimetric quasigeoid models for Australia and New Zealand, gravimetric terrain corrections on a 30 m grid over the whole of the Australian continent, an astronomical profile of vertical deflections across the Perth Basin, and high-resolution (2 km) gravity field models of the Moon. Quasigeoid models are commonly used to transform GPS heights to heights based on mean sea level and thus be compatible with topographic maps.

Further to the 2017 report and papers cited therein, papers on the Australian and New Zealand geoid models have now been published on their full development

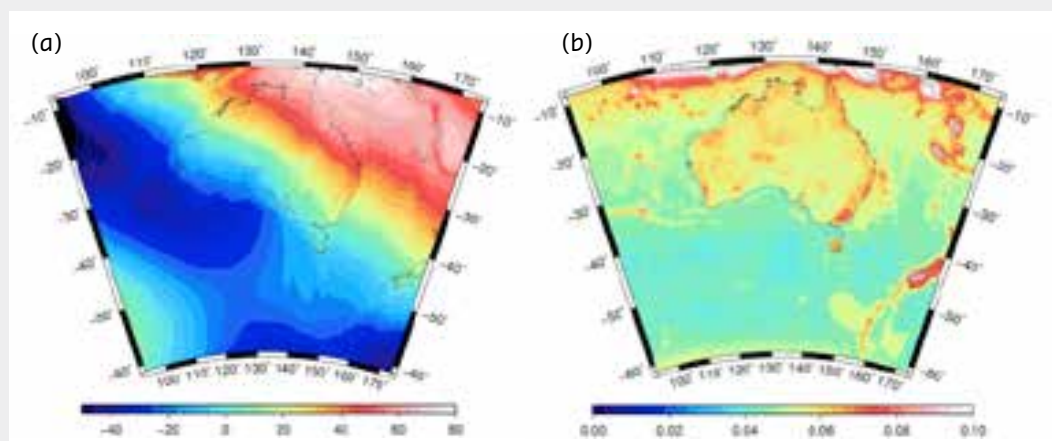
(Featherstone *et al.*, 2018a,b; Brown *et al.*, 2018; McCubbine *et al.*, 2018). These models are public-domain and used by all GPS users in Australia and New Zealand.

Featherstone W.E., McCubbine J.C., Brown N.J., Claessens S.J., Filmer M.S., Kirby J.F. (2018a). The First Australian Gravimetric Quasigeoid Model with Location-specific Uncertainty Estimates. *Journal of Geodesy*, 92, 149-168.

Featherstone W.E., Brown N.J., McCubbine J.C., Filmer M.S. (2018b). Description and Release of Australian Gravity Field Model Testing Data. *Australian Journal of Earth Sciences*, 65, 1-7.

Brown, N.J., McCubbine J.C., Featherstone W.E., Woods A., Baran I., Gowans, N. (2018). AUSGeoid2020 Combined Gravimetric-geometric Model with Location-specific Uncertainties and Baseline-length-dependent Error Decorrelation. *Journal of Geodesy*, 92, 1457-1465, 1467.

McCubbine, J.C., Amos M.J., Tontini F.C., Smith E., Winefield R., Stagpoole V., Featherstone W.E. (2018). The New Zealand Gravimetric Quasigeoid Model 2017 that Incorporates Nation-wide Airborne Gravimetry. *Journal of Geodesy*, 92, 923-937.

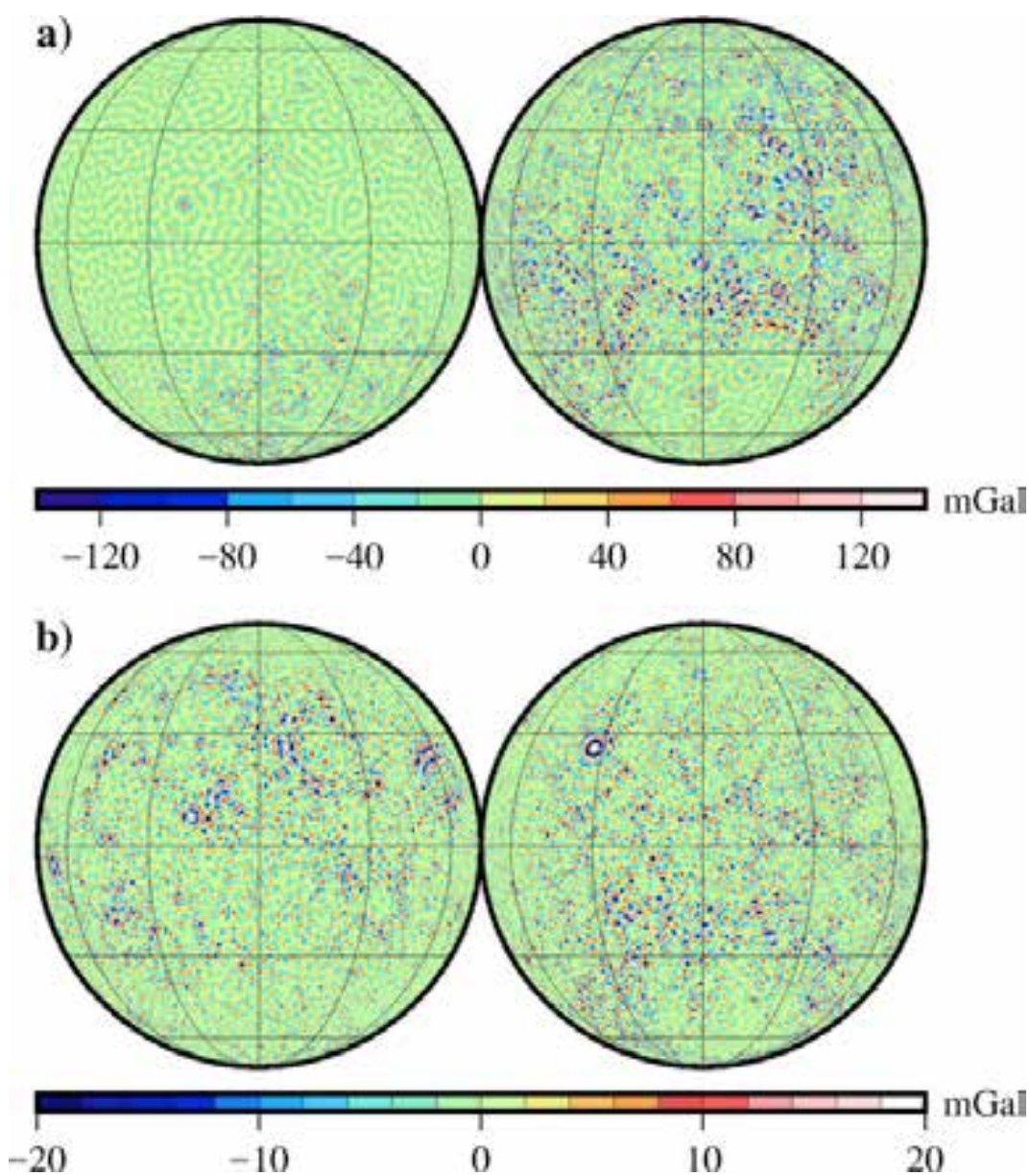


(a) The Australian gravimetric quasigeoid model 2017 (AGQG2017), and (b) its associated location-specific error map/chart. Units in metres.

Moon gravity field modelling

Funded by ARC Discovery Grant DP160104095, we have devised a forward modelling technique that can account for variations in density and topography, and applied it to the gravity field of the Moon.

Šprlák M., Han S-C., Featherstone W.E. (2018). Forward Modelling of Global Gravity Fields with 3D Density Structures and an Application to the High-resolution (~2 km) Gravity Fields of the Moon. *Journal of Geodesy*, 92, 847-862.



Šprlák M., Han S-C., Featherstone W.E. (2018). Forward Modelling of Global Gravity Fields with 3D Density Structures and an Application to the High-resolution (~2 km) Gravity Fields of the Moon. *Journal of Geodesy*, 92, 847-862.



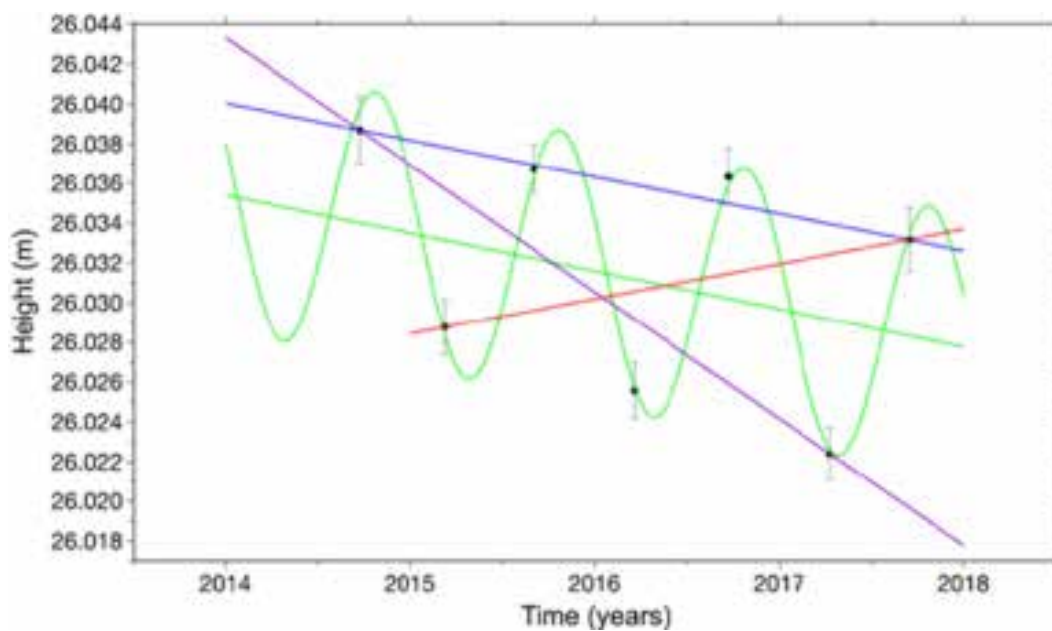


Land motion from levelling

Lyon *et al.* (2018) have provided some potential reasons why temporal changes in height (uplift or subsidence) measured by modern geodetic techniques, principally levelling, do not always agree with those inferred from the geological record. In some extreme cases, the repeat levelling can even indicate uplift in the case of subsidence (see figure). The study also shows that over the past 45 years, the Perth Basin has

subsided by a total of 80 mm (~3mm/yr), due principally to groundwater extraction. This work is funded by ARC Linkage Grant LP140100155 Landgate, WA Department of Water and Curtin.

Lyon, T.J., Filmer M.S., Featherstone, W.E. (2018) On the use of Repeat Leveling for the Determination of Vertical Land Motion: Artifacts, Aliasing and Extrapolation. *Journal of Geophysical Research - Solid Earth*, 123, 7021-7039.



Unification of vertical datums using the ocean's mean dynamic topography

Research conducted by Curtin University (Dr Mick Filmer and Prof Will Featherstone) in collaboration with UK researchers at the National Oceanographic Centre (Prof. Chris Hughes, and Dr Phil Woodworth) and Bristol University (Dr Rory Bingham) investigated models of the ocean's time-mean dynamic topography (MDT) at tide gauges around Australia (Fig 1). The ocean MDT is the separation between the geoid (equipotential surface) and the mean sea surface, and is the cause of vertical offsets between different height datums around the world. We compared MDT at Australian tide

gauges for 13 different physics-based ocean models and six models based on geodetic or ocean observations, finding that some physics based models have a standard deviation of differences of around ± 50 mm. This suggests that the ocean models can not only be used to directly unify vertical datums separated by ocean, but also be used to identify errors in geoid models at the coast (Filmer *et al.*, 2018).

Filmer M.S., Hughes C.W., Woodworth P.L., Featherstone W.E., Bingham R.J. (2018) Comparison between the geodetic and oceanographic approaches to estimate mean dynamic topography for vertical datum unification. *Journal of Geodesy*, 92(12): 1413–1437, doi: 10.1007/s00190-018-1131-5.

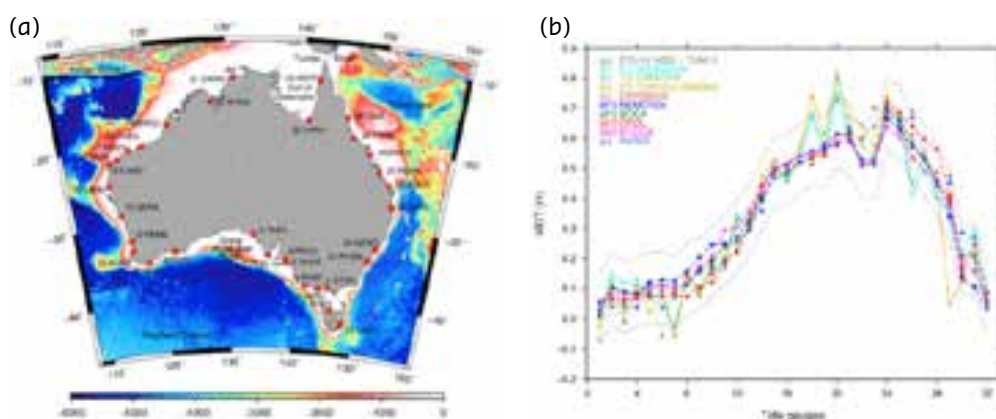


Fig. 1 (a) The 32 Australian tide gauges used in this study, shown as red squares. Bathymetric data are in metres and obtained from http://topex.ucsd.edu/cgi-bin/get_data.cgi (Smith and Sandwell 1997). (b) MDT profiles at 32 tide gauges (numbered as per Fig. 1) for the period 2003–2007. Black dotted lines are 99% confidence from the mean MDT value at each tide gauge.

TIGeR – supported visit by Dr Simon Williams, Senior Research Scientist at the National Oceanographic Centre (UK)

In November 2018, Dr Simon Williams visited the Geodesy Research Group in the School of Earth and Planetary Sciences as a TIGeR Visiting Research Fellow. During Dr Williams visit, he worked with Dr Mick Filmer on the noise characteristics of InSAR satellite radar signals that are used to measure vertical

land motion in the Perth Basin. These results suggested that the short time series (5 years) of the InSAR rates may be biasing the true noise characteristics of the time series. Dr Williams also worked with PhD students Todd Lyon and Khac Luyen Bui on the application of maximum likelihood estimation in noise analysis of geodetic measurements. He also gave a presentation on his research project at the NOC investigating GNSS reflectometry which uses GNSS signal multipath to measure sea level at coastal GNSS stations.



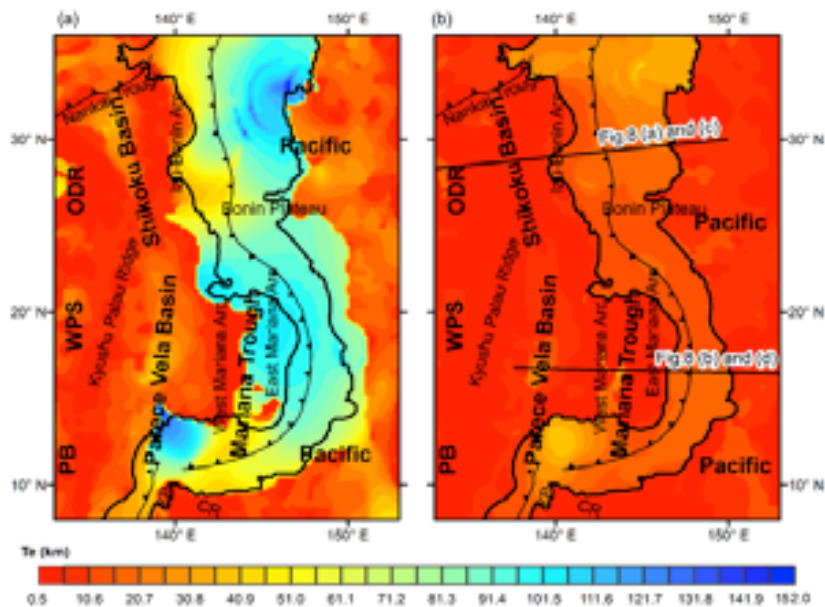
Fig 1: Dr Simon Williams presenting his research on GNSS reflectometry during his research visit to Curtin University, November 2018.

The effect of dynamic topography and gravity on lithospheric effective elastic thickness estimation: a case study

Lithospheric effective elastic thickness (T_e), a proxy for plate strength, is helpful for the understanding of subduction characteristics. Affected by curvature, faulting and magma activity, lithospheric strength near trenches should be weakened but some regional inversion studies have shown much higher T_e values along some trenches than in their surroundings. In order to improve T_e estimation accuracy, here we discuss the long-wavelength effect of dynamic topography and gravity on T_e estimation by taking the Izu-Bonin-Mariana (IBM) Trench as a case study area. We estimate the long-wavelength influence of the density and negative buoyancy of the subducting slab on observed gravity anomalies and seafloor topography. The residual topography and gravity are used to map T_e using the fan-wavelet coherence

method. Maps of T_e , both with and without the effects of dynamic topography and slab gravity anomaly, contain a band of high- T_e values along the IBM Trench, though these values and their errors are lower when slab effects are accounted for. Nevertheless, tests show that the T_e map is relatively insensitive to the choice of slab-density modelling method, even though the dynamic topography and slab-induced gravity anomaly vary considerably when the slab density is modelled by different methods. The continued presence of a high- T_e band along the trench after application of dynamic corrections shows that, before using 2D inversion methods to estimate T_e variations in subduction zones, there are other factors that should be considered besides the slab dynamic effects on the overriding plate.

Bai Y., Dong D., Kirby J.F., Williams S.E., Wang Z. (2018). The effect of dynamic topography and gravity on lithospheric effective elastic thickness estimation: a case study. *Geophysical Journal International*, 214, 623-634.



T_e maps (a) before and (b) after considering the influence of pull-force by the subducted slab of the Pacific plate on topography and gravity ($CW = 2.668$). The solid black lines in (a) and (b) are the outer boundaries of the high- T_e band from Figure 5b. (a) is a reproduction of Figure 3a, while (b) is a reproduction of Figure 5b. All abbreviations are the same as Figure 1. [Source: *Geophysical Journal International*.]





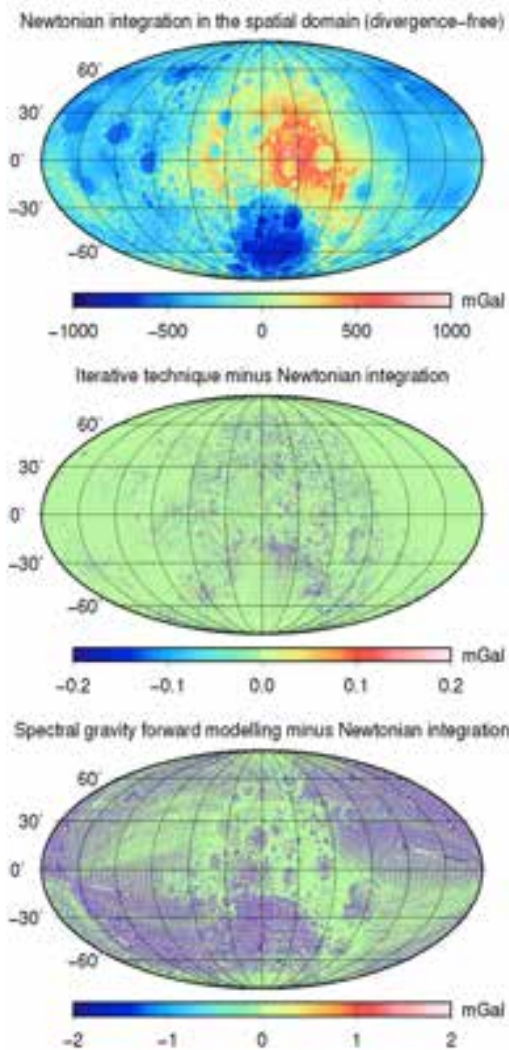
Divergence-free spherical harmonic gravity field modelling based on the Runge–Krup theorem: a case study for the Moon

External spherical harmonic series are widely used in gravity field modelling of Earth and other planetary bodies. However, recent studies have shown that the series may diverge when evaluating on or close to the surface of the generating masses and for increasing expansion of the spherical harmonic series (e.g. increased spectral resolution).

Bucha *et al.* (2018) have investigated an alternative solution that is still based on external spherical harmonic series, but capable of avoiding the divergence effect. The proposed approach relies on the Runge–Krup theorem stating that, theoretically, the external gravitational potential of a star-shaped body can be approximated to arbitrarily high level of accuracy by a single convergent series of spherical harmonics. In practice the regularized iterative downward continuation in combination with spherical harmonic calculus is used. This generates a set of external spherical harmonic coefficients on a sphere inside the generating masses (known as the Bjerhammar sphere), that, when upward continued generate the gravitational potential on or above the surface of the generating masses.

The new approach has been tested using gravity implied by the lunar topography with a 5-arc-minute spatial resolution. Numerical results demonstrate that the technique indeed avoids the divergence effect, at least at the spatial resolution used. This is demonstrated by a considerable drop in differences when compared to an independent (divergence-free) Newtonian integration.

Bucha B., Hirt C., Kuhn M. (2018). Divergence-free spherical harmonic gravity field modelling based on the Runge–Krup theorem: a case study for the Moon. *Journal of Geodesy*, <https://doi.org/10.1007/s00190-018-1177-4>.



Top panel: gravity implied by lunar topography obtained from (divergence-free) Newtonian integration in the spatial domain.

Middle panel: gravity implied by the new approach minus Newtonian integration.

Bottom panel: gravity implied by 'conventional' use of external spherical harmonic series minus Newtonian integration.

Precise Point Positioning

El-Mowafy *et al.* (2018a-c) have analysed the performance of the new second-generation Satellite-Based Augmentation System (SBAS) with focus on digital mining applications such as digital pegging and autonomous operations of trucks and drill machines. The second generation dual-frequency multi-constellation (DFMC) SBAS service transmits over the L5 frequency for GPS L1/L2 and Galileo E1/E5a signals. Performance analysis shows that the SBAS solutions have generally better positioning than the traditional standalone solutions, and the SBAS DFMC solutions have better precision than the SBAS L1. The PPP offers the best solution, provided that enough convergence time is available.

In another project a method is presented to solve a major problem in using Real-time Precise Point Positioning (RT PPP) as a primary positioning method used in natural hazard warning systems (NHWS) such as monitoring tsunamis and earthquakes. The method bridges outages in precise orbit and clock corrections needed for RT PPP by reliable prediction of these corrections.

In a further project, a new integrity monitoring method is presented to ensure reliable continuing positioning as a critical requirement for Intelligent Transportation Systems (ITS). An integrated positioning system is used comprising the Global Navigation Satellite Systems (GNSS) Real-Time Kinematic (RTK) integrated with low-cost inertial measurement unit (IMU) coupled with car odometer measurements.

El-Mowafy, A., Kubo, N. (2018a) Integrity monitoring for Positioning of intelligent transport systems using integrated RTK-GNSS, IMU and vehicle odometer, *IET Intelligent Transport Systems* 12(8): 901–908. DOI: 10.1049/iet-its.2018.0106.

El-Mowafy, A. (2018b). Real-Time Precise Point Positioning Using Orbit and Clock Corrections as Quasi-Observations for Improved Detection of Faults. *J. of Navigation*, 71(4), 769–787.

El-Mowafy, A. (2018c). Predicting Real-Time Orbit and Clock Corrections for Positioning Using GPS, GLONASS and QZSS in Natural Hazard Warning Systems, *Journal of Applied Geodesy*, DOI: 10.1515/jag-2018-0043.



Environmental Geoinformatics

Joseph Awange, John Kiema

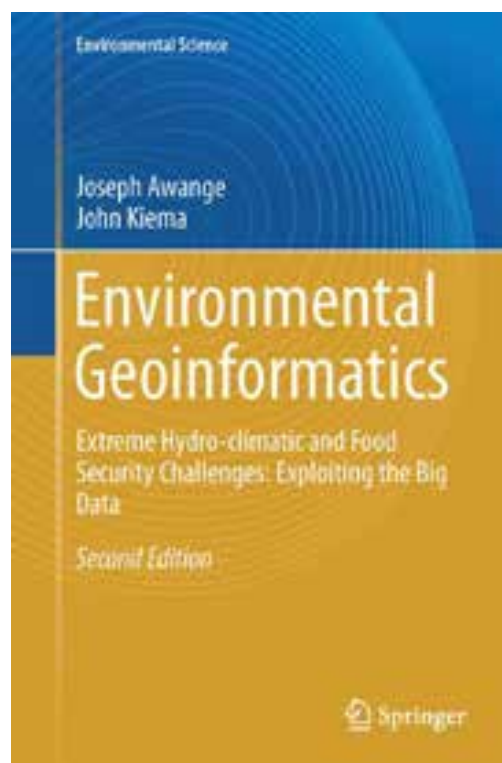
Environmental
Geoinformatics

Extreme Hydro-climatic and Food Security Challenges: Exploiting the Big Data Series: Environmental Science

- Brings together multi-disciplinary techniques to support the acquisition, analysis, and visualisation of geodata
- Includes numerous colour photos, as well as relevant and practical examples
- Features special chapters on applications and updated technologies involving big data and new challenges

This second edition includes updated chapters from the first edition as well as five additional new chapters (Light detection and ranging (LiDAR), CORONA historical de-classified products, Unmanned Aircraft Vehicles (UAVs), GNSS-reflectometry and GNSS applications to climate variability), shifting the main focus from monitoring and management to extreme hydro-climatic and food security challenges and exploiting big data. Since the publication of first edition, much has changed in terms of technology, and the demand for geospatial data has increased with the advent of the big data era. For instance, the use of laser scanning has advanced so much that it is unavoidable in most environmental monitoring tasks, whereas unmanned aircraft vehicles (UAVs)/drones are emerging as efficient tools that address food security issues as well as many other contemporary challenges. Furthermore, global navigation satellite systems (GNSS) are now responding to challenges posed by climate change by unravelling the impacts of teleconnection (e.g., ENSO) as well as advancing the use of reflected signals (GNSSreflectometry) to monitor, e.g., soil moisture variations. Indeed all these rely on the explosive use of “big data” in many fields of human endeavour.

Moreover, with the ever-increasing global population, intense pressure is being exerted on the Earth’s resources, leading to significant changes in its land cover (e.g., deforestation), diminishing biodiversity and natural habitats, dwindling fresh water supplies, and changing weather and climatic patterns (e.g., global warming, changing sea level). Environmental monitoring techniques that provide information on these are under scrutiny from an increasingly environmentally conscious society that demands the efficient delivery of such information at a minimal cost.



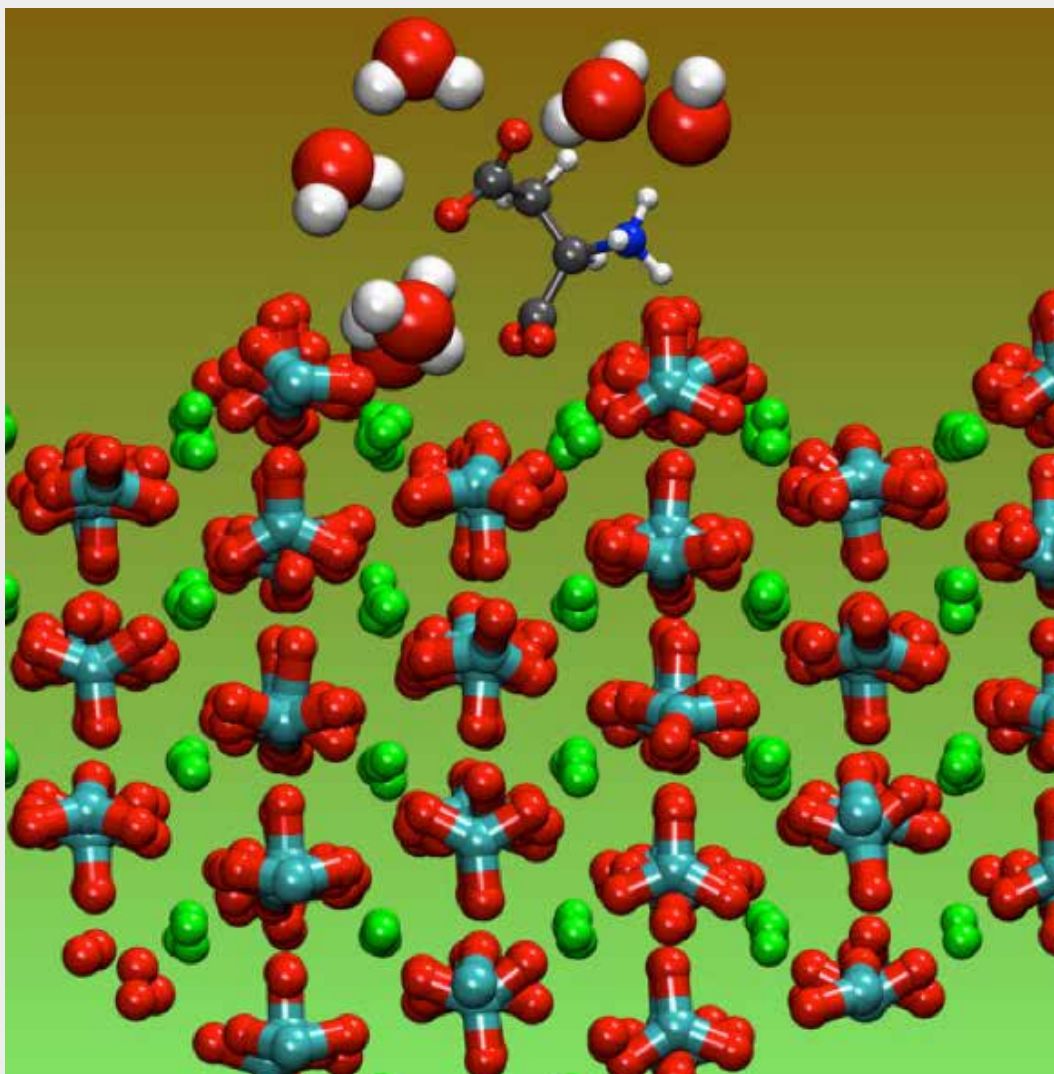
Research reports

COMPUTATIONAL GEOSCIENCES

Computational geochemistry

The research in computational geochemistry involves studying the nucleation and growth of minerals from aqueous solution using computer simulation based on both force fields and *ab initio* quantum mechanics. In particular, we are focusing on minerals relevant to biomineralisation including those composed of calcium in combination with carbonate, oxalate, sulphate or phosphate. This spans processes from ion pairing and formation of pre-nucleation clusters through to mineralogy and polymorphism.

During the past year, we have reported significant progress and findings. We have provided the biomineralization community with an appropriate classical force field that is suitable to model the phosphate speciation in water and we have applied it in a combined computational-experimental study to investigate the solid-water solution interface. In addition, we have begun developing new more accurate models for carbonate systems that include the important effects of polarisation.



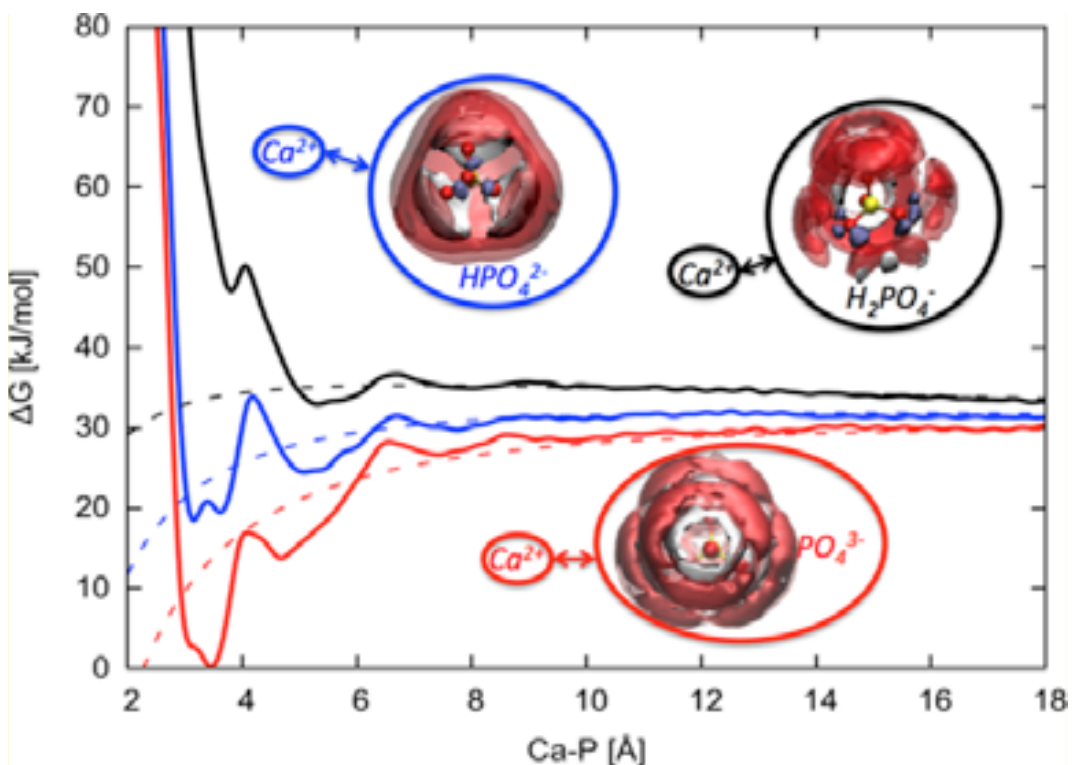
Interaction of aspartate negative zwitterion with the surface of CaCO_3 vaterite; first water coordination sphere shown.

Simulation of Calcium Phosphate Species in Aqueous Solution

A new force field has been derived for the aqueous calcium phosphate system that aims to reproduce the key thermodynamic properties of the system, including free energies of hydration of the ions and the solubility of the solid mineral phases. Interactions of three phosphate anions (PO_4^{3-} , HPO_4^{2-} , and H_2PO_4^-) with water were calibrated through comparison with the results obtained from *ab initio* molecular dynamics using both GGA and hybrid density functional theory with dispersion corrections. In the solid state, the force field has been evaluated by benchmarking against

experiment and other existing models and is shown to reproduce the structural and mechanical properties well, despite the primary focus being on thermodynamics. To validate the force field, the thermodynamics of ion pairing for calcium phosphate species in water has been computed and shown to be in excellent agreement with experimental data.

Demichelis, R., Garcia N.A., Raiteri P., Innocenti Malini R., Freeman C.L., Harding J.H., Gale J.D. (2018). Simulation of Calcium Phosphate Species in Aqueous Solution: Force Field Derivation. *Journal of Physical Chemistry B*, 122, 1471-1483.



Free energy representation of the water structure around the phosphate species; from left to right: PO_4^{3-} , HPO_4^{2-} , and H_2PO_4^- . Isosurfaces for O and H atoms of water are represented in red and white, respectively; isosurfaces for H atoms of phosphate are represented in purple. Oxygen and phosphorus atoms are colored in red and yellow, respectively.





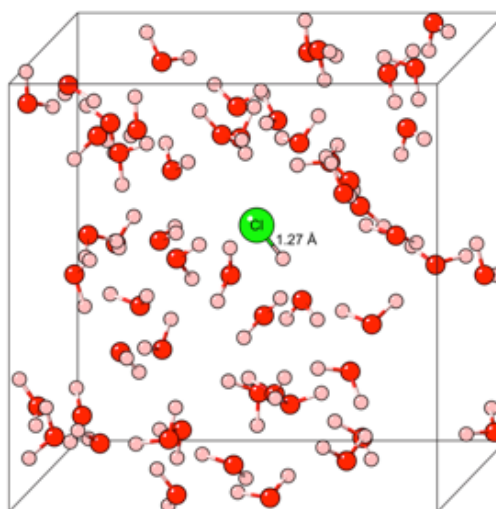
The dissociation mechanism and thermodynamic properties of HCl(aq) in hydrothermal fluids (to 700 °C, 60 kbar) by *ab initio* molecular dynamics simulations

HCl is one of the most significant volatiles in the Earth's crust. It is well established that chloride activity and acidity (pH) play important roles in controlling the solubility of metals in aqueous hydrothermal fluids. Thus, quantifying the dissociation of HCl in aqueous solutions over a wide range of temperature and pressure is crucial for the understanding and numerical modeling of element mobility in hydrothermal fluids. Mei *et al.* (2018) have conducted *ab initio* molecular dynamics (MD) simulations to investigate the mechanism of HCl(aq) dissociation and to calculate the thermodynamic properties for the dissociation reaction at 25–700 °C, 1 bar to 60 kbar, i.e. including high temperature and pressure conditions that are geologically important, but difficult to investigate via experiments.

Their results predict that HCl(aq) tends to associate with increasing temperature, and dissociate with increasing pressure. In particular, HCl(aq) is highly dissociated at extremely high pressures, even at high temperatures (e.g., 60 kbar, 600–700 °C). At 25°C, the calculated logK_d values (6.79 ± 0.81) are close to the value (7.0) recommended by IUPAC (International Union of Pure and Applied Chemistry) and some previous experimental and theoretical studies. The MD simulations indicate full dissociation of HCl at low temperature; in contrast, some experiments were interpreted assuming significant association at high HCl concentrations even at room T. This discrepancy is most likely the result of difficulties in the experimental determination of minor (if any) concentration of associated HCl(aq) under ambient conditions, and thus reflects differences in the activity models used for the interpretation of the

experiments. With increasing temperature, the discrepancy between our MD results and previous experimental studies, and between different studies, becomes smaller as the degree of HCl association increases. The results will enable prediction of the role of HCl in controlling element mobility in deep earth hydrothermal systems, including fluids associated with ultra-high pressure metasomatism in subduction zones.

Mei, Y., Liu W., Brugger J., Sherman D.M., Gale J.D. (2018). The dissociation mechanism and thermodynamic properties of HCl(aq) in hydrothermal fluids (to 700 °C, 60 kbar) by *ab initio* molecular dynamics simulations. *Geochimica Cosmochimica Acta*, 226, 84.

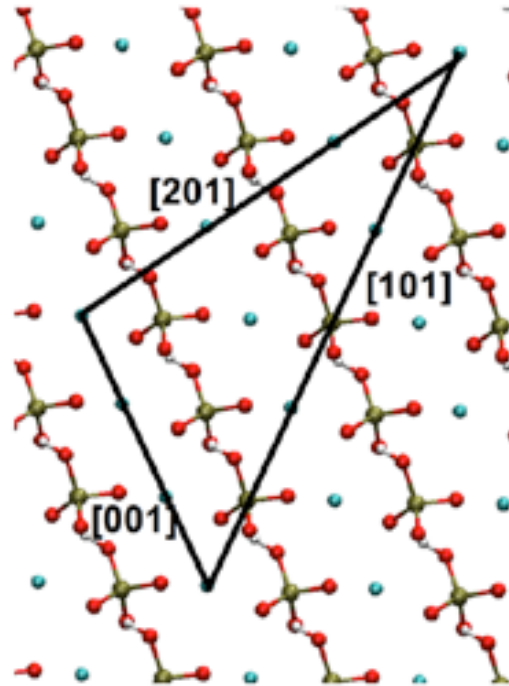


Simulation set up for HCl in aqueous solution (atom colors are green, red and pink for chlorine, oxygen and hydrogen, respectively).

Water structure, dynamics and ion adsorption at the aqueous {010} brushite surface

Understanding the growth processes of calcium phosphate minerals in aqueous environments has implications for both health and geology. Brushite, in particular, is a component of certain kidney stones and is used as a bone implant coating. Understanding the water-brushite interface at the molecular scale will help inform the control of its growth. Liquid-ordering and the rates of water exchange at the brushite-solution interface have been examined through the use of molecular dynamics simulation and the results compared to surface X-ray diffraction data. This comparison highlights discrepancies between the two sets of results, regardless of whether force field or first principles methods are used in the simulations, or the extent of water coverage. In order to probe other possible reasons for this difference, the free energies for the adsorption of several ions on brushite were computed. Given the exothermic nature found in some cases, it is possible that the discrepancy in the surface electron density may be caused by adsorption of excessions.

Garcia, N.A., Raiteri P., Vlieg E., Gale J.D. (2018). Water structure, dynamics and ion adsorption at the aqueous {010} brushite surface. *Minerals*, 8, 334.



One of the two Brushite {010} surfaces viewed from above with crystallographic directions indicated with solid black lines. Water is omitted for clarity. H is white, O is red, P is tan, and Ca is cyan.

Experimental crystal growth at the nanoscale

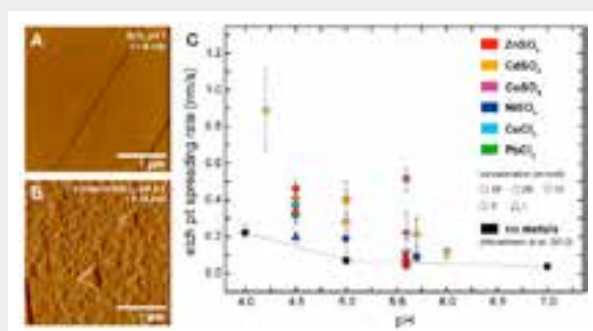
Computations and experiments are complementary and Atomic Force Microscopy (AFM) enables crystal growth to be observed in situ in a fluid cell at the nanoscale. The results of such experiments identify research questions that can be resolved with modelling techniques as well as provide constraints on the molecular modelling. In turn, molecular modelling provides the theoretical basis to explain the experimental observations. Some examples of published work during 2018 are given below.

Metal sequestration through coupled dissolution-precipitation at the brucite-water interface.

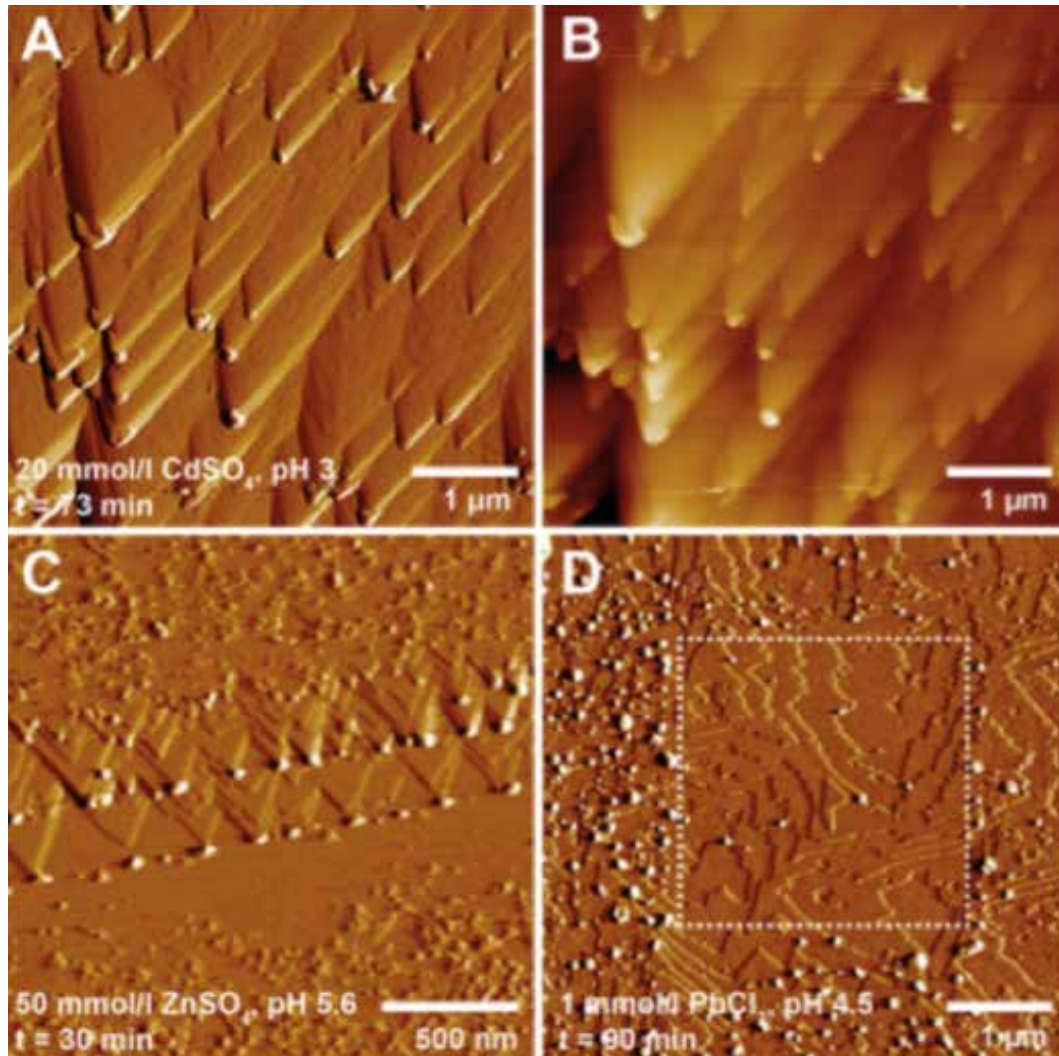
The increasing release of potentially toxic metals from industrial processes can lead to highly elevated concentrations of these metals in soil, and ground- and surface-waters. Today, metal pollution is one of the most serious environmental problems and thus, the development of effective remediation strategies is of paramount importance. In this context, it is critical to understand how dissolved metals interact with mineral surfaces in

soil-water environments. Here, we assessed the processes that govern the interactions between six common metals (Zn, Cd, Co, Ni, Cu, and Pb) with natural brucite ($\text{Mg}(\text{OH})_2$) surfaces. Using atomic force microscopy and a flow-through cell, we followed the coupled process of brucite dissolution and subsequent nucleation and growth of various metal bearing precipitates at a nanometer scale. Scanning electron microscopy and Raman spectroscopy allowed for the identification of the precipitates as metal hydroxide phases. Our observations and thermodynamic calculations indicate that this coupled dissolution-precipitation process is governed by a fluid boundary layer at the brucite-water interface. Importantly, this layer differs in composition and pH from the bulk solution. These results contribute to an improved mechanistic understanding of sorption reactions at mineral surfaces that control the mobility and fate of toxic metals in the environment.

Hövelmann J., Putnis C.V., Benning L.G. (2018). Metal sequestration through coupled dissolution-precipitation at the brucite-water interface. *Minerals*, 8, 346.



Brucite dissolution in the presence of dissolved metals. (A) In situ atomic force microscope (AFM) deflection image of a brucite (001) surface taken after 6 min in contact with pure water. (B) In situ AFM deflection image of a brucite surface taken after 24 min in contact with 1 mmol/L NiSO_4 , pH 4.5. The dissolution of brucite in acidic metal solutions resulted in the formation of triangular etch pits; (C) Comparison of etch pit spreading rates in the absence (black symbols) and presence (coloured symbols) of dissolved metals.



In situ atomic force microscopy (AFM) images of A deflection and B height images showing the nucleation of nanometer-size particles of $\text{Cd}(\text{OH})_2$ on a brucite ($\text{Mg}(\text{OH})_2$) surface in contact a solution of CdSO_4 (pH 3). C deflection image shows a surface of brucite in contact with a ZnSO_4 solution revealing the formation of 2 generations of nanoparticles formed along kink sites on a retreating brucite surface. D deflection image shows a brucite surface in contact with a PbCl_2 solution. The central area shows the position of previous scanning where the scanning tip was able to remove some of the particles, indicating that the particles were initially weakly attached to the surface. The precipitation of stable metal hydroxide particles has been shown to indicate the potential of a brucite surface to sequester metal contaminants in the environment.





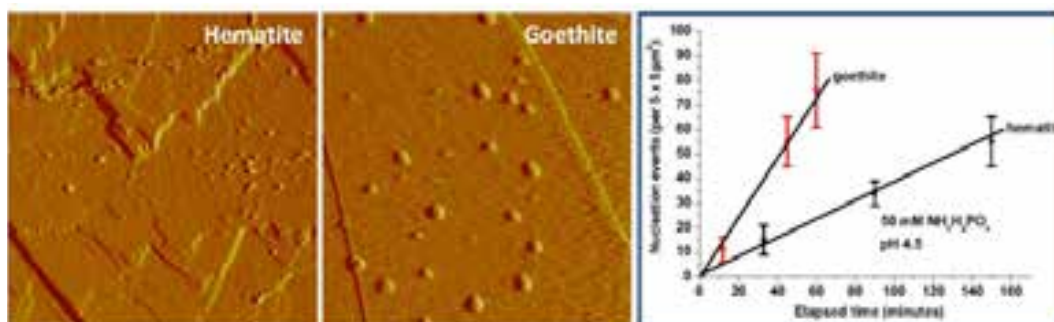
Interfacial precipitation of phosphate on hematite and goethite

Adsorption and subsequent precipitation of dissolved phosphates on iron oxides, such as hematite and goethite, is of considerable importance in predicting the bioavailability of phosphates. We used in situ atomic force microscopy (AFM) to image the kinetic processes of phosphate-bearing solutions interacting with hematite or goethite surfaces. The nucleation of nanoparticles (1.0–4.0 nm in height) of iron phosphate (Fe(III)-P) phases, possibly an amorphous phase at the initial stages, was observed during the dissolution of both hematite and goethite at the earliest crystallization stages. This was followed by a subsequent aggregation stage where larger particles and layered precipitates are formed under different pH values, ionic strengths, and organic additives. Kinetic analysis of the surface nucleation of Fe-P phases in 50 mM $\text{NH}_4\text{H}_2\text{PO}_4$ at pH 4.5 showed the nucleation rate was greater on goethite than hematite. Enhanced goethite and hematite dissolution in the presence of 10 mM AlCl_3 resulted in a rapid increase in Fe-P nucleation rates. A low concentration of citrate promoted the nucleation, whereas nucleation was inhibited at higher concentrations of citrate. By modeling using PHREEQC, calculated saturation indices (SI) showed that the three Fe(III)-P phases of cacoxenite, tenticite, and strengite may be supersaturated in the reacted solutions. Cacoxenite is predicted

to be more thermodynamically favorable in all the phosphate solutions if equilibrium is reached with respect to hematite or goethite, although possibly only amorphous precipitates were observed at the earliest stages. These direct observations at the nanoscale may improve our understanding of phosphate immobilization in iron oxide-rich acid soils.

Wang L., Putnis C.V., Hövelmann J., Putnis, A. (2018). Interfacial precipitation of phosphate on hematite and goethite. *Minerals*, 8, 207.

Two of the papers from 2018 (Hövelmann *et al.* and Wang *et al.*) were published in a special issue of the MDPI journal *Minerals*, Vol 8 “Mineral surface reactions at the nanoscale” (https://www.mdpi.com/journal/minerals/special_issues/Surface_Reactions) where Christine Putnis served as the guest editor. The special issue comprises 12 papers. All the contributions are connected by mineral surface reactions at the nanoscale and as such indicate the importance of detailed and careful analysis of mineral surfaces before, during and after reactions in aqueous fluids. The knowledge gained from interpretations of mineral surface reactivity spans a wide range of important Earth processes as well as potential environmental remediation. The mechanism highlighted in these contributions, whereby one mineral phase is replaced by another more stable phase, is interface-coupled dissolution-precipitation.



In situ Atomic Force Microscopy was used to image the kinetic processes of phosphate-bearing solutions interacting with hematite or goethite surfaces. The nucleation and growth of nanoparticles of iron phosphate phases were observed during the dissolution of both hematite and goethite at the earliest crystallisation stages.

Computational geoscience

Multiscale Modelling

In 2018, the group led by Prof Victor Calo published nineteen papers on the multiscale and multiphysics modelling of materials. The research group works on a wide range of topics. Some examples are given below.

Dispersion-minimized mass for isogeometric analysis

Deng and Calo (2018) introduce the dispersion-minimized mass for isogeometric analysis to approximate the structural vibration, which was modeled as a second-order differential eigenvalue problem. The dispersion-minimized mass reduces the eigenvalue error significantly, which leads to a more accurate method. The work establishes the dispersion error, where the leading error term is explicitly written in terms of the stiffness and mass entries, for arbitrary polynomial order isogeometric elements. The work also shows that the dispersion-minimized mass can also be obtained by approximating the mass matrix using optimally-blended quadratures. Generalization to higher-order methods are considered and discussed.

Deng Q., Calo V.M. (2018). Dispersion-minimized mass for isogeometric analysis. *Computer Methods in Applied Mechanics and Engineering*, 341, 71-92.

Spectral approximation of elliptic operators by the Hybrid High-Order method.

Calo *et al.* (2018) studied the approximation of the spectrum of a second-order elliptic differential operator by the Hybrid High-Order (HHO) method. The HHO method is formulated using cell and face unknowns which are polynomials. The key idea for the discrete eigenvalue problem is to introduce a discrete operator where the face unknowns have been eliminated. Using the abstract theory of spectral approximation of compact operators in Hilbert spaces, the work proves that the eigenvalues and eigenfunctions converge. The theoretical findings, which improve recent error estimates for Hybridizable Discontinuous Galerkin (HDG) methods, are verified on various numerical examples including smooth and non-smooth eigenfunctions. Moreover, the work reports superconvergence results numerically in one work reports superconvergence results numerically in one dimension for smooth eigenfunctions when using a specific value of the stabilization parameter.

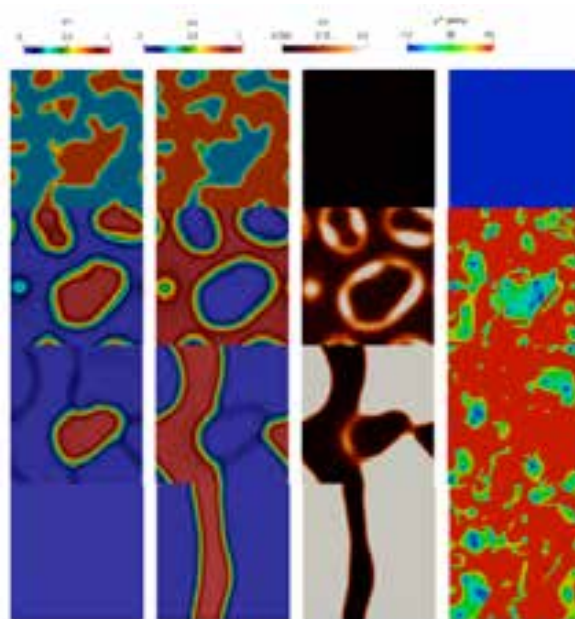
Calo V.M., Cicuttin M., Deng Q., Ern A. (2018). Spectral approximation of elliptic operators by the Hybrid High-Order method. *Mathematics of Computation*.

Modelling the effects of heterogeneous pressure in solids solutions far from equilibrium

Clavijo *et al.* (2018) studied chemically active solid solutions subject to mechanical effects due to heterogeneous stresses distributions driven by volume changes. In discussing systems undergoing volume changes, the thermodynamical pressure is identified as the conjugate power expenditure to this thermo-kinematic process, that is, change of volume versus thermodynamic pressure. The spherical part of the Cauchy tensor only provides the 'mechanical' contribution which is indeed an essential part of the thermodynamic pressure. Nevertheless, the spherical part of the Cauchy tensor does not represent a complete description of the pressure. Thermodynamically speaking, the thermodynamic pressure is defined as the negative variation of the Helmholtz free-energy with respect to the specific volume variations, and at the steady state, this thermodynamic pressure can be spatially

inhomogeneous. The latter entails that the system reaches equilibrium under non-hydrostatic stresses. To model these systems, they present a fully coupled thermodynamically-consistent framework for the chemo-mechanical responses of solid solutions. The Helmholtz free energy of a multicomponent elastic solid undergoing both mass transport and chemical reactions is described. The constitutive equations describe the evolution of the system towards equilibrium and satisfy the second law of thermodynamics by construction. Simulation results provide insights into understanding the heterogeneous pressure in metamorphic rocks and verify the interleaving between the chemical and mechanical that leads to inhomogeneous thermodynamic pressure.

Clavijo SP., Putnis A., Espath L., Fried E., Calo VM. (2018). Modelling the effects of heterogeneous pressure in solids solutions far from equilibrium. *Asia Oceania Geosciences Society*.



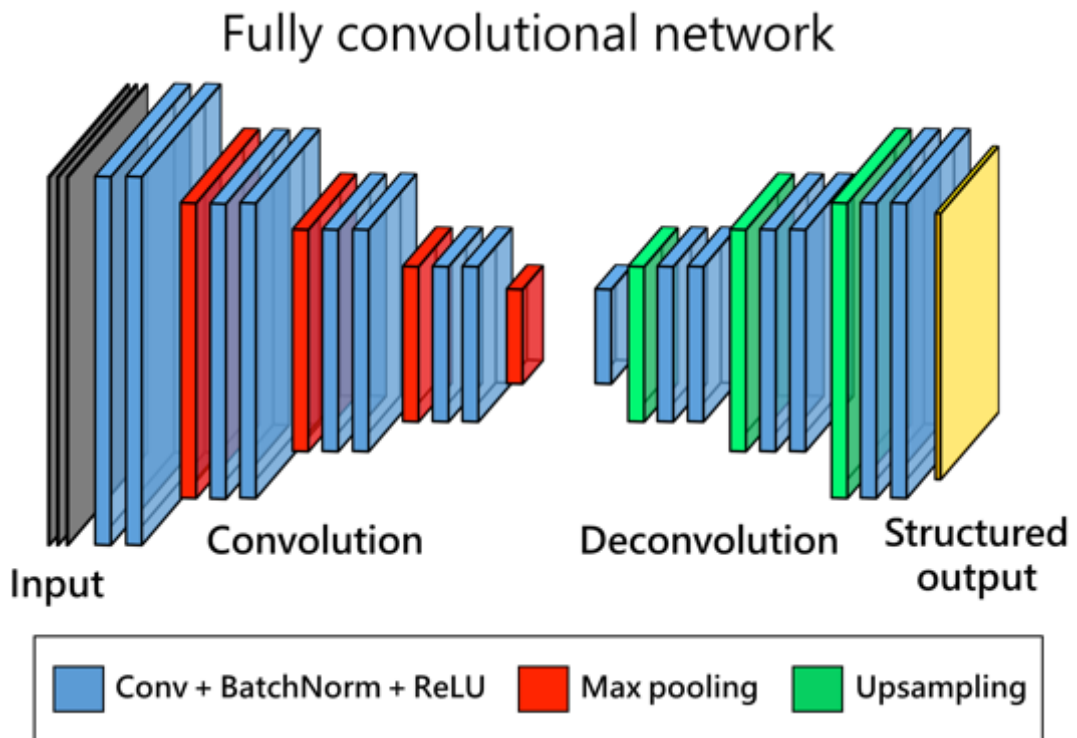
The evolution of a three phases system undergoing mass transport, a forward chemical reaction such as $A + B \rightarrow C$, and deformation. The concentrations ϕ_1 , ϕ_2 , and ϕ_3 represent the mass fraction of the phases A, B, and C, respectively. Moreover, p_{th} corresponds to the thermodynamic pressure.

Deep learning electromagnetic inversion with convolutional neural networks

Puzyrev (2018) proposes a new approach to electromagnetic inversion based on deep learning methods. While traditional techniques are largely based on deterministic methods, which are limited by nonlinearity and nonuniqueness of the inverse problem and require large computational resources, the proposed method avoids calculation of the gradient and provides results instantaneously. Deep neural networks

based on fully convolutional architecture are trained on large synthetic datasets obtained by full 3-D simulations. The performance is demonstrated on models of strong practical relevance representing an onshore controlled source electromagnetic CO₂ monitoring scenario. The method can reliably estimate the subsurface resistivity distribution in real time.

Puzyrev V. (2018) Deep learning electromagnetic inversion with convolutional neural networks. *arXiv:1812.10247*.



Puzyrev V. (2018) Deep learning electromagnetic inversion with convolutional neural networks. *arXiv:1812.10247*.



Labradorite partially replaced by non-iridescent feldspar.

Research reports

TIGeR
PUBLICATION
LIST 2018

TIGeR publication list 2018

Books

Awange JL (2018) GNSS Environmental Sensing. Revolutionizing Environmental Monitoring. Springer International Publishing AG. ISBN 978-3-319-58417-1, doi: 10.1007/978-3-319-58418-8.

Awange JL, Palancz B, Lewis R, Lajos V (2018) Mathematical Geosciences. Hybrid Symbolic-Numerical Solutions. Springer International Publishing AG. ISBN 978-3-319-58417-1, doi: 10.1007/978-3-319-67371-4.

Book Chapters

Blum T.B., Darling J.R., Kelly T.F., Larson D.J., Moser D.E., Perez-Huerta A., Prosa T.J., Reddy S.M., Reinhard D.A., Saxey D.W., Ulfing R.M., Valley J.W. (2018). Best practices for reporting atom probe analysis of geological materials. *Microstructural Geochronology: Planetary Records Down to Atom Scale*, 369–373. AGU/Wiley Publishing.

Cavosie, A.J., Erickson, E.M., Montalvo, P.E., Prado, D.C., Cintron, N.O., and Gibbon, R.J. (2018). The Rietputs Formation in South Africa: A Pleistocene Fluvial Archive of Meteorite Impact Unique to the Kaapvaal Craton. In: Moser, D.E., Corfu, F., Reddy, S.M., Darling, J., and Tait, K., (eds) *Microstructural Geochronology; Lattice to Atom-Scale Records of Planetary Evolution*. AGU Geophysical Monograph. AGU-Wiley, New Jersey, p. 203-224.

Ding, M., Zhang, N., 2018. Early Geologic History of the Moon. In: Cudnik B. (eds), *Encyclopedia of Lunar Science*. Springer. https://doi.org/10.1007/978-3-319-05546-6_8-1

Imparato, D., El-Mowafy, A. and Rizos, C. (2018). Positioning Integrity Monitoring: from Aviation to Land Applications, Chapter 2, Book: *Multifunctional Operation and Application of GPS*. InTech Publisher, ISBN 978-1-78923-214-1.

Kusiak M.A., Wilde S.A., Wirth R., Whitehouse M.J., Dunkley D.J., Lyon I., Reddy S.M., Berry A., De Jonge M. (2018). Detecting micro- and nano-scale variations in element mobility in high-grade metamorphic rocks: implication for precise U-Pb dating of zircon. *Microstructural Geochronology: Planetary Records Down to Atom Scale*, 279–291. AGU/Wiley Publishing.

Moser D., Corfu F., Darling J., Reddy S.M., Tait. K. (eds.). (2018). *Microstructural Geochronology: Planetary Records Down to Atom Scale*, Geophysical Monograph 232, AGU/Wiley Publishing. pp. 373.

Saxey D. W., Reddy S.M., Fougereuse D., Rickard W.D. (2018). The Optimization of Zircon Analyses by Laser-Assisted Atom Probe Microscopy: Insights from the 91500 Zircon Standard. *Microstructural Geochronology: Planetary Records Down to Atom Scale*, 293–313. AGU/Wiley Publishing

Refereed Publications

- Ai N., He S., Li N., Zhang Q., Rickard W.D.A., Chen K., Zhang T., Jiang S.P. (2018). Suppressed Sr segregation and performance of directly assembled $\text{La}_{0.6}\text{Sr}_{0.4}\text{Co}_{0.2}\text{Fe}_{0.8}\text{O}_{3-\delta}$ oxygen electrode on $\text{Y}_2\text{O}_3\text{-ZrO}_2$ electrolyte of solid oxide electrolysis cells. *Journal of Power Sources*, 384, 125-135.
- Aitken, C.M., Head, I.M., Jones, D.M., Rowland, S.J., Scarlett, A.G., West, C.E., 2018. Comprehensive two-dimensional gas chromatography-mass spectrometry of complex mixtures of anaerobic bacterial metabolites of petroleum hydrocarbons. *Journal of Chromatography A*, 1536, 96-109.
- Alessio, B., Blades, M., Murray G., Thorpe B., Collins A.S., Kelsey D.E, Foden J., Payne J., Al-Khribash S., and Jourdan F. 2018. "Origin and tectonic evolution of the NE basement of Oman: a window into the Neoproterozoic accretionary growth of India?" *Geological Magazine* 155 (July): 1150-74.
- Ameen, S.M.M., Wilde, S.A. (2018). Multiple sources for Archean granitoids in the Yalgoo area, Yilgarn Craton, Western Australia: Geochemical and isotopic evidence. *Precambrian Research*, 314, 76-110.
- Antill, L.M., Beardmore, J.P., Woodward, J.R., 2018. Time-resolved optical absorption microspectroscopy of magnetic field sensitive flavin photochemistry. *Review of Scientific Instruments*, 89, 023707
- Anyah R.O., Forootan E., Awange J.L., Khaki M. (2018) Understanding linkages between global climate indices and terrestrial water storage changes over Africa using GRACE products. *Science of the Total Environment* 635: 1405-1416.
- Archibald D., Murphy B., Reddy S.M., Jourdan F., Gillispie J., Glorie S. Post-accretionary uplift of the Meguma Terrane relative to the Avalon Terrane in the Canadian Appalachians. *Tectonophysics* 747, 343-356. 2018.
- Armandola S., Barham M., Reddy S.M., Clark C., Spinks, S. (2018). Footprint of a large intracontinental rifting event, zircon geochronology from the Mesoproterozoic Collier Basin, Western Australia. *Precambrian Research*, 318, 156-169.
- Awange J.L. (2018): Environmental Geodesy: state of the art. In: A. Heck, K. Seitz, T. Grombein, M. Mayer, J.-M. Stövhase, H. Sumaya, M. Wampach, M. Westerhaus, L. Dalheimer, P. Senger (ed.): (Schw)Ehre, wem (Schw)Ehre gebührt - Festschrift zur Verabschiedung von Prof. Dr.-Ing. Dr. h.c. Bernhard Heck: 19-28; Schriftenreihe des Studiengangs Geodäsie und Geoinformatik, vol. 2018-1, Karlsruhe (KIT Scientific Publishing), doi: 10.5445/KSP/1000080205.
- Awange J.L., Paláncz B., Völgyesi L., Rózsa S (2018): Hybrid symbolic-numeric methods in geosciences. In: A. Heck, K. Seitz, T. Grombein, M. Mayer, J.-M. Stövhase, H. Sumaya, M. Wampach, M. Westerhaus, L. Dalheimer, P. Senger (ed.): (Schw)Ehre, wem (Schw)Ehre gebührt - Festschrift zur Verabschiedung von Prof. Dr.-Ing. Dr. h.c. Bernhard Heck: 19-28; Schriftenreihe des Studiengangs Geodäsie und Geoinformatik, vol. 2018-1, Karlsruhe (KIT Scientific Publishing), doi: 10.5445/KSP/1000080205.

- Aylmore M.G., Merigot K., Quadir Z., Rickard W.D.A., Evans N.J., McDonald B.J., Catovic E., Spitalny P. (2018). Applications of advanced analytical and mass spectrometry techniques to the characterisation of micaceous lithium-bearing ores. *Minerals Engineering*, 116, 182-195.
- Aylmore M.G., Merigot K., Rickard W.D.A., Evans N.J., McDonald B.J., Catovic E., Spitalny P. (2018). Assessment of a spodumene ore by advanced analytical and mass spectrometry techniques to determine its amenability to processing for the extraction of lithium. *Minerals Engineering*, 119, 137-148.
- Bachtadse, V., Aubele, K., Muttoni, G., Ronchi, A., Kirscher, U., Kent, D.V., 2018. New early Permian paleopoles from Sardinia confirm intra-Pangea mobility. *Tectonophysics*, 749, 21-34.
- Bai Y., Dong D., Kirby J.F., Williams S.E., Wang Z. (2018). The effect of dynamic topography and gravity on lithospheric effective elastic thickness estimation: a case study. *Geophysical Journal International*, 214, 623-634.
- Barham M., Reynolds S., Kirkland C.L., O'Leary M.J., Evans N.J., Allen H., Haines P.W., Hocking R.M. and McDonald B.J. (2018). Sediment routing and basin evolution in Proterozoic to Mesozoic east Gondwana: a case study from southern Australia. *Gondwana Research*, 58, 122-140.
- Barton M., Calo V., Deng Q., Puzyrev V. (2018). Generalization of the Pythagorean eigenvalue error theorem and its application to isogeometric analysis. *Numerical methods for PDEs. Lectures from the fall 2016 thematic quarter at Institut Henri Poincaré*, Eds: Di Pietro, D., Ern, A., Formaggia, L., SEMA-SIMAI Series, Springer 15, 147-170.
- Beinlich A., Austrheim H., Mavromatis V., Grguric B., Putnis C.V., Putnis A. (2018). Peridotite weathering is the missing ingredient of Earth's continental crust composition. *Nature communications*, 9, 634.
- Bellucci, J. J., A. A. Nemchin, M. J. Whitehouse, J. F. Snape, P. Bland, G. K. Benedix, and J. Roszjar. 2018. Pb evolution in the Martian mantle. *Earth and Planetary Science Letters* 485 (March): 79–87. doi:10.1016/j.epsl.2017.12.039.
- Bellucci, J. J., A. A. Nemchin, M. J. Whitehouse, R. B. Kielman, J. F. Snape, and R. T. Pidgeon. 2018. Geochronology of Hadean zircon grains from the Jack Hills, Western Australia constrained by quantitative scanning ion imaging. *Chemical Geology* 476 (January): 469–80. doi:10.1016/j.chemgeo.2017.11.042.
- Bhattacharya, S., Kemp, A.I.S., Collins, W.J. (2018). Response of zircon to melting and metamorphism in deep arc crust, Fiordland (New Zealand): implications for zircon inheritance in cordilleran granites. *Contributions to Mineralogy and Petrology*, 173:28
- Bhowany, K., Hand, M., Clark, C., Kelsey, D. E., Reddy, S. M., Pearce, M. A., . . . Morrissey, L. J. (2018). Phase equilibria modelling constraints on P-T conditions during fluid catalysed conversion of granulite to eclogite in the Bergen Arcs, Norway. *Journal of Metamorphic Geology*, 36(3), 315-342. doi:10.1111/jmg.12294

- Bouvier, Laura C., Maria M. Costa, James N. Connelly, Ninna K. Jensen, Daniel Wielandt, Michael Storey, Alexander A. Nemchin, *et al.* (2018). "Evidence for extremely rapid magma ocean crystallization and crust formation on Mars." *Nature* 558 (June): 568–89. doi:10.1038/s41586-018-0222-z.
- Breckenridge, J., Maravelis, A.G., Catuneanu, O., Ruming, K., Holmes, E., Collins, W.J. (2018). Outcrop analysis and facies model of an Upper Permian tidally influenced fluviodeltaic system: Northern Sydney Basin, SE Australia. *Geological Magazine* <https://doi.org/10.1017/S0016756818000973>
- Brown, M. & Johnson, T.E. (2018). Invited Centennial Article: Secular change in metamorphism and the onset of global plate tectonics. *American Mineralogist*, 103, 181–196.
- Brown, N.J., McCubbine J.C., Featherstone W.E., Woods A., Baran I., Gowans, N. (2018). AUSGeoid2020 Combined Gravimetric-geometric Model with Location-specific Uncertainties and Baseline-length-dependent Error Decorrelation. *Journal of Geodesy*, 92, 1457-1465, 1467.
- Bucha B., Hirt C., Kuhn M. (2018). Divergence-free spherical harmonic gravity field modelling based on the Runge-Krarp theorem: a case study for the Moon. *Journal of Geodesy*, <https://doi.org/10.1007/s00190-018-1177-4>.
- Calo V.M., Cicuttin M., Deng Q., Ern A. (2018). Spectral approximation of elliptic operators by the Hybrid High-Order method. *Mathematics of Computation*.
- Calo VM., Badia S., Principe J. (2018). Algorithmic Aspects of High-Performance Computing for Mechanics and Physics. *Journal of Computational and Applied Mathematics*. 100, 739.
- Calo VM., Iliev O., Nunes SP., Printsypar G., Shi M. (2018). Cell-element simulations to optimize the performance of osmotic processes in porous membranes. *Computers & Mathematics with Applications*. 76, 361-376.
- Cammack, J. N., M. J. Spicuzza, A. J. Cavosie, M. J. Van Kranendonk, A. H. Hickman, R. Kozdon, I. J. Orland, K. Kitajima, and J. W. Valley. 2018. "SIMS microanalysis of the Strelley Pool Formation cherts and the implications for the secular-temporal oxygen-isotope trend of cherts." *Precambrian Research* 304 (January): 125–39. doi:10.1016/j.precamres.2017.11.005.
- Cao M.J., Evans N.J., Hollings P., Cooke D.R., McInnes B.I.A., Qin K.Z. and L, G.M. (2018). Phenocryst Zonation in Porphyry-related rocks of the Baguio District, Philippines: Evidence for magmatic and metallogenic processes. *Journal of Petrology*, 59(5), 825-848.
- Cao M.J., Qin K., Li G.M., Evans N.J., Li J.X and Zhao J.X. (2018). Oxidation state inherited from the magma source and implications for mineralization: Late Jurassic to Early Cretaceous granitoids, central Lhasa subterane, Tibet. *Mineralium Deposita*. 53(3), 299-309. (IF = 2.561)
- Cavosie, A. J., Timms, N. E., Ferrière, L., Rochette, P. (2018). FRIGN zircon—The only terrestrial mineral diagnostic of high-pressure and high-temperature shock deformation. *Geology*, 46, 891-894.

- Cavosie, A.J. (2018). The Enduring Mystery of Australasian Tektites. *Elements*, 14,
- Cavosie, A.J., Timms, N.E., Erickson, T.M., Koeberl, C. (2018). New clues from Earth's most elusive impact crater: Evidence of reidite in Australasian tektites from Thailand. *Geology*, 46, 203–206.
- Cavosie, A.J., Valley, J.W., Wilde, S.A. (2018). The oldest terrestrial mineral record: Thirty years of research on Hadean zircon from Jack Hills, Western Australia. In: *Earth's Oldest Rocks (2nd Edition)*, Van Kranendonk, M.J., Bennett, V. C., Hoffman, J.E. (Eds), Elsevier, pp. 255-278.
- Cawood P.A., Hawkesworth C.J., Pisarevsky S.A., Dhuime B., Capitanio F.A., Nebel O. (2018). Geological archive of the onset of plate tectonics. *Phil. Trans. R. Soc. A* 376: 20170405,
- Centrella S., Putnis A., Lanari P. and Austrheim H. Textural and chemical evolution of pyroxene during hydration and deformation: a consequence of retrograde metamorphism. *Lithos* 296-299, 245-264 (2018)
- Cesar, J. and Grice K. (2018) Drimane-type compounds in source rocks and fluids from fluvial-deltaic depositional settings in the North-West Shelf of Australia. *Organic Geochemistry* 116, 103-112
- Chen K., He S., Li N., Cheng Y., Ai N., Chen M., Rickard W.D.A., Zhang T., Jiang S.P. (2018). Nb and Pd co-doped $\text{La}_{0.57}\text{Sr}_{0.38}\text{Co}_{0.19}\text{Fe}_{0.665}\text{Nb}_{0.095}\text{Pd}_{0.05}\text{O}_{3-\delta}$ as a stable, high performance electrode for barrier-layer-free $\text{Y}_2\text{O}_3\text{-ZrO}_2$ electrolyte of solid oxide fuel cells. *Journal of Power Sources*, 378, 433-442.
- Chen M., Cheng Y., He S., Ai N., Veder J.-P., Rickard W.D.A., Saunders M., Chen K., Zhang T., Jiang S.P. (2018). Active, durable bismuth oxide-manganite composite oxygen electrodes: Interface formation induced by cathodic polarization. *Journal of Power Sources*, 397, 16-24.
- Christeson, G. L., S. P. S. Gulick, J. V. Morgan, C. Gebhardt, D. A. et al. (2018). Extraordinary rocks from the peak ring of the Chicxulub impact crater: P-wave velocity, density, and porosity measurements from IODP/ICDP Expedition 364. *Earth and Planetary Science Letters* 495: 1-11.
- Clark, C., Taylor, R. J. M., Kylander-Clark, A. R. C., & Hacker, B. (2018). Prolonged (>100 Ma) ultrahigh temperature metamorphism in the Napier Complex, East Antarctica: A petrochronological investigation of Earth's hottest crust. *Journal of Metamorphic Geology*, 36(9), 1117-1139.
- Clavijo SP., Putnis A., Espath L., Fried E., Calo VM. (2018). Modelling the effects of heterogeneous pressure in solids solutions far from equilibrium. *Asia Oceania Geosciences Society*.
- Collins, W.J., Purdy, D. J. (2018) Evolution of the Southern Thomson Orogen and environs: evaluating the missing link of the Tasmanides. *Australian Journal of Earth Sciences*, 65, 889-891.
- Corbett M. K., Eksteen J. J., Niu X-Z., Watkin E.L.J. (2018). Syntrophic Effect of Indigenous and Inoculated Microorganisms in the Leaching of Rare Earth Elements from Western Australian Monazite. *Research in Microbiology* 169;558-568.

- Corbett M. K., Watkin E. L. J. (2018). Microbial cooperation improves bioleaching recovery rates. *Microbiology Australia*. Published online 16 February 2018
- Cox, M.A., Cavosie, A.J., Bland, P.A., Miljković, K., and Wingate, M.T.D. (2018). Crustal Dynamics of Central Uplifts Revealed: Reidite Off-set by Zircon Twins at the Woodleigh Impact Structure, Australia. *Geology*, 46, 983-986. Cox, G.M., Lyons, T.W., Mitchell, R.N., Hasteroka, D., Garda, M., 2018. Linking the rise of atmospheric oxygen to growth in the continental phosphorus inventory. *Earth and Planetary Science Letters*, 489, 28-36.
- Cox, M.A., Cavosie A.J., Bland P.A., Miljković K., and Wingate M.T.D.. 2018. Microstructural dynamics of central uplifts: Reidite offset by zircon twins at the Woodleigh impact structure, Australia." *Geology* 46 (November): 983-86.
- Crede, L.S., Rempel, K.U., Hu, S.Y., Evans, K.A., (2018). An experimental method for gold partitioning between two immiscible fluids: Brine and n-dodecane. *Chemical Geology* 501, 35-50.
- Crossley, R.J., Evans, K.A., Jeon, H., Kilburn, M.R., (2018). Insights into sulfur cycling at subduction zones from in-situ isotopic analysis of sulfides in high-pressure serpentinites and 'hybrid' samples from Alpine Corsica. *Chemical Geology* 493, 359-378.
- Cucciniello C., le Roex A., Jourdan F., Morra V., Grifa C., Franciosi L. and Melluso L.. Late Cenozoic non-plume volcanism in SW Madagascar (Ankililoaka district, Tulear): 40Ar/39Ar ages, geochemistry, tectonic setting and comparisons with the Cretaceous volcanic rocks. *Journal of the Geological Society* 175, 627-641. 2018.
- Cumberland, S.A., Etschmann, B., Brugger, J., Douglas, G., Evans, K.A., Fisher, L., Kappen, P., Moreau, J.W., (2018). Characterization of uranium redox state in organic-rich Eocene sediments. *Chemosphere* 194, 602-613.
- Daczko N.R., Halpin J.A., Fitzsimons I.C.W., Whittaker J.M. (2018). A cryptic Gondwana-forming orogen located in Antarctica. *Scientific Reports*, 8(1), 8371. <http://doi.org/10.1038/s41598-018-26530-1>
- Dallanave, E., Kirscher, U., Hauck, J., Hesse, R., Bachtadse, V., Wortmann, U.G., 2018. Paleomagnetic time and space constraints of the Early Cretaceous Rhenodanubian Flyschzone (Eastern Alps). *Geophysical Journal International*, ggy077. <https://doi.org/10.1093/gji/ggy077>
- Daly L., Bland P.A., Tessalina S., Saxey D.W., Reddy S.M., Fougereuse D., Rickard W.D.A., Forman L.V., Fontaine A.L., Cairney J.M., Ringer S.P., Schaefer B.F., Schwander D. (2018). Defining the Potential of Nanoscale Re-Os Isotope Systematics Using Atom Probe Microscopy. *Geostandards and Geoanalytical Research*, 42 (3), 279-299.
- Daubar, Ingrid, Philippe Lognonné, Nicholas A. Teanby, Katarina Miljkovic, Jennifer Stevanović, Jeremie Vaubaillon, Balthasar Kenda, et al. 2018. Impact-Seismic Investigations of the InSight Mission. *Space Science Reviews* 214 (December): 132. doi:10.1007/s11214-018-0562-x.
- De Gromard R.Q., Kirkland C.L., Howard H.M., Smithies R.H., Wingate M.T.D., Jourdan, F., McInnes B.I.A., Danisik M., Evans N.J., and McDonald B.J. (2018). Will it ever end? long lived intracontinental compressional in central Australia. *Geoscience Frontiers Special Issue "Timescale of geological processes"*. 10(1), 149-164. doi. org/10.1016/j.gsf.(2018).09.003

- De Silva D., Gerald Swor, Evans N.J. and Nummer T. (2018). (U-Th)/He ages from the fluorite mineralization of the Tangua alkaline intrusion. *Anuario do Instituto de Geociencias UFRJ*, Vol 41(2), 14-21.
- Delle Piane C., Raven M.D., Bourdet J., Clennell M.B., Rickard W.D.A., Saunders M., Sherwood N., Li Z., Dewhurst D.N. (2018). Organic matter network in post-mature Marcellus Shale: Effects on petrophysical properties. *AAPG Bulletin*, 102, 2305-2332.
- Delle Piane, C., Piazzolo, S., Timms, N.E., Luzin, V., Saunders, M., Bourdet, J., Giwelli, A., Ben Clennell, M., Kong, C., Rickard, W.D. Verrall, M. (2018). Generation of amorphous carbon and crystallographic texture during low-temperature subseismic slip in calcite fault gouge. *Geology*, 46, 163-166.
- Dallanave, E., Kirscher, U., Hauck, J., Hesse, R., Bachtadse, V., Wortmann, U.G., 2018. Paleomagnetic time and space constraints of the Early Cretaceous Rhenodanubian Flyschzone (Eastern Alps). *Geophysical Journal International*, ggy077. <https://doi.org/10.1093/gji/ggy077>
- Demichelis, R., Garcia N.A., Raiteri P., Innocenti Malini R., Freeman C.L, Harding J.H., Gale J.D. (2018). Simulation of Calcium Phosphate Species in Aqueous Solution: Force Field Derivation. *Journal of Physical Chemistry B*, 122, 1471-1483.
- Demichelis, R., Schuitemaker A., Garcia N.A., Koziara K.B., De La Pierre M., Raiteri P., Gale J.D. (2018). Simulation of crystallization of biominerals. *Annual Review of Materials Research*, 48, 327-352.
- Deng Q., Barton M., Puzyrev V., Calo V.M. (2018). Dispersion-minimizing quadrature rules for C1 quadratic isogeometric analysis. *Computer Methods in Applied Mechanics and Engineering*, 328, 554-564.
- Deng Q., Calo V.M. (2018). Dispersion-minimized mass for isogeometric analysis. *Computer Methods in Applied Mechanics and Engineering*, 341, 71-92.
- Deng Q., Puzyrev V., Calo V. (2018). Isogeometric spectral approximation for elliptic differential operators. *Journal of Computational Science (In Press)*. doi.org/10.1016/j.jocs.2018.05.009.
- Deo M., El-Mowafy A. (2018). Comparison of Advanced Troposphere Models for Aiding Reduction of PPP Convergence Time in Australia, *Journal of Spatial Science, Journal of Spatial Science*, doi.org/10.1080/14498596.2018.1472046
- Deo, M. and El-Mowafy (2018). Triple-frequency GNSS models for PPP with float ambiguity estimation: performance comparison using GPS. *Survey Review*. 50-(360), 249-261. doi.org/10.1080/00396265.2016.1263179
- Devillepoix, Hadrien A. R., Eleanor K. Sansom, Philip A. Bland, Martin C. Towner, Martin Cupák, Robert M. Howie, Trent Jansen-Sturgeon, et al. 2018. The Dingle Dell meteorite: A Halloween treat from the Main Belt. *Meteoritics and Planetary Science* 53 (October): 2212-27.
- Dew R.E.C., Collins A.S., Glorie S., Morley C.K., King R., Foden H., De Grave, J., Kanjanapayont P., Evans N.J., Alessio B.L. and Charusiri P. (2018). Probing Thailand's basement: New insights from U-Pb geochronology, Sr, Sm-Nd, Pb and Lu-Hf isotopic systems. *Lithos* 320-321, 332-354.

- Dew R.E.C., Nachtergaele S., Collins A.S., Glorie S., Foden J.D., De Grave J., Blades M.L., Morley C.K., Evans N.J., Alessio B.L., Kanjanapayont P., King R., and Charusiri P. (2018). Analysis of the U-Pb geochronology and Lu-Hf system in zircon and whole-rock Sr, Sm-Nd and Pb isotopic systems for the granitoids of Thailand. *Data in Brief*, [https://doi.org/10.1016/j.dib.\(2018\).10.176](https://doi.org/10.1016/j.dib.(2018).10.176)
- Dogra, Y., Scarlett, A.G., Rowe, D., Galloway, T.S., Rowland, S.J., 2018. Predicted and measured acute toxicity and developmental abnormalities in zebrafish embryos produced by exposure to individual aromatic acids. *Chemosphere*, 205, 98-107.
- Donskaya T.V., Gladkochub D.P., Ernst R. E., Pisarevsky S. A., Mazukabzov A. M., Demonterova E. I. (2018). Geochemistry and petrogenesis of Mesoproterozoic Dykes of the Irkutsk Promontory, southern part of the Siberian Craton. *Minerals*, 8, 545, doi:10.3390/min8120545
- Donskaya T.V., Gladkochub D.P., Mazukabzov A. M., Denyszyn S., Pisarevsky S. A., Motova Z.L., Demonterova E. I. (2018). The oldest (~1.9 Ga) metadolerites of the southern Siberian craton: age, petrogenesis, and tectonic setting. *Russian Geology and Geophysics*, 59, 1548-1559.
- Doucet, L.S., Laurent, O., Mattielli, N., Debouge, W., 2018. Zn isotope heterogeneity in the continental lithosphere: New evidence from Archean granitoids of the northern Kaapvaal craton, South Africa. *Chemical Geology*, 476, 260-271. <https://doi.org/10.1016/j.chemgeo.2017.11.022>
- Dwyer, R.C., Collins, W.J., Hack, A.C., Hegarty, R., Huang, H-Q. (2018) Age and tectonic significance of the Louth Volcanics: implications for the evolution of the Tasmanides of eastern Australia, *Australian Journal of Earth Sciences*, 65, 1049-1069, DOI: 10.1080/08120099.2018.1469392
- Egorov A., Correa J., Bona A., Pevzner R., Tertyshnikov K., Glubokovskikh S., Puzyrev V., Gurevich B. (2018). Elastic full waveform inversion of vertical seismic profile data acquired with distributed acoustic sensors. *Geophysics*, 83 (3), R273-R281.
- El-Mowafy, A. (2018) A New Model for Precise Point Positioning to Improve Fault Detection, Proceedings IGSS Symposium 2018, Sydney, 7 – 9 February 2018, 1-9.
- El-Mowafy, A. (2018). Predicting Real-Time Orbit and Clock Corrections for Positioning Using GPS, GLONASS and QZSS in Natural Hazard Warning Systems, *Journal of Applied Geodesy*, DOI: 10.1515/jag-2018-0043.
- El-Mowafy, A. (2018). Real-Time Precise Point Positioning Using Orbit and Clock Corrections as Quasi-Observations for Improved Detection of Faults. *J. of Navigation*, 71(4), 769-787.
- El-Mowafy, A., Imperato, D. (2018). Positioning Integrity, Availability and Precision for Journey Planning and Navigation Using GNSS Integrated with Low-Cost Sensors. In the 31st International Technical Meeting of The Satellite Division of the Institute of Navigation (ION GNSS+ 2018), Sep 20-24, 2018, Miami, Florida, *The Institute of Navigation*. 2642 – 2653.

- El-Mowafy, A., Kubo, N. (2018) Integrity monitoring for Positioning of intelligent transport systems using integrated RTK-GNSS, IMU and vehicle odometer, *IET Intelligent Transport Systems* 12(8): 901–908. DOI: 10.1049/iet-its.2018.0106.
- Exertier F., La Fontaine A., Corcoran C., Piazzolo S., Belousova E., Peng Z., Gault B., Saxey D.W., Fougereuse D., Reddy S.M. (2018). Atom probe tomography analysis of the reference zircon gj-1: An interlaboratory study. *Chemical Geology*, 495, 27–35.
- Fathollahzadeh H., Eksteen J.J., Kaksonen A.H., Watkin E.L.J. (2018). Role of microorganisms in bioleaching of rare earth elements from primary and secondary resources. *Applied Microbiology and Biotechnology* <https://doi.org/10.1007/s00253-018-9526-z>
- Fathollahzadeh H., Hackett M.J., Khaleque H.N., Eksteen J.J., Kaksonen A.H., Watkin E.L.J. (2018). Better together: Potential of co-culture microorganisms to enhance bioleaching of rare earth elements from monazite. *Bioresource Technology Reports* 3 (2018)109–118
- Fathollahzadeh H., Eksteen J.J., Kaksonen A.H., Niu X-Z., Watkin E.L.J. (2018). Microbial Contact Enhances Bioleaching of Rare Earth Elements. *Bioresource Technology Reports* 3 (2018) 102–108
- Featherstone W.E., Brown N.J., McCubbine J.C., Filmer M.S. (2018) Description and release of Australian gravity field model testing data. *Australian Journal of Earth Sciences*, 65(1): 1-7.
- Featherstone W.E., McCubbine J.C., Brown N.J., Claessens S.J., Filmer M.S., Kirby J.F. (2018) The first Australian gravimetric quasigeoid model with location-specific uncertainty estimates. *Journal of Geodesy*, 92(2):149-168.
- Feisel, Y., White, R.W., Palin, R.M. & Johnson, T.E. (2018). New constraints on granulite-facies metamorphism and melt production in the Lewisian Complex, northwest Scotland. *Journal of Metamorphic Geology*, 36, 799–819.
- Filmer M.S., Hughes C.W., Woodworth P.L., Featherstone W.E., Bingham R.J. (2018) Comparison between the geodetic and oceanographic approaches to estimate mean dynamic topography for vertical datum unification. *Journal of Geodesy*, 92(12): 1413–1437.
- Foivos K., Rakoto V., Lognonné P., Larmat C., Daubar I., and Miljković K.. 2018. “Inversion of Meteor Rayleigh Waves on Earth and Modeling of Air Coupled Rayleigh Waves on Mars.” *Space Science Reviews* 214 (December): 127. doi:10.1007/s11214-018-0566-6.
- Fougereuse D., Reddy S.M., Saxey D.W., Erickson T.M., Kirkland C.L., Rickard W.D.A., Seydoux-Guillaume A.M., Clark C., Buick I.S. (2018). Nanoscale distribution of Pb in monazite revealed by atom probe microscopy. *Chemical Geology*, 479, 251–258.
- Fu, D., Huang, B, Kusky, T., Li, G.Z., Wilde, S.A., Zhou, W.X., Yu, Z. (2018). A Middle Permian Ophiolitic Melange Belt in the Solonker Suture Zone, Western Inner Mongolia, China: Implications for the Evolution of the Paleo-Asian Ocean. *Tectonics*, 37, 1292-1320.

- Garcia D., Ghommem M., Collier N., Varga BON., Calo V.M. (2018). PyFly: A fast, portable aerodynamics simulator. *Journal of Computational and Applied Mathematics*, 334, 875-903.
- Garcia D., Pardo D., Dalcin L., Calo VM. (2018). Refined isogeometric analysis for a preconditioned conjugate gradient solver. *Computer Methods in Applied Mechanics and Engineering*, 335, 490-509.
- Garcia, N.A., Raiteri P., Vlieg E., Gale J.D. (2018). Water structure, dynamics and ion adsorption at the aqueous {010} brushite surface. *Minerals*, 8, 334.
- Gardiner, N. J., Hickman, A. H., Kirkland, C. L., Lu, Y., Johnson, T. E. & Zhao, J-X. (2017). Processes of crust formation in the early Earth imaged through Hf isotopes from the East Pilbara Terrane. *Precambrian Research*, 297, 56-76.
- Gardiner, N. J., Johnson, T. E., Kirkland, C. L., and Smithies, R. H., 2018a, Melting controls on the lutetium-hafnium evolution of Archaean crust: *Precambrian Research*, v. 305, p. 479-488.
- Gardiner, N. J., Maidment, D. W., Kirkland, C. L., Bodorkos, S., Smithies, R. H., and Jeon, H., 2018b, Isotopic insight into the Proterozoic crustal evolution of the Rudall Province, Western Australia: *Precambrian Research*, v. 313, p. 31-50.
- Gardiner, N. J., Searle, M. P., Morley, C. K., Robb, L. J., Whitehouse, M. J., Roberts, N. M. W., Kirkland, C. L., and Spencer, C. J., 2018c, The crustal architecture of Myanmar imaged through zircon U-Pb, Lu-Hf and O isotopes: Tectonic and metallogenic implications: *Gondwana Research*, v. 62, p. 27-60.
- Ge, R., Wilde, S.A., Nemchin, A.A., Whitehouse, M.J., Bellucci, J.J., Erickson, T.M., Frew, A., Thern, E.R. (2018). A 4463 Ma apparent zircon age from the Jack Hills (Western Australia) resulting from ancient Pb mobilization. *Geology*, 46, 303-306.
- Ge, R.F., Zhu, W.B., Wilde, S.A. (2018). Remnants of Eoarchean continental crust derived from a subducted proto-arc. *Science Advances*, 4, article number eaao3159.
- Gebauer, D., Raiteri P., Gale J.D., Cölfen H. (2018). On classical and non-classical views on nucleation. *Am. J. Sci.*, 318, 969-988.
- Gilmer, A.K., Tapster, S., Sparks, R.S.J., Hauff, F., Blundy, J.D., Hoernle, K., Rust, A.C., Spencer, C.J., 2018, Petrogenesis and Assembly of the Don Manuel Igneous Complex, Miocene-Pliocene Porphyry Copper Belt, Central Chile: *Journal of Petrology*, v. 59, p. 1067-1108.
- Giosan, L., W. D. Orsi, M.J.L. Coolen, C. Wuchter, A. G. Dunlea, K. Thirumalai, S. E. Munoz, P. D. Clift, J. P. Donnelly, V. Galy and D. Q. Fuller (2018). Neoglacial climate anomalies and the Harappan metamorphosis. *Climate of the Past* 14: 1669-1686.
- Greenwood, P.F., Mohammed, L., Grice, K., McCulloch, M. and Schwark L. (2018) The application of compound-specific sulfur isotopes to the oil-source rock correlation of Kurdistan petroleum. *Organic Geochemistry* 117, 22-30
- Greenwood P.F., Shan C., Holman A.I., Grice K. (2018). The composition and radiolysis impact on aromatic hydrocarbons in sedimentary organic matter from the Mulga Rock (Australia) uranium deposit. *Organic Geochemistry*, 123, 103-112.

- Goncalves R, Awange JL et al., (2018) Research frame work at LACCOST, UFPE, Brazil. In: A. Heck, K. Seitz, T. Grombein, M. Mayer, J.-M. Stövhase, H. Sumaya, M. Wampach, M. Westerhaus, L. Dalheimer, P. Senger (ed.): (Schw)Ehre, wem (Schw)Ehre gebührt - Festschrift zur Verabschiedung von Prof. Dr.-Ing. Dr. h.c. Bernhard Heck: 95-100; Schriftenreihe des Studiengangs Geodäsie und Geoinformatik, vol. 2018-1, Karlsruhe (KIT Scientific Publishing), doi: 10.5445/KSP/1000080216.
- Gong, Z., Xu, X., Evans, D.A.D., Hoffman, P.F., Mitchell, R.N., Bleeker, W., 2017. Paleomagnetism and rock magnetism of the ca. 1.87 Ga Pearson Formation, Northwest Territories, Canada: A test of vertical-axis rotation within the Great Slave basin. *Precambrian Research*, 305, 295-309.
- Hall J.W., Glorie S., Reid A., Collins A.S., Jourdan F., Danisik M. and Evans N.J. (2018). Thermal history of the northern Olympic Domain, Gawler Craton; correlations between cooling ages and mineralising systems. *Gondwana Research*, 56, 90-104.
- He S., Saunders M., Chen K., Gao H., Suvorova A., Rickard W.D.A., Quadir Z., Cui C.Q., Jiang S.P. (2018). A FIB-STEM study of strontium segregation and interface formation of directly assembled $\text{La}_{0.6}\text{Sr}_{0.4}\text{Co}_{0.2}\text{Fe}_{0.8}\text{O}_3$ cathode on $\text{Y}_2\text{O}_3\text{-ZrO}_2$ electrolyte of solid oxide fuel cells. *Journal of The Electrochemical Society*, 165, F417-F429.
- Henderson, B.J., Collins, W.J., Murphy, J.B., Hand, M. (2018). A hafnium isotopic record of magmatic arcs and continental growth in the Iapetus Ocean: The contrasting evolution of Ganderia and the peri-Laurentian margin. *Gondwana Research*, 58, 141-160.
- Hidalgo L., Kuhar L., Beinlich A., Putnis A. (2018). Kinetic study of chalcopyrite dissolution with iron (III) chloride in methanesulfonic acid. *Minerals Engineering*, 125, 66-74.
- Holman A.I., Grice K. (2018). $\delta^{13}\text{C}$ of aromatic compounds in sediments, oils and atmospheric emissions: A review. *Organic Geochemistry*, 123, 27-37.
- Hövelmann J., Putnis C.V., Benning L.G. (2018). Metal sequestration through coupled dissolution-precipitation at the brucite-water interface. *Minerals*, 8, 346.
- Hu, S.Y., Evans, K., Rempel, K., Guagliardo, P., Kilburn, M., Craw, D., Grice, K., Dick, J., (2018). Sequestration of Zn into mixed pyrite-zinc sulfide framboids: A key to Zn cycling in the ocean? *Geochimica et Cosmochimica Acta* 241, 95-107.
- Imparato, D., El-Mowafy, A., Rizos, C. and Wang, J. (2018) A review of SBAS and RTK vulnerabilities in Intelligent Transport Systems applications, Proceedings IGNSS Symposium 2018, Sydney, 7 – 9 February 2018, 1-18.
- Ionov, D.A., Doucet, L.S., Carlson, R.W., Golovin, A.V., Oleinikov, O.B., 2018. Lost in interpretation: Facts and misconceptions about the mantle of the Siberian craton. A comment on: "Composition of the lithospheric mantle in the northern part of Siberian craton: Constraints from peridotites in the Obnazhennaya kimberlite" by Sun et al. (2017). *Lithos*, 314-315, 683-687.

- Ionov, D.A., Doucet, L.S., Pogge von Strandmann, P.A.E., Golovin, A.V., Korsakov, A.V., 2017. Links between deformation, chemical enrichments and Li-isotope compositions in the lithospheric mantle of the central Siberian craton. *Chemical Geology*, 475, 105-121.
- Ionov, D.A., Doucet, L.S., Xu, Y., Golovin, A.V., Oleinikov, O.B., 2018. Reworking of Archean mantle in the NE Siberian craton by carbonate-bearing and silicate melt metasomatism: Evidence from a carbonate-bearing, dunite-to-websterite xenolith suite from the Obnazhennaya kimberlite. *Geochimica et Cosmochimica Acta*, 224, 132-153.
- Jabaloy-Sánchez A., Talavera C., López-Sánchez-Vizcaino V., Gómez-Pugnaire M.T., Vázquez-Vílchez M., Rodríguez-Peces M.J. and Evans N.J. (2018). U-Pb ages of detrital zircons from the Internal Betics: a key to deciphering paleogeographic provenance and tectono-stratigraphic evolution. *Lithos*, 318-319, 244-266.
- Jepson, G., Glorie, S., Konopelko, D., Gillespie, J., Danišik, M., Evans, N.J., Mamadjanov, Y., Collins, A.S. (2018). Thermochronological insights into the structural contact between the Tian Shan and Pamirs, Tajikistan. *Terra Nova*, 30(2), 95-104.
- Jepson, G., Glorie, S., Konopelko, D., Gillespie, J., Danišik, M., Mirkamalov, R., Mamadjanov, Y., Collins, A. S. (2018). Low-Temperature Thermochronology of the Chatkal-Kurama Terrane (Uzbekistan-Tajikistan): Insights into the Meso-Cenozoic thermal history of the western Tian Shan. *Tectonics*, 37(10), 3954-3969.
- Jepson, G., Glorie, S., Konopelko, D., Mirkamalov, R., Danišik, M., Collins, A. S. (2018). The low-temperature thermo-tectonic evolution of the western Tian Shan, Uzbekistan. *Gondwana Research*, 64, 122-136.
- Jiang W.-C., Li H., Evans N.J., Wu. J.-H. and Cao J.-Y. (2018). Metal Sources of World-Class Polymetallic W-Sn Skarns in the Nanling Range, South China: Granites versus Sedimentary Rocks. *Minerals* 8(7), 265, <https://doi.org/10.3390/min8070265>
- Johnson, S. P., Kirkland, C. L., Evans, N. J., McDonald, B. J., and Cutten, H. N., 2018a, The complexity of sediment recycling as revealed by common Pb isotopes in K-feldspar: *Geoscience Frontiers*, v. 9, no. 5, p. 1515-1527.
- Johnson, T. E., Gardiner, N. J., Miljković, K., Spencer, C. J., Kirkland, C. L., Bland, P. A. & Smithies, R. H. (2018). An impact melt origin for Earth's oldest known evolved rocks. *Nature Geoscience*, 11, 795-799.
- Kemp, A.I.S., Wilde, S.A., Spaggiari, C. (2018). The Narryer Terrane, Yilgarn Craton, Western Australia: Review and Recent Developments. In: *Earth's Oldest Rocks (2nd Edition)*, Van Kranendonk, M.J., Bennett, V. C., Hoffman, J.E. (Eds), Elsevier, pp. 401-433.
- Khahi M, Forootan E, Kuhn M, Awange J, Papac F, Shum CK (2018) A study of Bangladesh's Sub-surface Water Storages Using Satellite Products and Data Assimilation Scheme. *Science of the Total Environment*, doi: 10.1016/j.scitotenv.2017.12.289.

- Khaki M, Ait-El-Fquih B, Hoteit I, Forootan E, Awange J, Kuhn M (2018) Unsupervised Ensemble Kalman Filtering with an Uncertain Constraint for Land Hydrological Data Assimilation. *Journal of Hydrology* 564: 175-190, doi: 10.1016/j.jhydrol.2018.06.080
- Khaki M, Awange J, Forootan E, Kuhn M (2018) Understanding the association between climate variability and the Nile's water level fluctuations and water storage changes during 1992–2016. *Science of the Total Environment* 645: 1509–1521, doi: 10.1016/j.scitotenv.2018.07.212
- Khaki M, Forootan E, Kuhn M, Awange J, Longuevergne L, Wada Y (2018) Efficient basin scale filtering of GRACE satellite products. *Remote Sensing of Environment* 204: 76-93, doi: 10.1016/j.rse.2017.10.040.
- Khaki M, Forootan E, Kuhn M, Awange J, Van Dijk A, Schumacher M, Sharifi M (2018) Determining Water Storage Depletion within Iran by Assimilating GRACE data into the W3RA Hydrological Model. *Advances in Water Resources* 114:1-18, doi: 10.1016/j.advwatres.2018.02.008. .
- Khaki M, Hamilton F, Forootan E, Hoteit I, Awange J, Kuhn M (2018) Non-parametric Data Assimilation Scheme for Land Hydrological Applications. *Water Resources Research* 54, 4946–4964, doi: 10.1029/2018WR022854.
- Khaki M, Hamilton F., Forootan E., Hoteit I., Awange J.L., Kuhn M. (2018). Non-parametric data assimilation scheme for land hydrological applications. *Water Resources Research*, 54(7), 4946–4964.
- Khaki M., Ait-El-Fquih B., Hoteit I., Forootan E., Awange J.L., Kuhn M. (2018). Unsupervised ensemble Kalman filtering with an uncertain constraint for land hydrological data assimilation. *Journal of Hydrology*, 564, 175-190.
- Khaki M., Awange J.L., Forootan E., Kuhn M. (2018). Understanding the association between climate variability and the Nile's water level fluctuations and water storage changes during 1992–2016. *Science of Total Environment*, 645, 1509-1521.
- Khaki M., Forootan E., Kuhn M., Awange J.L., Longuevergne L., Wada Y. (2018). Efficient Filtering of GRACE satellite products applied to remotely sensed basin-wide water storage changes. *Remote Sensing of Environment*, 204, 76-93.
- Khaki M., Forootan E., Kuhn M., Awange J.L., Papa F., Shum C.K. (2018). A study on Bangladesh's sub-surface water storages using satellite products and data assimilation scheme. *Advances in Water Resources*, 625, 963-977.
- Khaki M., Forootan E., Kuhn M., Awange J.L., vanDijk A.I.J.M., Schumacher M., Sharifi M.A. (2018). Determining water storage depletion within Iran by assimilating GRACE data into the W3RA Hydrological Model, *Advances in Water Resources*, 114, 1-18.
- Khaleque H.N., Kaksonen A.H., Boxall N.J., Watkin E.L.J. (2018). Quantitative proteomics using SWATH-MS identifies mechanisms of chloride tolerance in the halophilic acidophile *Acidihalobacter prosperus* DSM 14174. *Research in Microbiology* DOI: 10.1016/j.resmic.2018.07.002.

- Khaleque H.N., Kaksonen A.H., Boxall N.J., Watkin E.L.J. (2018). Chloride ion tolerance and pyrite bioleaching capabilities of pure and mixed halotolerant, acidophilic iron- and sulfur-oxidizing cultures. *Minerals Engineering* 120: 87-93.
- Kielman, Ross B., Alexander A. Nemchin, Martin J. Whitehouse, Robert T. Pidgeon, and Jeremy J. Bellucci. 2018. "U-Pb age distribution recorded in zircons from Archean quartzites in the Mt. Alfred area, Yilgarn Craton, Western Australia." *Precambrian Research* 310 (June): 278-90.
- Kielman, Ross, Martin Whitehouse, Alexander Nemchin, and Anthony Kemp. 2018. "A tonalitic analogue to ancient detrital zircon." *Chemical Geology* 499 (November): 43-57.
- Kirilova, Martina, Virginia G. Toy, Nick Timms, Angela Halfpenny, Catriona Menzies, Dave Craw, Olivier Beyssac, et al. 2018. "Textural changes of graphitic carbon by tectonic and hydrothermal processes in an active plate boundary fault zone, Alpine Fault, New Zealand." *Geological Society of London Special Publications* 453 (January): 205-23. doi:10.1144/SP453.13.
- Kirkland C., Yakymchuk C., Szilas K., Evans N.J., Hollis J. and McDonald B.J. (2018). Apatite; a U-Pb thermochronometer or geochronometer. *Lithos*, 318-319, 143-157.
- Kirkland C.L., Fougereuse D., Reddy S.M., Hollis J., Saxey D.W. (2018). Assessing the mechanisms of common Pb incorporation into titanite. *Chemical Geology*, 483, 558-566.
- Kirkland, C. L., Slagstad, T. & Johnson, T. E. (2018). Zircon as a metamorphic timekeeper: a case study from the Caledonides of central Norway. *Gondwana Research*, 61, 63-72.
- Kirkland, C. L., Yakymchuk, C., Hollis, J., Heide-Jørgensen, H., Danišik, M. (2018). Mesoarchean exhumation of the Akia terrane and a common Neoproterozoic tectonothermal history for West Greenland. *Precambrian Research*, 314, 129-144.
- Kirkland, C. L., Yakymchuk, C., Szilas, K., Evans, N., Hollis, J., McDonald, B., and Gardiner, N. J., 2018d, Apatite: a U-Pb thermochronometer or geochronometer?: *Lithos*, v. 318-319, p. 143-157.
- Kirscher, U., Winklhofer, M., Hackl, M., Bachtadse, V., 2018. Detailed Jaramillo field reversals recorded in lake sediments from Armenia - Lower mantle influence on the magnetic field revisited. *Earth and Planetary Science Letters*, 484, 124-134.
- Kitano I., Osanai Y., Nakano N., Adachi T., Fitzsimons I.C.W. (2018). Detrital zircon and igneous protolith ages of high-grade metamorphic rocks in the Highland and Wannu Complexes, Sri Lanka: Their geochronological correlation with southern India and East Antarctica. *Journal of Asian Earth Sciences*, 156, 122-144. <http://doi.org/10.1016/j.jseaes.2018.01.017>
- Konopelko, D., Wilde, S.A., Seltnann, R., Romer, R.L., Biske, Yu.S. (2018). Early Permian intrusions of the Alai range: Understanding tectonic settings of Hercynian post-collisional magmatism in the South Tien Shan, Kyrgyzstan. *Lithos*, 302-303, 405-420.
- Kose, S.H., K. Grice, W. D. Orsi, M. Ballal and M. J. L. Coolen (2018). "Metagenomics of pigmented and cholesterol gallstones: the putative role of bacteria." *Scientific Reports* 8.

- Kozdon, R., Orland, I.J., Kitajima, K., and Valley, J.W. (2018). SIMS Microanalysis of the Strelley Pool Formation Cherts and the Implications for the Secular-Temporal Oxygen-isotope Trend of Cherts, *Precambrian Research*, 304, 125-139.
- Kranendonk, M., and Bennett, V. (Series Eds.), *Developments in Precambrian Geology 255-278, World's Oldest Rocks*, Elsevier, Amsterdam.
- Krijgsman, W., Tesakov, A., Yanina, T., Lazarev, S., Danukalova, G., Van Baak, C.G.C., Agustí, J., Alçiçek, M.C., Aliyeva, E., Bista, D., Bruch, A., Büyükmeriç, Y., Bukhsianidze, M., Flecker, R., Frolov, P., Hoyle, T.M., Jorissen, E.L., Kirscher, U., Koriche, S.A., Kroonenberg, S.B., Lordkipanidze, D., Oms, O., Rausch, L., Singarayer, J., Stoica, M., van de Velde, S., Titov, V.V., Wesselingh, F.P., 2018. Quaternary time scales for the Pontocaspian domain: Interbasinal connectivity and faunal evolution. *Earth-Science Reviews*, 188, 1-40.
- Kuhn M. (2018). On the approximation of a tesseroid by a rectangular prism. In: (*Schw*) *Ehre wem (Schw) Ehre gebührt, Festschrift zur Verabschiedung von Prof Dr-Ing Dr hc Bernhard Heck*, Karlsruhe Institute of Technology (KIT) Scientific Publishing, Geodesy and Geo-informatic, 2018, No. 1, p. 153-161.
- Kusiak, M.A., Dunkley, D.J., Whitehouse, M.J., Wilde, S.A., Sałacińska, A., Konečný, P., Szopa, K., Gawęda, A., Chew, A. (2018). Peak to post-peak thermal history of the Saglek Block of Labrador: A multiphase and multi-instrumental approach to geochronology. *Chemical Geology*, 484, 210-223.
- Kuznetsov, N.B., Priyatkina, N.S., Rud'ko, S.V., Shatsillo, A.V., Collins, W.J., Romanyuk, T.V., (2018). Primary Data on U/Pb-Isotope Ages and Lu/Hf-Isotope Geochemical Systematization of Detrital Zircons from the Lopatinskii Formation (Vendian-Cambrian Transition Levels) and the Tectonic Nature of Teya-Chapa Depression (Northeastern Yenisei Ridge). *Doklady Akademii Nauk*, 479, 49-53.
- Laber, C. P., J. E. Hunter, F. Carvalho, J. R. Collins et al. (2018). Coccolithovirus facilitation of carbon export in the North Atlantic. *Nature Microbiology* 3: 537-547.
- Le Gall B., Leleu S, Pik R., Jourdan F., Chazot G., Ayale D., Gezahegn Y., Cloquet C. (2018) The Red Beds series in the Erta Ale segment, North Afar. Evidence for a 6 Ma-old post-rift basin prior to continental rifting. *Tectonophysics* 747, 373-389.
- Leng, C., Cooke, D., Hou, Z., Evans, N., Zhang, X., Chen, W., Danišik, M., McInnes, B.I.A., Yang, J. (2018). Quantifying exhumation at the giant pulang porphyry Cu-Au deposit using U-Pb-He dating. *Economic Geology*, 113(5), 1077-1092.
- Lewis R., Paláncz B., Awange J. (2018) Fitting a Sphere via Gröbner Basis. In: Davenport J., Kauers M., Labahn G., Urban J. (eds) *Mathematical Software – ICMS 2018. ICMS 2018. Lecture Notes in Computer Science*, vol 10931. Springer, Cham, pp 319-327, doi: 10.1007/978-3-319-96418-8_38
- Li H., Wu J.-H., Evans N.J., Jiang W.-C. and Zhou Z.-K. (2018). Zircon geochronology and geochemistry of the Xianghualing A-type granitic rocks: Insights into multi-stage Sn-polymetallic mineralization in South China. *Lithos* 312-313. 1-20.

- Li J.X., Qin K.Z., Li G.M., Evans N.J., Huang F. and Zhao J.X. (2018) Iron isotope fractionation during magmatic-hydrothermal evolution: A case study from the Duolong porphyry Cu-Au deposit, Tibet. *Geochimica et Cosmochimica Acta*, 238, 1-15.
- Li J.X., Qin K.Z., Li G.M., Evans N.J., Zhao J.X., Yue Y.H., and Xie J. (2018). Volatile variations in magmas related to porphyry Cu-Au deposits: Insights from amphibole geochemistry, Duolong district, Central Tibet. *Ore Geology Reviews*, 95, 649-662.
- Li M., Wang L., Putnis C.V. 2018. Atomic force microscopy imaging of classical and nonclassical surface growth dynamics of calcium orthophosphates. *CrystEngComm.*, doi.org/10.1039/C7CE02100C
- Li M., Zhang J., Wang L., Wang B, Putnis C.V. (2018). Mechanisms of modulation of calcium phosphate pathological mineralization by mobile and immobile small-molecule inhibitors. *Journal of Physical Chemistry B* 122 (5): 1580-1587.
- Li N., Ai N., He S., Cheng Y., Rickard W.D.A., Chen K., Zhang T., Jiang S.P. (2018). Effect of Pd doping on the activity and stability of directly assembled $\text{La}_{0.95}\text{Co}_{0.19}\text{Fe}_{0.76}\text{Pd}_{0.05}\text{O}_{3-\delta}$ cathodes of solid oxide fuel cells. *Solid State Ionics*, 316, 38-46.
- Li, S., Chung, S.L., Wang, T., Wilde, S.A., Chu, M.F., Pang, C.J., Guo, Q.Q. (2018). Water-fluxed crustal melting and petrogenesis of large-scale Early Cretaceous intracontinental granitoids in the southern Great Xing'an Range, North China. *Geological Society of America Bulletin*, 130, 580-597.
- Li, Z., Wang, X-C., Wilde, S.A., Liu, L., Li, W.X., Yang, X.M. (2018). Role of deep-Earth water cycling in the growth and evolution of continental crust: constraints from Cretaceous magmatism in southeast China. *Lithos*, 302, 126-141.
- Li,H., Wu Q.H., Evans N.J., Zhou Z.K., Kong H. and Xi X.S. (2018). Geochemistry and geochronology of the Banxi Sb deposit: Implications for fluid origin and evolution of Sb mineralization in central-western Hunan, South China. *Gondwana Research*, 55. 112-134.
- Liu, Y., Li, Z.-X., Pisarevsky, S., Kirscher, U., Mitchell, R.N., Stark, J.C., 2018. Palaeomagnetism of the 1.89 Ga Boonadgin dykes of the Yilgarn Craton: Possible connection with India, *Precambrian Research*, In Press. <https://doi.org/10.1016/j.precamres.2018.05.021>
- Liu, Y., Li, Z.-X., Pisarevsky, S., Kirscher, U., Mitchell, R.N., Stark, J.C., Clark, C., Hand, M., 2018. First Precambrian palaeomagnetic data from the Mawson Craton (East Antarctica) and tectonic implications. *Scientific Reports* 8: 16403. <https://doi.org/10.1038/s41598-018-34748-2>
- Lowery, C. M., T. J. Bralower, J. D. Owens, F. J. Rodriguez-Tovar et al. (2018). Rapid recovery of life at ground zero of the end-Cretaceous mass extinction. *Nature* 558:288-291.
- Lyon T.J., Filmer M.S., Featherstone W.F. (2018). On the use of repeat leveling for the determination of vertical land motion: artifacts, aliasing and extrapolation errors. *Journal of Geophysical Research: Solid Earth*, 123(8):7021-7039, doi: 10.1029/2018JB015705.

- Makuluni, P., Kirkland, C.L., Barham, M. (2018). Zircon grain shape holds provenance information: A case study from southwestern Australia. *Geological Journal*, 1-15.
- Markwitz, V., and Kirkland, C. L., 2018, Source to sink zircon grain shape: Constraints on selective preservation and significance for Western Australian Proterozoic basin provenance: *Geoscience Frontiers*, v. 9, no. 2, p. 415-430.
- Marzoli A. , Callegaro S., Dal Corso J., Davies J., Youbi N., Bertrand,H., Reisberg L., Chiaradia M., Merle R. and Jourdan F. (2018) InThe Central Atlantic magmatic province: a review. pSpecial publication: *The Late Triassic world, special publication, 91-125. 2018*
- McCubbine, J.C., Amos M.J., Tontini F.C., Smith E., Winefied R., Stagpoole V., Featherstone W.E. (2018). The New Zealand Gravimetric Quasigeoid Model 2017 that Incorporates Nation-wide Airborne Gravimetry. *Journal of Geodesy*, 92, 923-937.
- Meadows, H. R., Reddy, S. M., Clark, C., Harris, C., Martin, L., & White, A. J. R. (2018). Isotopic constraints on fluid evolution and ore precipitation in a sediment-hosted Pb-Ag-Ba-Zn-Cu-Au deposit in the Capricorn Orogen, Western Australia. *Applied Geochemistry*, 96, 217-232. doi:10.1016/j.apgeochem.2018.06.012
- Mei, Y., Liu W., Brugger J., Sherman D.M., Gale J.D. (2018). The dissociation mechanism and thermodynamic properties of HCl(aq) in hydrothermal fluids (to 700 °C, 60 kbar) by ab initio molecular dynamics simulations. *Geochimica Cosmochimica Acta*, 226, 84.
- Merle, R., F. Jourdan, and J. Girardeau. 2018. "Geochronology of the Tore-Madeira Rise seamounts and surrounding areas: a review." *Australian Journal of Earth Sciences* 65 (July): 591-605. doi:10.1080/08120099.2018.1471005.
- Mitchell, R. J., Johnson, T. E., Clark, C., Gupta, S., Brown, M., Harley, S. L., & Taylor, R. (2018). Neoproterozoic evolution and Cambrian reworking of ultrahigh temperature granulites in the Eastern Ghats Province, India. *Journal of Metamorphic Geology*. doi:10.1111/jmg.12451
- Mole D.R., Barnes S.J., Taylor R.J.M., Kinny P.D., Fritz H. (2018) A relic of the Mozambique Ocean in south-east Tanzania. *Precambrian Research*, 305, 386-426.
- Mole, D. R., Barnes, S. J., Yao, Z., White, A. J. R., Maas, R., and Kirkland, C. L., 2018, The Archean Fortescue large igneous province: A result of komatiite contamination by a distinct Eo-Paleoarchean crust: *Precambrian Research*, v. 310, p. 365-390.
- Montalvo Jimenez P.E., Cavosie A.J., Erikson T.M., Kirkland C.L., Evans N.J., McDonald B.J., Talavera C. and Lugo-Centeno C. (2018). Detrital shocked zircon provides first radiometric age constraint (1472Ma) for the Santa Fe impact structure, New Mexico, USA. *GSA Bulletin*, <https://doi.org/10.1130/B31761.1>
- More, K. D., W. D. Orsi, V. Galy, L. Giosan, L. J. He, K. Grice and M. J. L. Coolen (2018). A 43 kyr record of protist communities and their response to oxygen minimum zone variability in the Northeastern Arabian Sea. *Earth and Planetary Science Letters* 496: 248-256.

- Mpelasoka F, Awange JL, Goncalves RM (2018) Accounting for dynamics of mean precipitation in drought projections: A case study of Brazil for the 2050 and 2070 periods. *Science of the Total Environment*, 622–623: 1519–1531, doi: 10.1016/j.scitotenv.2017.10.032.
- Mpelasoka F, Awange JL, Zerihun A (2018) Influence of coupled ocean-atmosphere phenomena on the Greater Horn of Africa droughts and their implications. *Science of the Total Environment*, 610-611: 691-702, doi: 10.1016/j.scitotenv.2017.08.109.
- Mulder, J.A., McDonald, B., Merdith, A.S., Berry, R.F., Karlstrom, K.E., Halpin, J.A., and Spencer, C.J., 2018, Rodinian devil in disguise: Correlation of 1.25–1.10 Ga strata between Tasmania and Grand Canyon: *Geology*, v. 46, p. 991–994.
- Murphy, J.B., Shellnutt, J.G., Collins, W.J. (2018). Late Neoproterozoic to Carboniferous genesis of A-type magmas in Avalonia of northern Nova Scotia: repeated partial melting of anhydrous lower crust in contrasting tectonic environments. *Int J Earth Sci (Geol Rundsch)*, 107, 587–599. <https://doi.org/10.1007/s00531-017-1512-7>
- Nachtergaele, S., De Pelsmaeker, E., Glorie, S., Zhimulev, F., Jolivet, M., Danišik, M., Buslov, M.M., De Grave, J. (2018). Meso-Cenozoic tectonic evolution of the Talas-Fergana region of the Kyrgyz Tien Shan revealed by low-temperature basement and detrital thermochronology. *Geoscience Frontiers*, 9(5), 1495-1514.
- Ndehedehea CE, Awange JL, Agutu NO, Okwuash O (2018) Changes in hydro-meteorological conditions over tropical West Africa (1980–2015) and links to global climate. *Global Planetary Change*, doi: 10.1016/j.gloplacha.2018.01.020.
- Nie, J., Ruetenik, G., Gallagher, K., Hoke, G., Garzzone, C. N., Wang, W., Stockli, D., Hu, X., Wang, Z., Wang, Y., Stevens, T., Danišik, M., Liu, S. (2018). Rapid incision of the Mekong River in the middle Miocene linked to monsoonal precipitation. *Nature Geoscience*, 11(12), 944.
- Nordsvan, A.R., Collins, W.J., Li, Z.-X., Spencer, C.J., Pourteau, A., Withnall, I.W., Betts, P.G., Volante, S., 2018, Laurentian crust in northeast Australia: Implications for the assembly of the supercontinent Nuna. *Geology*, 46, 251–254. <https://doi.org/10.1130/G39980.1>.
- Occhipinti, S. A., Tyler, I. M., Spaggiari, C. V., Korsch, R. J., Kirkland, C. L., Smithies, R. H., Martin, K., and Wingate, M. T. D., 2018, Tropicana translated: A foreland thrust system imbricate fan setting for c. 2520 Ma orogenic gold mineralization at the northern margin of the Albany-Fraser Orogen, Western Australia, Geological Society Special Publication, Volume 453, p. 225-245.
- Olierook, H. K. H., Sheppard, S., Johnson, S. P., Occhipinti, S. A., Reddy, S. M., Clark, C., . . . Erickson, T. M. (2018). Extensional episodes in the Paleoproterozoic Capricorn Orogen, Western Australia, revealed by petrogenesis and geochronology of mafic-ultramafic rocks. *Precambrian Research*, 306, 22-40. doi:10.1016/j.precamres.2017.12.015
- Olierook, H.K.H., Agangi, A., Plavsá, D., Reddy, S.M., Yao, W., Clark, C., Occhipinti, S.A., Kylander-Clark, A.R.C., 2018. Neoproterozoic hydrothermal activity in the West Australian Craton related to Rodinia assembly or breakup? *Gondwana Research*, 68, 1-12.

- Pages, A., Barnes, S., Schmid, S., Coveney R.M. Jr, Schwark, L., Liu, W., Grice, K., ... (2018) Geochemical investigation of the Lower Cambrian mineralised black shales of South China and the Devonian Nick deposit, Canada. *Ore Geology Reviews* 94, 396-413.
- Palozzi, J., Pantopoulos, G., Maravelis, A.G., Nordsvan, A., Zeligidis, A., 2017. Sedimentological analysis and bed thickness statistics from a Carboniferous deep-water channel-levee complex: Myall Trough, SE Australia. *Sedimentary Geology*, 364, 160-179.
- Parrish, M.D., Collins, W.J., Hegarty, R.A., Gilmore, P.J., Huang, H-Q. (2018) Depositional age and provenance of the Cobar Supergroup, *Australian Journal of Earth Sciences*, 65, 1035-1048, DOI: 10.1080/08120099.2018.1501422
- Pastor-Galán, D., Nance, R.D., Murphy, J.B., and Spencer, C.J., 2018, Supercontinents: myths, mysteries, and milestones: Geological Society, London, Special Publications, v. 470, p. SP470-16.
- Philippot P., Ávila J.N., Killingsworth B.A., Tessalina S., Baton F., Caquineau T., Muller E., Pecoits E., Cartigny P., Lalonde S.V., Ireland T.R., Thomazo C., Kranendonk M.J., Busigny V. (2018). Globally asynchronous sulphur isotope signals require re-definition of the Great Oxidation Event. *Nature Communications*, 9 (1), doi:10.1038/s41467-018-04621-x.
- Pidgeon, R. T., R. E. Merle, M. L. Grange, and A. A. Nemchin. 2018. "Annealing history of zircons from Apollo 14083 and 14303 impact breccias." *Meteoritics and Planetary Science* 53 (December): 2632-43.
- Piechocka A.M., Sheppard S., Fitzsimons I.C.W., Johnson S.P., Rasmussen B., Jourdan F. (2018). Neoproterozoic $^{40}\text{Ar}/^{39}\text{Ar}$ mica ages mark the termination of a billion years of intraplate reworking in the Capricorn Orogen, Western Australia. *Precambrian Research*, 310, 391-406. <http://doi.org/10.1016/j.precamres.2018.04.006>
- Piilonen, P., Sutherland, F., Danišik, M., Poirier, G., Valley, J., Rowe, R. (2018). Zircon Xenocrysts from Cenozoic Alkaline Basalts of the Ratanakiri Volcanic Province (Cambodia), Southeast Asia — Trace Element Geochemistry, O-Hf Isotopic Composition, U-Pb and (U-Th)/He Geochronology — Revelations into the Underlying Lithospheric Mantle. *Minerals*, 8(12), 556.
- Plavsa, D., Reddy, S. M., Agangi, A., Clark, C., Kylander-Clark, A., & Tiddy, C. J. (2018). Microstructural, trace element and geochronological characterization of TiO_2 polymorphs and implications for mineral exploration. *Chemical Geology*, 476, 130-149.
- Plet, C., Pagès A., Holman A.I., Madden R.H.C., Grice K. (2018). From supratidal to subtidal, an integrated characterisation of Carbla Beach shallow microbial mats (Hamelin Pool, Shark Bay, WA): Lipid biomarkers, stable carbon isotopes and microfabrics. *Chemical Geology*, 493, 338-352.
- Plotinskaya O.Y., Abramova V.D., Groznova E.O., Tessalina S.G., Seltmann R., Spratt J. (2018). 'Trace-element geochemistry of molybdenite from porphyry Cu deposits of the Birgilda-Tomino ore cluster (South Urals, Russia). *Mineralogical Magazine*, 82 (S1), S281-S306.

- Pourteau, A., Scherer, E.E., Schorn, S., Bast, R., Schmidt, A., Ebert, L., 2018. Thermal evolution of an ancient subduction interface revealed by Lu-Hf garnet geochronology, Halilbağı Complex (Anatolia). *Geoscience Frontiers*, 10(1), 127-148. <https://doi.org/10.1016/j.gsf.2018.03.004>
- Pourteau, A., Smit, M.A., Li, Z.-X., Collins, W.J., Nordsvan, A.R., Volante, S., Li, J. (2018). 1.6 Ga crustal thickening along the final Nuna suture: *Geology*, 46, 959-962. <https://doi.org/10.1130/G45198.1>
- Poveda LA., Galvis J., Calo VM. (2018). Localized harmonic characteristic basis functions for multiscale finite element methods. *Journal of Computational and Applied Mathematics*. 37, 1982-2000.
- Powell, R., Evans, K.A., Green, E.C.R., White, R.W., (2018). On equilibrium in non-hydrostatic metamorphic systems. *Journal of Metamorphic Geology* 36, 419-438.
- Priyatkina, N., Collins, W.J., Khudoley, A.K., Letnikova, E.F., Huang, H-Q. (2018). The Neoproterozoic evolution of the western Siberian Craton margin: U-Pb-Hf isotopic records of detrital zircons from the Yenisey Ridge and the Prisayan Uplift. *Precambrian Research*, 305, 197-217.
- Proborukmi, Maria Sekar, Brigitte Urban, Steffen Mischke, Henk K. Mienis, Yoel Melamed, Guillaume Dupont-Nivet, Fred Jourdan, and Naama Goren-Inbar. 2018. "Evidence for climatic changes around the Matuyama-Brunhes Boundary (MBB) inferred from a multi-proxy palaeoenvironmental study of the GBY#2 core, Jordan River Valley, Israel." *Palaeogeography Palaeoclimatology Palaeoecology* 489 (January): 166-85. doi:10.1016/j.palaeo.2017.10.007.
- Puzyrev V., Deng Q., Calo V. (2018). Spectral approximation properties of isogeometric analysis with variable continuity. *Computer Methods in Applied Mechanics and Engineering*, 334, 22-39.
- Puzyrev V., Ghommem M., Meka S., Calo V. (2018). Reduced Order Modeling in Geophysics: pyROM Open-source Framework. *80th EAGE Conference and Exhibition*.
- Puzyrev V., Torres-Verdin C., Calo V. (2018). 3D inversion-based interpretation of deep directional resistivity measurements in high-angle and horizontal wells. *Geophysical Journal International*, 213 (2), 1135-1145.
- Renard F., Putnis C.V., Montes-Hernandez G., King H.E., Breedveld G.D., Okkenhaug G. (2018). Sequestration of antimony on calcite observed by time-resolved nanoscale imaging. *Environ. Sci. Technol.* 52 (1): 107-113.
- Riller, U., M. H. Poelchau, A. S. P. Rae, F. M. Schulte, G. S. Collins et al. (2018). Rock fluidization during peak-ring formation of large impact structures. *Nature* 562: 511-518.
- Roda, M., Zucali, M., Li, Z.-X., Spalla, M.I., Yao, W., 2018. Pre-Alpine contrasting tectono-metamorphic evolutions within the Southern Steep Belt, Central Alps. *Lithos*, 310-311, 31-49.
- Roger L.M., George A.D., Shaw J., Hart R.D., Roberts M., Becker T., Evans N.J. and McDonald B.J. (2018). Geochemical and crystallographic study of *Turbo torquatus* (Mollusca: Gastropoda) from southwestern Australia. *Geochemistry, Geophysics, Geosystems* 19(1), 214-231.

Rowland, S.J., Sutton, P.A., Belt, S.T., Fitzsimmons-Thoss, V., Scarlett, A.G., 2018. Further spectral and chromatographic studies of ambergris. *Natural Product Research*, 1-7.

Salacinska, A., Kusiak, M.A., Whitehouse, M.J., Dunkley, D., Wilde, S.A., Kielman, R. (2018). Complexity of the early Archean Uivak Gneiss: Insights from Tigigakyuk Inlet, Saglek Block, Labrador, Canada and possible correlations with south West Greenland. *Precambrian Research*, 315, 103-119.

Saleem A, Corner R, Awange JL (2018) On the Possibility of Using CORONA and Landsat Data for Evaluating and Mapping Long-term LULC: Case study of Iraqi Kurdistan. *Applied Geography* 90: 145-154, doi: 10.1016/j.apgeog.2017.12.007.

Sarmiento AF., Espath LFR., Vignal P., Dalcin L., Parsani M., Calo VM. (2018). An energy-stable generalized- α method for the Swift-Hohenberg equation. *Journal of Computational and Applied Mathematics*. 334, 836-851.

Saxey D. W., Moser D. E., Piazzolo S., Reddy S. M., & Valley J. W. (2018). Atomic worlds: Current state and future of atom probe tomography in geoscience. *Scripta Materialia*, 148, 115-121.

Schack, P., Hirt C., Hauk M., Featherstone W.E., Lyon T.J., Guillaume S. (2018). A High-precision Digital Astrogeodetic Traverse in an Area of Steep Geoid Gradients and Close to the Coast of Perth, Western Australia, *Journal of Geodesy*, 92, 1143-1153.

Schmieder, M., Kennedy, T., Jourdan, F., Buchner, E. and Reimold, W.U. 2018a. "A high-precision $^{40}\text{Ar}/^{39}\text{Ar}$ age for the Nördlinger Ries impact crater, Germany, and implications for the accurate dating of terrestrial impact events." *Geochimica et Cosmochimica Acta* 220 (January): 146-57.

Schmieder, M., Kennedy, T., Jourdan, F., Buchner, E. and Reimold, W.U. "Response to Comment on "A high-precision $^{40}\text{Ar}/^{39}\text{Ar}$ age for the Nördlinger Ries impact crater, Germany, and implications for the accurate dating of terrestrial impact events" by Schmieder et al. *Geochimica et Cosmochimica Acta* 220 (2018) 146-157. *Geochimica et Cosmochimica Acta* 238, 602-605.

Scicchitano M.R., Rubatto D., Hermann J., Majumdar A.S. and Putnis A. Oxygen isotope analysis of olivine by ion microprobe: Matrix effects and applications to a serpentinised dunite. *Chemical Geology* 499, 126-137 (2018)

Shahriari M., Rojas S., Pardo D., Rodríguez-Rozas A., Bakr S., Calo VM., Muga I. (2018). A numerical 1.5 D method for the rapid simulation of geophysical resistivity measurements. *Geosciences*. 8, 225.

Siwik L., Wozniak M., Trujillo V., Pardo D., Calo VM., Paszynski M. (2018). Parallel refined Isogeometric Analysis in 3D. *IEEE Transactions on Parallel and Distributed Systems*.

Slagstad, T., and Kirkland, C. L., 2018, Timing of collision initiation and location of the Scandian orogenic suture in the Scandinavian Caledonides: *Terra Nova*, v. 30, no. 3, p. 179-188.

- Slagstad, T., Roberts, N. M. W., Coint, N., Høy, I., Sauer, S., Kirkland, C. L., Marker, M., Røhr, T. S., Henderson, I. H. C., Stormoen, M. A., Skår, Ø., Sørensen, B. E., and Bybee, G., 2018, Magma-driven, high-grade metamorphism in the Sveconorwegian Province, southwest Norway, during the terminal stages of Fennoscandian Shield evolution: *Geosphere*, v. 14, no. 2, p. 861-882.
- Snape, J. F., B. Davids, A. A. Nemchin, M. J. Whitehouse, and J. J. Bellucci. 2018. Constraining the timing and sources of volcanism at the Apollo 12 landing site using new Pb isotopic compositions and crystallisation ages. *Chemical Geology* 482 (April): 101-12. doi:10.1016/j.chemgeo.2018.02.009.
- Snape, Joshua F., Natalie M. Curran, Martin J. Whitehouse, Alexander A. Nemchin, Katherine H. Joy, Tom Hopkinson, Mahesh Anand, Jeremy J. Bellucci, and Gavin G. Kenny. 2018. Ancient volcanism on the Moon: Insights from Pb isotopes in the MIL 13317 and Kalahari 009 lunar meteorites. *Earth and Planetary Science Letters* 502 (November): 84-95. doi:10.1016/j.epsl.2018.08.035.
- Söngen, H., Reischl B., Miyata K., Bechstein R., Raiteri P., Rohl A.L., Gale J.D., Fukuma T., Kühnle A. (2018). Resolving point defects in the hydration structure of calcite (10.4) with three-dimensional atomic force microscopy. *Physical Review Letters*, 120, 116101.
- Spaak, G., D. S. Edwards, H. J. Allen, H. Grotheer, R. E. Summons, M. J. L. Coolen and K. Grice (2018). Extent and persistence of photic zone euxinia in Middle-Late Devonian seas - Insights from the Canning Basin and implications for petroleum source rock formation. *Marine and Petroleum Geology* 93: 33-56.
- Spaggiari, C. V., Smithies, R. H., Kirkland, C. L., Wingate, M. T. D., England, R. N., and Lu, Y. J., 2018, Buried but preserved: The Proterozoic Arubiddy Ophiolite, Madura Province, Western Australia: *Precambrian Research*, v. 317, p. 137-158.
- Spencer, C. J., Kirkland, C. L., and Roberts, N. M. W., 2018a, Implications of erosion and bedrock composition on zircon fertility: Examples from South America and Western Australia: *Terra Nova*, v. 30, no. 4, p. 289-295.
- Spencer, C. J., Murphy, J. B., Kirkland, C. L., Liu, Y., and Mitchell, R. N., 2018b, A Palaeoproterozoic tectono-magmatic lull as a potential trigger for the supercontinent cycle: *Nature Geoscience*, v. 11, no. 2, p. 97-101.
- Spencer, C.J., Dyck, B., Mottram, C.M., Roberts, N.M.W., Yao, W., Martin, E.L., 2018. Deconvolving the pre-Himalayan Indian margin – Tales of crustal growth and destruction. *Geoscience Frontiers*, In Press. <https://doi.org/10.1016/j.gsf.2018.02.007>
- Šprlák M., Han S-C., Featherstone W.E. (2018). Forward Modelling of Global Gravity Fields with 3D Density Structures and an Application to the High-resolution (~2 km) Gravity Fields of the Moon. *Journal of Geodesy*, 92, 847-862.
- Stark, J. C., Wang, X. C., Li, Z. X., Rasmussen, B., Sheppard, S., Zi, J. W., . . . Li, W. X. (2018). In situ U-Pb geochronology and geochemistry of a 1.13 Ga mafic dyke suite at Bunger Hills, East Antarctica: The end of the Albany-Fraser Orogeny. *Precambrian Research*, 310, 76-92. doi:10.1016/j.precamres.2018.02.023

- Stark, J.C., Wang, X.-C., Li, Z.-X., Denyszyn, S.W., Rasmussen, B., Zi, J.-W., Sheppard, S., 2018. 1.39 Ga mafic dyke swarm in southwestern Yilgarn Craton marks Nuna to Rodinia transition in the West Australian Craton. *Precambrian Research*, 316, 291-304.
- Stark, J.C., Wilde, S.A., Söderlund, U., Li, Z.-X., Rasmussen, B., Zi, J.-W., 2018. First evidence of Archean mafic dykes at 2.62 Ga in the Yilgarn Craton, Western Australia: links to cratonisation and the Zimbabwe Craton. *Precambrian Research*, 317, 1-13.
- Sukhorukov V.P., Turkina O.M., Tessalina S., Talavera C. (2018). Sapphirine-bearing Fe-rich granulites in the SW Siberian craton (Angara-Kan block): Implications for Paleoproterozoic ultrahigh-temperature metamorphism. *Gondwana Research*, 57, 26-47.
- Sun M., Chen H., Milan L.A., Wilde S.A., Jourdan F. and Xu Y. (2018) Continental arc and back-arc migration in eastern NE China: New constraints on Cretaceous Paleo-Pacific subduction and roll-back. *Tectonics* 37, 3293-3915.
- Sun, M.D., Chen, H.L., Milam, L.A., Wilde, S.A., Jourdan, F., Xu, Y.G. (2018). Continental Arc and Back-Arc Migration in Eastern NE China: New Constraints on Cretaceous Paleo-Pacific Subduction and Rollback. *Tectonics*, 37, 3893-3915.
- Thébaud N., Sugiono D., LaFlamme C., Miller J., Fisher L., Voute F., Tessalina S., Sonntag I., Fiorentini M. (2018). Protracted and polyphased gold mineralisation in the Agnew District (Yilgarn Craton, Western Australia). *Precambrian Research*, 310, 291-304.
- Thiessen, F., A. A. Nemchin, J. F. Snape, J. J. Bellucci, and M. J. Whitehouse. 2018. "Apollo 12 breccia 12013: Impact-induced partial Pb loss in zircon and its implications for lunar geochronology." *Geochimica et Cosmochimica Acta* 230 (June): 94-111.
- Timms, N.E., Healy, D., Erickson, T.M., Nemchin, A.A., Pearce, M.A., Cavosie, A.J. (2018). The role of elastic anisotropy in the development of deformation microstructures in zircon. In: Moser, D., Corfu, F., Reddy, S., Darling, J., Tait, K. (Eds.), AGU Monograph: Microstructural Geochronology; Lattice to Atom-Scale Records of Planetary Evolution. AGU-Wiley, 183-202.
- Tohver E., Schmieder M., Lana C., Jourdan F., Mendes P.S.T, Warren L. and Riccomini C. End-Permian impactogenic earthquake and tsunami deposits in the intracratonic Paraná Basin of Brazil. *GSA bulletin* 130, 1099-1120. 2018.
- Travis, B. J., P. A. Bland, W. C. Feldman, and M. V. Sykes. 2018. "Hydrothermal dynamics in a CM-based model of Ceres." *Meteoritics and Planetary Science* 53 (September): 2008-32.
- Turvey C.C., Wilson S.A., Hamilton J.L., Tait A.W., McCutcheon J., Beinlich A., Fallon S.J., Dipple G.M., Southam G. (2018). Hydrotalcites and hydrated Mg-carbonates as carbon sinks in serpentinite mineral wastes from the Woodsreef chrysotile mine, New South Wales, Australia: Controls on carbonate mineralogy and efficiency of CO₂ air capture in mine tailings. *International Journal of Greenhouse Gas Control*, 79, 38-60.

- Venkataramani, D., Musgrave, R.J., Boutelier, D.A., Alistair C. Hack, A.C., Collins, W.J., 2018. Revised potential field model of the Gilmore Fault Zone. *Exploration Geophysics*, 49, 572-583. <https://doi.org/10.1071/EG16148>
- Wan, Y.S., Xie, H.Q., Dong, C.Y., Kroner, A., Wilde, S.A., Bai, W.Q., Liu, S.J., Xie, S.W., Ma, M.Z., Li, Y., Liu D.Y. (2018). Hadean to Paleoproterozoic Rocks and Zircons in China. In: *Earth's Oldest Rocks (2nd Edition)*, Van Kranendonk, M.J., Bennett, V. C., Hoffman, J.E. (Eds), Elsevier, pp. 293-327.
- Wang C.L., Qin K.Z., Zhou Q.F., Evans N.J., Tang D.M. and Yang Y.H. (2018). Rapid two-stage evolution of the Kelumute No.112 Li-Be-Nb-Ta pegmatite, Chinese Altai: constraints from columbite-tantalite mineralogy and U-Pb geochronology. *American Mineralogist*, 103, 1891-1905.
- Wang C.L., Wang Y.T., Dong L.H., Qin K.Z., Evans N.J., Zhang B. and Ren Y. (2018). Iron mineralization at the Songhu deposit, Chinese Western Tianshan: A type locality with regional metallogenic implications. *International Journal of Earth Sciences* 107, 291-319. <https://doi.org/10.1007/s00531-017-1490-9>. (IF = 2.093)
- Wang L., Putnis C.V., Hövelmann J. and Putnis A. Interfacial precipitation of phosphate on hematite and goethite. *Minerals*, 8, 207 (2018) doi:10.3390/min8050207
- Wang Y., Chen H., Xiao B., Han J., Fang J., Yang J., Jourdan F.. Overprinting mineralization in the Paleozoic Yandong porphyry copper deposit, Eastern Tianshan, NW China—Evidence from geology, fluid inclusions and geochronology. *Ore Geology Reviews* 100, 148-167. 2018.
- Wang, K., Dong, S., Li, Z.-X., Han, B., 2018. Age and chemical composition of Archean metapelites in the Zhongxiang Complex and implications for early crustal evolution of the Yangtze Craton. *Lithos*, 321-321, 280-301. <https://doi.org/10.1016/j.lithos.2018.09.027>
- Wang, K., Li, Z.-X., Dong, S., Cui, J., Han, B., Zheng, T., Xu, Y., 2018. Early crustal evolution of the Yangtze Craton, South China: New constraints from zircon U-Pb-Hf isotopes and geochemistry of ca. 2.9–2.6 Ga granitic rocks in the Zhongxiang Complex. *Precambrian Research*, 314, 325-352. <https://doi.org/10.1016/j.precamres.2018.05.016>
- Wang, L.-J., Guo, J.-H., Yin, C., Peng, P., Zhang, J., Spencer, C.J., and Qian, J.-H., 2018, High-temperature S-type granitoids (charnockites) in the Jining complex, North China Craton: Restite entrainment and hybridization with mafic magma: *Lithos*, v. 320, p. 435-453.
- Wang, Q., Wilde, S.A. (2018). New constraints on the Hadean to Proterozoic history of the Jack Hills belt, Western Australia. *Gondwana Research*, 55, 74-91.
- Wang, R., Weinberg, R.F., Collins, W.J., Richards, J.P. and Di-cheng Zhu, D.C., 2018. Origin of post-collisional magmas and formation of porphyry Cu deposits in southern Tibet. *Earth Science Reviews*, 181, 122-143. <https://doi.org/10.1016/j.earscirev.2018.02.019>
- Wang, R., Weinberg, R.F., Collins, W.J., Richards, J.P., Zhu, D-C. (2018). Origin of postcollisional magmas and formation of porphyry Cu deposits in southern Tibet. *Earth-Science Reviews* 181, 122-143.

- Ware B., Jourdan F., Tohver E., Fernandes K.G. and Chiaradia M. (2018) Primary Hydrous Minerals from the Karoo LIP Magmas: Evidence for a Hydrated Source Component. *Earth and Planetary Science Letters* 503, 181-193.
- Ware B.D., Jourdan F., Merle, R. M. Chiaradia, K. Hodges. Major, Trace, and Isotope Geochemistry of the Kalkarindji Large Igneous Province, Australia: Petrogenesis of the oldest province of the Phanerozoic. *Journal of Petrology* 59, 635-666. 2018.
- Ware, B. and Jourdan F.. $^{40}\text{Ar}/^{39}\text{Ar}$ dating of terrestrial pyroxene. *Geochimica Cosmochimica Acta* 230, 112-136. 2018
- Ware, B., and FJourdan F.. 2018. " $^{40}\text{Ar}/^{39}\text{Ar}$ geochronology of terrestrial pyroxene." *Geochimica et Cosmochimica Acta* 230 (June): 112-36. doi:10.1016/j.gca.2018.04.002.
- Ware, Bryant D., Fred Jourdan, Renaud Merle, Massimo Chiaradia, and Kyle Hodges. 2018. "The Kalkarindji Large Igneous Province, Australia: Petrogenesis of the Oldest and Most Compositionally Homogenous Province of the Phanerozoic." *Journal of Petrology* 59 (April): 635-65. doi:10.1093/petrology/egy040.
- Ware, Bryant, Fred Jourdan, Eric Tohver, Kamila G. Fernandes, and Massimo Chiaradia. 2018. "Primary hydrous minerals from the Karoo LIP magmas: Evidence for a hydrated source component." *Earth and Planetary Science Letters* 503 (December): 181-93. doi:10.1016/j.epsl.2018.09.017.
- Wei, X., Zheng, H., Wang, P., Tada, R., Clift, P.D., Jourdan, F. and Luo C. Miocene Volcaniclastic Sequence within Xiyu Formation from Source to Sink: Implications for Northward Indention of Pamir in Northern Tibet. *Tectonics* 37, 3261-3284. 2018
- Wong, S.C.T., Collins, W.J., Hack, A.C., Huang, H., 2018. Provenance and structure of the Yancannia Formation, southern Thomson Orogen: implications for the tectono-stratigraphic evolution of the Cambro-Ordovician western Tasmanides. *Australian Journal of Earth Sciences*. <https://doi.org/10.1080/08120099.2018.1464062>
- Wu Y.-F., Li J.-W., Evans K., Vasconcelos P.M., Thiede D.S., Fougereuse D., Rempel K. (2018) Late Jurassic to Early Cretaceous age of the Daqiao gold deposit, West Qinling Orogen, China: implications for regional metallogeny. *Mineralium Deposita*, 1-14.
- Wu, T., Wang, X-C., Li, X.H., Li, W.X., Wilde, S.A., Tian, L., Pang, C-J., Li, J. (2018). The 825 Ma Yiyang High-MgO basalts of central South China: insights from Os-Hf-Nd data. *Chemical Geology*, 502, 107-121.
- Wu, T., Zhou, J.X., Wang, X.C., Li, W.X., Wilde, S.A., Sun, H.R., Wang, J.S., Li Z. (2018). Identification of ca. 850 Ma high-temperature strongly peraluminous granitoids in southeastern Guizhou Province, South China: A result of early extension along the southern margin of the Yangtze Block. *Precambrian Research*, 308, 18-34.

- Wu, Y.F., Li, J.W., Evans, K., Koenig, A.E., Li, Z.K., O'Brien, H., Lahaye, Y., Rempel, K., Hu, S.Y., Zhang, Z.P., Yu, J.P., (2018). Ore-forming processes of the Daqiao epizonal orogenic gold deposit, West Qinling Orogen, China: Constraints from textures, trace elements, and sulfur isotopes of pyrite and marcasite, and raman spectroscopy of carbonaceous material. *Economic Geology* 113, 1093-1132.
- Yakymchuk, C., Kirkland, C. L., and Clark, C., 2018, Th/U ratios in metamorphic zircon: *Journal of Metamorphic Geology*, v. 36, no. 6, p. 715-737.
- Yao J., Chen H., Xiang X., Sun W., Jourdan F., Lai, C-K., Song W., Luo X. A 20 m.y. long-lived successive mineralization in the giant Dahutang W-Cu-Mo deposit, South China. *Ore Geology Reviews* 95, 401-407. 2018.
- Yao, W., Li, Z.-X., Spencer, C.J., and Martin, E.L., 2018, Indian-derived sediments deposited in Australia during Gondwana assembly: *Precambrian Research*, v. 312, p. 23-37.
- Zhai H., Qin L., Zhang, W., Putnis, C.V., Wang L. (2018). Dynamics and molecular mechanism of phosphate binding to biomimetic hexapeptide. *Environ. Sci. Technol.*, DOI:10.1021/acs.est.8b03062
- Zhai H., Wang L., Qin L., ZhangW., Putnis C.V., Putnis A. (2018). Direct observation of simultaneous immobilization of cadmium and arsenate at the brushite–fluid interface. *Environ. Sci. Technol.* 52, 3493-3502.
- Zhang B., Puzyrev V., Calo V., Yang D., Müller T. (2018). Poroelastic Seismic Modelling Using the Viscosity-extended Biot Framework. *80th EAGE Conference and Exhibition*.
- Zhang B., Puzyrev V., Calo V., Yang D., Müller T. (2018). Seismic modeling in porous media using the viscosity-extended Biot framework. *SEG Technical Program Expanded Abstracts*. 3918-3922.
- Zhang, J.H., Yang, J.H., Chen, J.Y., Wu, F.Y., Wilde, S.A. (2018). Genesis of late Early Cretaceous high-silica rhyolites in eastern Zhejiang Province, southeast China: A crystal mush origin with mantle input. *Lithos*, 269-299, 482-495.
- Zhang, N., Dang, Z., Huang, C., Li, Z.X., 2018. The dominant driving force for supercontinent breakup: Plume push or subduction retreat? *Geoscience Frontiers*, 9(4), 997-1007.
- Zhang, N., Li, Z.-X., 2017. Formation of mantle "lone plumes" in the global downwelling zone — A multiscale modelling of subduction-controlled plume generation beneath the South China Sea. *Tectonophysics*, 723, 1-13
- Zhang, X., P. Hancock, H. A. R. Devillepoix, R. B. Wayth, A. Beardsley, B. Crosse, D. Emrich, et al. 2018. "Limits on radio emission from meteors using the MWA." *Monthly Notices of the RAS* 477 (July): 5167-76. doi:10.1093/mnras/sty930.
- Zhou Q., Sun H., Li C., Liu Z., Lai Y., Yan G. and Evans N.J. (2018). Contemporaneous east-west extension and north-south compression at 43Ma in south Tibet. *Journal of Structural Geology*, 117, 124-135.
- Zhou, J.X., Luo K., Wang, X.C., Wilde, S.A., Wu, T., Huang, Z.L., Cui, Y.L., Zhao, J.X. (2018). Ore genesis of the Fule Pb-Zn deposit and its relationship with the Emeishan Large Igneous Province: Evidence from mineralogy, bulk c-O-S and in situ S-Pb isotopes. *Gondwana Research*, 54, 161-179.

Zhou, J.B., Wilde, S.A., Zhao, G.C., Han, J. (2018). Nature and assembly of microcontinental blocks within the Paleo-Asian Ocean. *Earth-Science Reviews*, 186, 76-93.

Zhou, J.X., Wang, X.C., Wilde, S.A., Luo, K., Huang, Z.L., Wu, T., Jin, Z.G. (2018). New insights into the metallogeny of MVT Zn-Pb deposits: A case study from the Nayongzhi in South China, using field data, fluid compositions, and in situ S-Pb isotopes. *American Mineralogist*, 103, 91-108.

Zhou, Y., Zhang, B., Stuart-Williams, H., Grice, K., Hocart, C.H. Gessler, A. ... (2018) On the contributions of photorespiration and compartmentation to the contrasting intramolecular 2H profiles of C3 and C4 plant sugars. *Phytochemistry* 145, 197-206.

Zhu, G., Zhang, Y., Zhang, Z., Li, T., He, N., Grice, K., Neng, Y. and Greenwood P. (2018) High abundance of alkylated diamondoids, thiadiamondoids and thioaromatics in recently discovered sulfur-rich LS2 condensate in the Tarim Basin. *Organic Geochemistry* 123, 136-143

Research reports

TIGeR MEMBERSHIP 2018



TIGeR membership 2018

Director

Andrew Putnis

TIGeR Business Manager

Yacoob Padia

The TIGeR Executive Committee

Andrew Putnis

Chris Clark

Will Featherstone

Kliti Grice

Boris Gurevich

Brent McInnes

Academic and Research Staff

Joseph Awange

Milo Barham

Andreas Beinlich

Gretchen Benedix

Phil Bland

Alison Blyth

Victor Calo

Aaron Cavosie

Sten Claessens

Chris Clark

Bill Collins

Marco Coolen

Jane Cuneen

Martin Danisik

Raffaella Demichelis

Jacques Eksteen

Ahmed El-Mowafy

Chris Elders

Katy Evans

Noreen Evans

Will Featherstone

Mick Filmer

Ian Fitzsimons

Lucy Forman

Denis Fougereuse

Julian Gale

Nicholas Gardiner

Rongfeng Ge

Paul Greenwood

Kliti Grice

Daive Imparato

Tim Johnson

Fred Jourdan

Pete Kinny

Jon Kirby

Chris Kirkland

Uwe Kirscher

Kasia Koziara

Michael Kuhn

Zhen Li

Zheng-Xiang Li

Brent McInnes

Neal McNaughton

Katarina Miljkovic

Ross Mitchell

Alexander Nemchin

Amy Parker

Bob Pidgeon

Sergei Pisarevskiy

Amaury Porteau

Christine Putnis

Vladimir Puzyrev

Paolo Raiteri

Steven Reddy

William Rickard

Ellie Sansom

David Saxey

Alan Scarlett

Gregory Smith

Christopher Spencer

Svetlana Tossalina

Nick Timms

Martin Towner

Kate Trinajstic

Svenja Tulipani

Stephanie Vialle

Xuan-Ce Wang

Elizabeth Watkin

Simon Wilde

Domenik Wolff-Boenisch

Weihua Yao

Nan Zhang

Jianwei Zi

TIGeR Research students

Khalid Mohammad AlHamoud
Seamus Anderson
Sonia Armandola
Samuel John Bain
Vitor Barrote
Pouria Behnoudfar
Rodney William Berrell
Daniel T. Brennan
Giada Buferale
Julian Chard
Santiago Peña Clavijo
Morgan Cox
Darren Shawn Tek-Suen Cheah
Hamed Gamal El Dien
Peng Chen
Melissa Corbett
Hadrien Devillepoix
Homayoun Fathallahzadeh
Imogen Fielding
Natalya Garcia
David Hollingsworth
Benjamin Hartig
Michael Hartnady
Johanna Heeb
Tania Hidalgo
Trent Jansen-Sturgeon
Yalimay Jimenez de Duarte
Inalee Jahn
Qiang Jiang
Liu Kai
Mehdi Khaki
Himel Nahreen Khaleque
Jiangyu Li
Shaojie Li
Janne Liebmann
Yebo Liu

Erin Martin
Sam McHarg
Ruby Marsden
Ruairidh Mitchell
Stephanie Montalvo Delgado
Josephine Moore
Kikis Muchlis
Tanja Neidhart
Nicole Nevill
Adam Nordsvan
Kenneth Orr
Agnieszka Piechocka
Correia Guerreiro Pinto Bravo
Jennifer Karin Porter
Alexander Prent
Hayley Rohead-O'Brien
Mattia Sacco
Patrick Shober
Tommaso Tacchetto
Rick Verberne
Silvia Volante
Alexander Walker
Chong Wang
Danlei Wang
Qian Wang
Tobias Wengorsch
Mulky Winata
Yafei Wu
Xuemei Yang





Curtin University



Curtin University

THE INSTITUTE FOR
GEOSCIENCE RESEARCH (TIGeR)

Disclaimer and copyright information

Information in this publication is correct at the time of printing and valid for 2018, but may be subject to change. In particular, the University reserves the right to change the content and/or method of assessment, to change or alter tuition fees of any unit of study, to withdraw any unit of study or program which it offers, to impose limitations on enrolment in any unit or program, and/or to vary arrangements for any program.

Curtin will not be liable to you or any other person for any loss or damage (including direct, consequential or economic damage) however caused and whether by negligence or otherwise that may result directly or indirectly from the use of this publication.

© Curtin University 2019
CRICOS Provider Code 00301J
ADV117714

CONTACT:

Andrew Putnis

Director

The Institute for Geoscience Research (TIGeR)

Curtin University
Kent Street Bentley WA 6102
GPO Box U1987 Perth WA 6845

Tel: +61 8 9266 7978

Email: andrew.putnis@curtin.edu.au

scieng.curtin.edu.au